AD-A150 443 DESIGN DEVELOPMENT AND TESTING OF A PROTOTYPE DIGITAL RIDE CONTROL SYSTEM.. (U) MARITIME DYNAMICS INC TACOMA WA J D ADAMS ET AL. JUN 83 MD-AR-1195-1 USCG-D-31-84 1/2

UNCLASSIFIED N00167-82-C-0079 F/G 13/10 NL

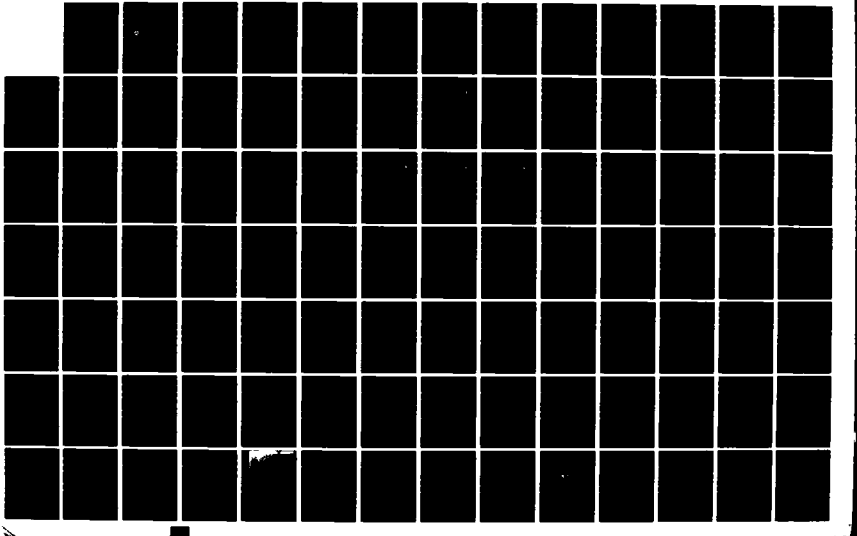

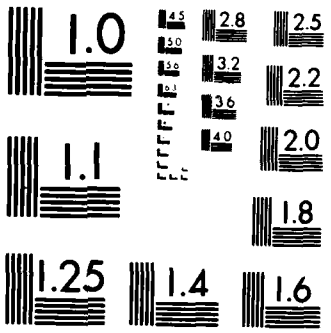

Report No. CG-D-31-84

DESIGN, DEVELOPMENT AND TESTING OF A PROTOTYPE DIGITAL RIDE CONTROL SYSTEM FOR SURFACE EFFECT SHIPS

PART VIII: TEST ON XR-1E SES

JUNE 1983

Prepared for:

U.S. Department of Transportation
United States Coast Guard

Office of Research and Development
Washington, D.C. 20593

METRIC CONVERSION FACTORS

Approximate Conversions to Metric Measures

Symbol	When You Know	Multiply by	To Find	Symbol
		LENGTH		
in	inches	*2.5	centimeters	cm
ft	feet	30	centimeters	cm
yd	yards	0.9	meters	m
mi	miles	1.6	kilometers	km
		AREA		
in^2	square inches	6.5	square centimeters	cm^2
ft^2	square feet	0.09	square meters	m^2
yd^2	square yards	0.8	square meters	m^2
mi^2	square miles	2.6	square kilometers	km^2
	acres	0.4	hectares	ha
		MASS (weight)		
oz	ounces	28	grams	g
lb	pounds	0.45	kilograms	kg
	short tons (2000 lb)	0.9	tonnes	t
		VOLUME		
tsp	teaspoons	5	milliliters	ml
Tbsp	tablespoons	15	milliliters	ml
fl oz	fluid ounces	30	milliliters	ml
c	cups	0.24	liters	l
pt	pints	0.47	liters	l
qt	quarts	0.95	liters	l
gal	gallons	3.8	liters	l
ft^3	cubic feet	0.03	cubic meters	m^3
yd^3	cubic yards	0.76	cubic meters	m^3
		TEMPERATURE (exact)		
°F	Fahrenheit temperature	5/9 (after subtracting 32)	Celsius temperature	°C

*1 in = 2.54 (exactly). For other exact conversions and more detailed tables, see NBS Misc. Publ. 286, Units of Weights and Measures, Price $2.25, SD Catalog No. C13.10:286.

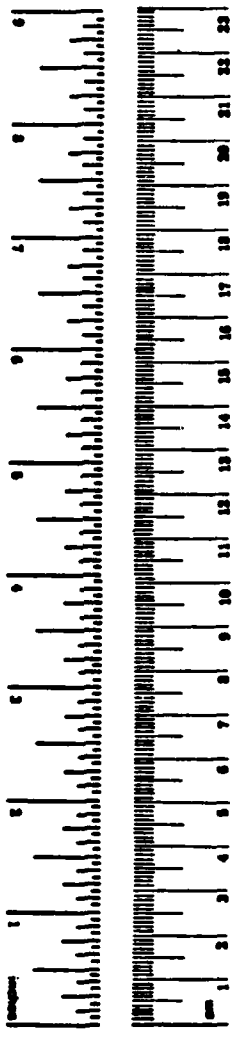

Approximate Conversions from Metric Measures

Symbol	When You Know	Multiply by	To Find	Symbol
		LENGTH		
mm	millimeters	0.04	inches	in
cm	centimeters	0.4	inches	in
m	meters	3.3	feet	ft
m	meters	1.1	yards	yd
km	kilometers	0.6	miles	mi
		AREA		
cm^2	square centimeters	0.16	square inches	in^2
m^2	square meters	1.2	square yards	yd^2
km^2	square kilometers	0.4	square miles	mi^2
ha	hectares (10,000 m^2)	2.5	acres	
		MASS (weight)		
g	grams	0.035	ounces	oz
kg	kilograms	2.2	pounds	lb
t	tonnes (1000 kg)	1.1	short tons	
		VOLUME		
ml	milliliters	0.03	fluid ounces	fl oz
l	liters	2.1	pints	pt
l	liters	1.06	quarts	qt
l	liters	0.26	gallons	gal
m^3	cubic meters	35	cubic feet	ft^3
m^3	cubic meters	1.3	cubic yards	yd^3
		TEMPERATURE (exact)		
°C	Celsius temperature	9/5 (then add 32)	Fahrenheit temperature	°F

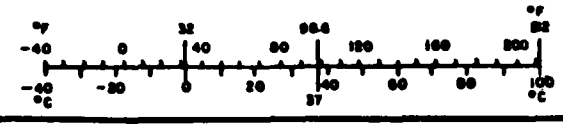

Technical Report Documentation Page

1. Report No.	2. Government Accession No. AD-A150 443 CG-D-31-84	3. Recipient's Catalog No.
4. Title and Subtitle Design, Development and Testing of a Pro-Type Digital Ride Control System for Surface Effect Ships Part VIII: Test On XR-1E SES		5. Report Date June 1983 6. Performing Organization Code
7. Author(s) John D. Adams, A. W. Ernest, J. H. Lewis		8. Performing Organization Report No. MD-AR-1195-1
9. Performing Organization Name and Address Maritime Dynamics, Inc. 1169 East Ash Avenue Fullerton, CA 92631 8100 27th Street W., Tacoma, WA. 98466		10. Work Unit No. (TRAIS) 11. Contract or Grant No. N00167-83-C-0079
12. Sponsoring Agency Name and Address United States Coast Guard Headquarters G-DMT-2/54 Washington, D. C. 20593		13. Type of Report and Period Covered Final 14. Sponsoring Agency Code

15 Supplementary Notes

16. Abstract

The prototype digital ride control system (RCS) developed by Maritime Dynamics was installed and tested on the 26-ton XR-1E SES. Open and closed loop tests were conducted. Stability of the digital controller was compared with that of the experimental analog RCS developed for the XR-1D SES. Closed loop test data was used to make RCS performance predictions for the USCG Sea Bird Class SES. A tradeoff study was performed and a candidate RCS configuration was selected for the Sea Bird Class SES. A preliminary design was developed for the RCS configuration identified as most desirable.

17. Key Words	18. Distribution Statement		
Surface Effect Ship Ride Control XR-1E SES SES Test and Evaluation			
19. Security Classif. (of this report) Unclassified	20. Security Classif. (of this page) Unclassified	21. No. of Pages	22. Price

Form DOT F 1700.7 (8-72) Reproduction of completed page authorized

TABLE OF CONTENTS

TABLE OF CONTENTS (Cont.)

TABLE OF CONTENTS (Cont.)

LIST OF FIGURES

LIST OF FIGURES (Cont.)

LIST OF FIGURES (Cont.)

LIST OF TABLES

1. INTRODUCTION

Under Contract N00024-80-C-5338, Maritime Dynamics, Inc. (MariDyne) developed a prototype digital ride control system (RCS) for surface effect ships (SES). Initial application of this system is oriented toward the U. S. Navy 200-ton high length-to-beam ratio SES designated the SES-200. However, prior to installation on the SES-200, the system was installed and tested on the 26-ton low length-to-beam ratio XR-1E SES between 7 September and 8 October 1982. This testcraft is stationed at the USN Surface Effect Ship Test Facility (SESTF) located at the Naval Air Test Center, Patuxent River, MD.

The XR-1E digital RCS test program was sponsored jointly by the U. S. Navy Surface Effect Ship Project (NAVSEA05R47) and the U. S. Coast Guard Office of Research and Development. Testcraft instrumentation, test planning, testcraft operations and data reduction were accomplished by the Surface Effect Ship Test Facility. Maritime Dynamics provided initial instrumentation, test and data requirements in addition to analyzing and reporting the test data contained in this report. The MariDyne effort was funded under Contract N00167-82-C-0079.

Principal objectives of testing the digital RCS on the XR-1E included the following:

1. Verify proper shipboard operation of the system prior to installation on the SES-200.

2. Compare performance and stability of the digital RCS with the experimental analog RCS tested on the XR-1D SES (see References 1 and 2).

3. Predict RCS performance on the USCG Sea Bird Class SES from data gathered during XR-1E tests.

4. Specify RCS configuration and installation requirements for the USCG Sea Bird Class SES from experience obtained on the XR-1E and SES-200.

This report describes how each of these test program objectives has been satisfied. It has been designated as Part VIII of an eight-part report which will be issued by Maritime Dynamics under Contract N00167-82-C-0079. Parts I and VII have been published and are listed as References 3 and 4.

2. SUMMARY

The prototype digital ride control system (RCS) developed by Maritime Dynamics (MariDyne) was installed and tested on the low length-to-beam ratio 26 L.T. XR-1E SES. Two (2) open loop hover tests and three (3) closed loop underway missions were conducted between 7 September and 8 October 1982.

Open loop test conditions matched those used for testing the experimental analog RCS developed for the XR-1D SES (References 1 and 2). Therefore, direct comparison of the stability characteristics of the two controllers were made.

XR-1E cushion dimensions (length, beam, height) and loading (pressure) are such that the testcraft is an acceptable 1/2 scale Froude model of the USCG Sea Bird Class SES. Digital RCS closed loop tests were conducted at scaled Sea Bird fan flow rates, speeds and sea conditions. The data base obtained was used to make RCS performance predictions for the Sea Bird Class SES.

A tradeoff study was performed and a candidate RCS configuration was selected for the Sea Bird Class SES. As part of this tradeoff study, an inspection of the Seahawk was made at the USCG SES Squadron Headquarters at Key West, Florida on 7 and 8 April 1983. Discussions were held with the SES operators regarding the impact of various configurations on vessel operation and maintenance.

A preliminary design was developed for the RCS configuration identified as most desirable. This design effort addressed the impact of the selected RCS configuration on the Sea Bird's arrangements, structure, weight, LCG location, stability, machinery and operation. Preliminary hardware specifications were developed for the RCS vent valve modules, the hydraulic system and the electronic components. Operation and maintenance requirements were specified.

3. MAJOR RESULTS

The digital RCS was developed as a general purpose controller which could be used to perform the ride control function on surface effect ships and air cushion vehicles. Initial application of the system was focused on the SES-200. Installation and successful testing of the system on the XR-1E during this test program demonstrated the system's general purpose nature.

Measured controller transfer functions and RCS-plus-craft open loop transfer functions were compared to and found to be in agreement with analytical predictions. This validates design of the digital RCS software and hardware plus its integration with the XR-1E SES.

Digital RCS open loop transfer functions were compared to similar data for the experimental analog RCS tested on the XR-1D SES. As predicted, the digital RCS gain margin was 1 to 2 db lower than that of the analog system. The sample-and-hold effect and computational delays in the digital system increase the high frequency phase lag which causes this small reduction in the gain margin. Closed loop testing demonstrated that the digital RCS stability and sample rate are adequate. In these tests, the digital RCS was operated at the same overall gain utilized during tests of the analog RCS. There was no evidence of instability, limit cycling or excessive pressure amplification in the acoustic frequency (10 to 20 Hz) due to the small reduction in gain margin.

The XR-1E SES is an acceptable 1/2 scale Froude model of the U. S. Coast Guard Sea Bird Class SES. Closed loop digital RCS tests were conducted at Froude scaled Sea Bird fan flow rates and speeds in head seas. The resulting data base was supplemented with XR-1D and SES-200 RCS data and then used to make RCS performance predictions for the Sea Bird SES.

These predictions are shown in Figure 3-1(a). They represent Sea Bird operation at maximum speed in head seas for Sea States I to IV. This is the operating condition for which heave accelerations are most detrimental to habitability. As shown, the RCS is predicted to reduce the standard deviation (RMS) of heave acceleration by 50 to 60% in Sea States I and II, 40 to 50% in Sea State III and 35% to 40% in Sea State IV. These levels of heave acceleration reduction can significantly reduce crew fatigue and improve efficiency and morale during transits, sweep, and search and rescue operations. For typical Gulf of Mexico Sea State II operations, the RCS can maintain the standard deviation of heave acceleration below 0.10 g. In the Sea Bird frequency range 1σ,vertical accelerations below 0.10 g are generaly considered tolerable for several days without physical impairment of crew functions. In higher sea states, the RCS effectiveness is somewhat less; however, system operation will be very noticeable due to attenuation of the pressure spikes associated with cushion venting.

In off head sea conditions, the RCS is expected to reduce the heave accelerations by the same percentages shown in Figure 3-1(a). Fatigue is caused by the cumulative effects of acceleration level and mission duration. Therefore, it is expected that a Sea Bird Crew would operate the RCS at all times during over hump operations in Sea States I through IV.

Figure 3-1(a) SEA BIRD CLASS SES - 1⁄ HEAVE ACCELERATION VERSUS WAVE HEIGHT, WITH AND WITHOUT RCS, MAXIMUM SPEED, HEAD SEAS

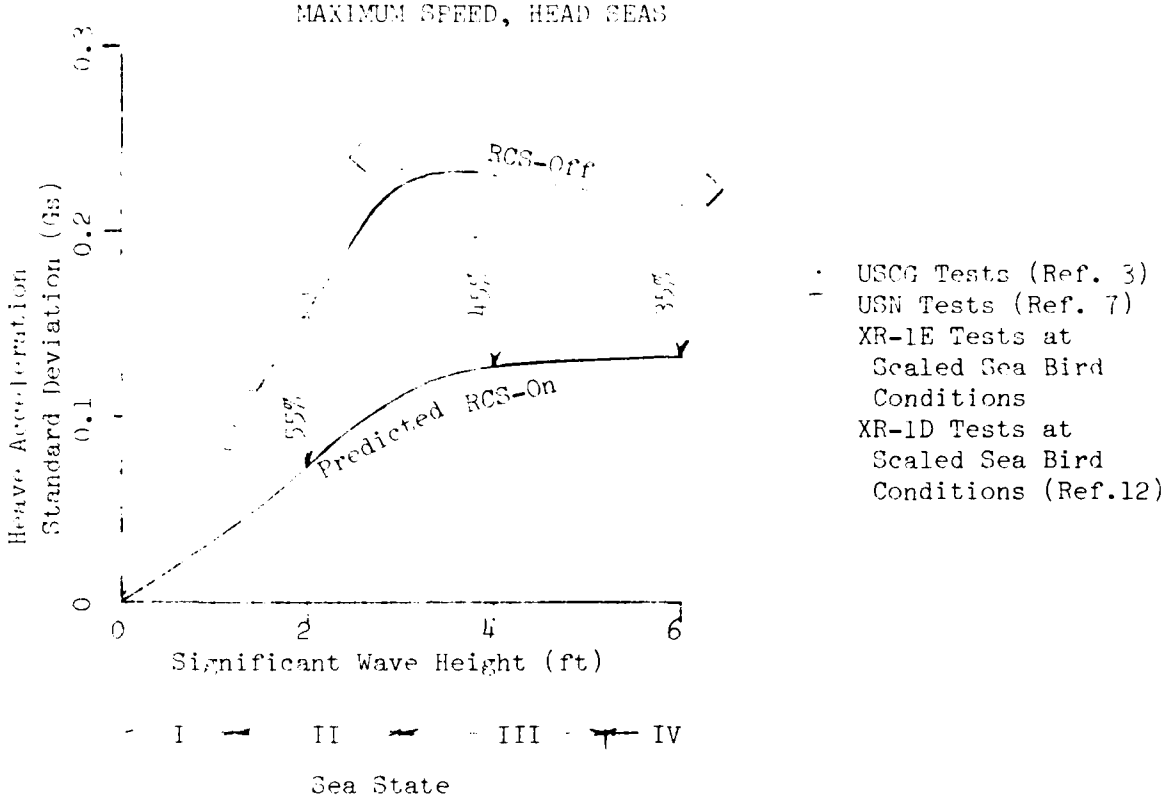

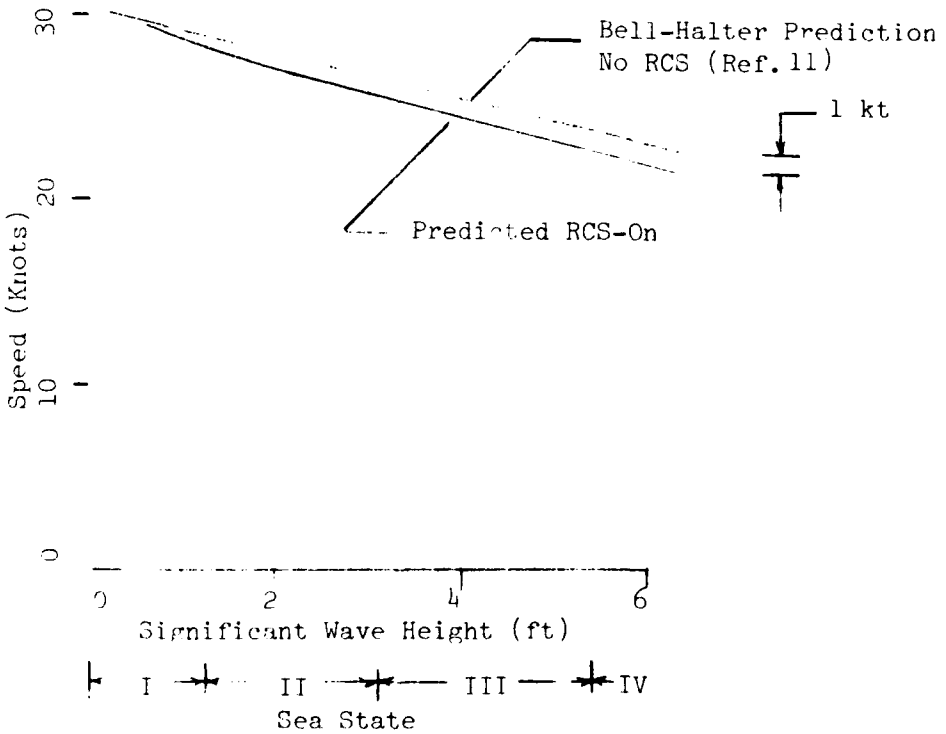

Figure 3-1(b) SEA BIRD CLASS SES, SPEED VERSUS WAVE HEIGHT, WITH AND WITHOUT RCS, MAXIMUM SPEED, HEAD SEAS

Figure 3-1(b) illustrates the predicted maximum boundary speed for head sea operation with and without ride control. As shown, a 1 knot loss of speed is predicted due to dumping pressurized air overboard through the vent valves. During an extended transit at maximum speed, this 1 knot loss would reduce the Sea Bird's range by 45 nm., from 1225 nm. to 1180 nm. This appears to be an acceptable penalty considering the significant reduction in heave acceleration which can be obtained using the RCS. One knot speed loss is considerably lower than predicted in Reference 13 because SES-200 data to assist in predicting trends in Sea States III and IV was previously unavailable.

A tradeoff study was performed to select an RCS configuration for the USCG Sea Bird Class SES. This study showed that there were two (2) key requirements to be satisfied:

1. Minimizing impact of the installation on existing ship systems.

2. Minimizing weight growth and forward movement of the vessel's LCG.

The selected configuration meets both of these key requirements. It is similar to the installation on the SES-200 except that the number of vent valve modules has been reduced from four to two. This reduction considerably simplifies the mechanical, hydraulic and electronic portions of the ride control system.

The vent valve installation involves installing two 3 by 5 ft flow trunks inside the Number 2 Centerline Fuel Tank. Vent valve modules will be bolted to short trunk stacks which extend approximately 2 ft above the weather deck. The vent valve louvers are oriented to discharge the airflow directly aft. This deck-mounted vent valve configuration was discussed with the USCG SES Squadron at Key West. The operators felt that cushion venting in waves makes the deck too wet for personnel use; therefore, they did not feel that the above deck vent valve exhaust would pose any operational problems.

Two non-integral fuel tanks (designated Number 3 Port and Starboard) will be installed in unused spaces aft of Frame 13 to replace the volume of fuel removed from the Number 2 Tank. Because it is presently necessary to carry ballast in the aft (Number 3) ballast tanks to maintain the LCG in the range required for best performance (i.e., 1.5 ft aft of amidships), this installation results in a favorable aft shift in the vessel's LCG.

Based on USCG draft readings and Bell-Halter draft tables, at full load displacement the vessel nominally carries 7515 gallons of fuel, 1390 gallons of ballast water and weighs 323,700 lb for an LCG location 1.5 ft aft of amidships. Following retrofit of the RCS, it is estimated that the vessel could carry as much as 8242 gallons of fuel without ballast and maintain a -1.5 ft LCG at a full load displacement of 319,800 lb. Therefore, the Sea Bird Class SES could carry approximately 10% more fuel and

which 3900 lb less at full load with the selected RCS configuration installed. The increased fuel capacity would more than compensate for the small range penalty due to RCS operation. This favorable situation is the result of rearranging the fuel tanks to shift the LCG aft and reduce the present requirement to carry ballast for LCG control. Of course, it will always be necessary to carry some small amount of ballast (≈100 - 200 gallons) to maintain the transverse center of gravity (TCG) on the centerline. At less than full load, the modified craft still requires less ballast than the present configuration for LCG control.

It should be noted that the USCG SES operators at Key West stated that ballast is carried in the aft tanks often but not always. They mentioned that, under certain very high wind and sea conditions, performance was best with the LCG further forward than Bell-Halter's recommended location of -1.5 ft aft of amidships. Since this behavior could not be predicted from either previous or present U. S. Navy SES test experience, possible causes are explored in Section 8 of this report. Regardless of the reason, it should be noted that the ballast system will not be disturbed by the RCS installation. It will always be possible to fine-tune the longitudinal and transverse center of gravity positions using the ship's three sets of ballast tanks.

The RCS hydraulic system will be located between Frames 9 and 10 in the lift engine compartment. Since the vent valve modules are located just aft of Frame 10, the plumbing requirements are minimal, and all components are in proximity to one another. The hydraulic pump will be driven via a belt-drive connected to the PTO pulley on the aft end of the starboard lift engine. A similar arrangement has proved satisfactory on the SES-200.

The RCS electronic control unit will be mounted on the bridge and interconnected with the various feedback sensors via a junction box located at Frame 10. Optional pitch and roll inputs are specified for the control unit. The RCS can display mean values of these parameters. USCG SES operators felt these displays would be very helpful in assessing the vessel's trim and list for purposes of transferring fuel or ballast to optimize performance. The mean value displays will not vary due to pitch and roll oscillations because the dynamic part of the signal will be digitally filtered out. This should be a considerable improvement over the present bridge inclinometers which oscillate too much to be used in waves.

In summary, the preliminary RCS design developed for the USCG Sea Bird Class SES satisfies the two principal design criteria mentioned earlier. The impact on existing ship systems is modest because it is not necessary to remove or relocate any machinery or electrical systems. The majority of the work requires only welding support to install the flow trunks and new fuel tanks in the hull. Machinery modifications required include installing plumbing for the new fuel tanks and installing the RCS hydraulic system. Both of these are straightforward tasks.

The RCS installation will have a favorable impact on weight and LCG position because the present requirement to carry ballast in the aft tanks to maintain an optimum LCG will be reduced. The aft shift in the LCG produced by the RCS installation could help other planned USCG retrofit projects such as vertical stacks, sound proofing and electronic gear installations. Without the RCS modifications, these installations will shift the Sea Bird LCG farther forward making it necessary to carry even more ballast in the aft tanks, thus adding more weight to the full load displacement.

4. RECOMMENDATIONS

A preliminary RCS design has been developed for the U. S. Coast Guard Sea Bird Class SES. It has a favorable impact on the vessel's weight, LCG and range and minimal impact on existing craft systems. Since the design satisfies these key requirements, it is recommended that the RCS be installed on the Sea Bird SES to reduce crew fatigue and improve efficiency.

The final design effort should produce a detailed weight and moment survey for all craft modifications. Floodable length calculations need to be performed to verify that the present two-compartment standard of subdivision can be met after installation of the flow trunks and new fuel tanks.

5. TEST PROGRAM DESCRIPTION

The principal objectives of testing the digital Ride Control System (RCS) on the XR-1E SES were to verify proper shipboard operation of the system and to compare the performance of the digital RCS with that of the analog RCS developed during the XR-1D RCS Program (see References 1 and 2). Therefore these tests served as a shakedown for the digital RCS prior to installation on the SES-200.

Another objective of the tests was to obtain data which could be used to predict RCS performance for the USCG Sea Bird Class SES (i.e., the Bell-Halter BH-110, Mark II). Since the XR-1E cushion dimensions approximate a 1/2 scale BH-110, all XR-1E RCS tests were conducted at Froude-scaled BH-110 fan flow rates and speeds to obtain the required data.

5.1 DIGITAL RIDE CONTROL SYSTEM DESCRIPTION

The purpose of the RCS on the surface effect ship is to modulate cushion airflow to increase SES heave damping and raise the heave resonant frequency. This action can substantially reduce vertical accelerations due to wave action thereby improving the ride quality by reducing fatigue and increasing crew effectiveness.

The digital RCS is a microprocessor-based controller intended for general SES/ACV useage. The system will accept from one to four pressure signals for control law feedback, perform a discrete or sampled data control algorithm, and output a single control signal to four vent valves. The initial application is directed primarily at the SES-200; however, as long as these basic input/output restrictions are complied with, the system can be utilized to perform the ride control function on other SES/ACV craft. The system is general purpose because a microprocessor is used to implement different control laws with the same hardware by modifying stored arrays of numerical coefficients used in the control law computations. In addition to performing the ride control function, the system also computes and displays the mean and standard deviation of craft parameters important to RCS operation. The system is designed for unattended operation and contains logic for performing self checks and shutdowns. A block diagram for the digital RCS is shown in Figure 5-1.

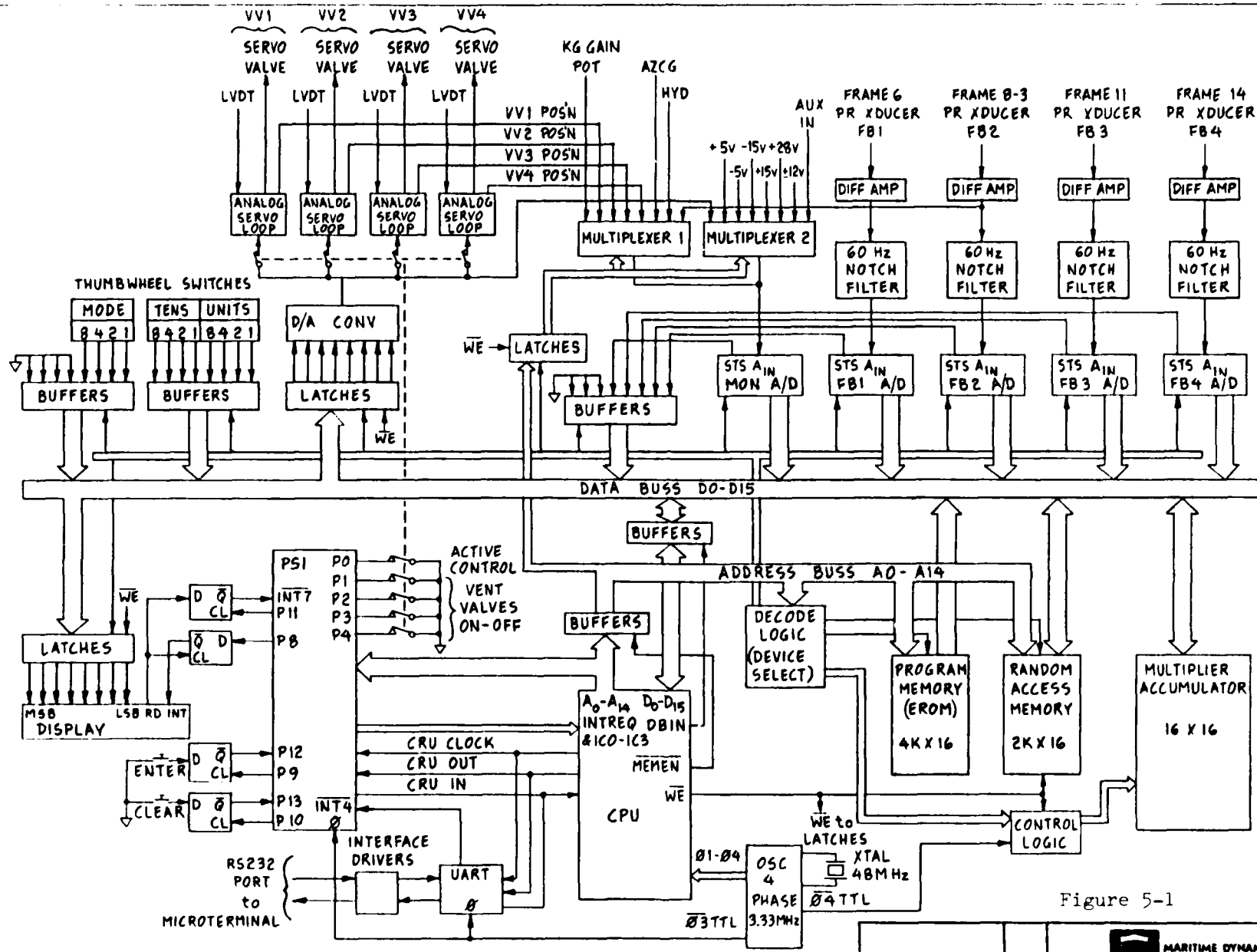

Figure 5-1

DRAWN J. ELERY 6/27/83		MARITIME DYNAMICS, INC
CHK		SES RIDE CONTROL SYSTEM BLOCK DIAGRAM
STRESS		
DES APPR		
SIZE C	CODE IDENT NUMBER	DWG NO 1193-0607-82 REV 1
SCALE		SHEET 1 OF 1

5.1.1 Digital Control Laws

Two digital RCS control laws were designed for the XR-1E test program. The first of these is a simple proportional control law similar to the proportional analog controller tested on the XR-1D (see References 1 and 2). The second law incorporates a compensation transfer function similar to the compensation laws arrived at by classical design techniques in Reference 1. Tests with these control laws then provide some basis for comparison of the digital controller performance with that of the analog controller of Reference 1. As was the case with the analog controllers, both laws operate on a single cushion pressure as a feedback signal and the output signal is a command to the four ganged vent valves (VVs). It may be noted that the basic digital controller is capable of handling multiple inputs and outputs. The controller program used for these tests is actually set up for four inputs and one output. However, a single-input/single-output arrangement is adequate for our present purposes. It is implemented in the controller program by merely inserting zero gain coefficients on the unwanted input channels.

Restricting attention to the single input/single output implementation, the control laws incorporated in the program are of the form

$$u\ (= u(0)) = \sum_{r=o}^{Q} Y(4)*y(r) - \sum_{r=1}^{P} X(r)*u(r) \qquad (5\text{-}1)$$

where the Xs and Ys are the control law coefficients, y is the input signal to the controller (in this case the mid-cushion pressure) and u is the control signal. The index r in Equation (5-1) indicates the indexed quantity is delayed r sampling intervals, e.g., u(3) is the control signal which was output three sampling intervals earlier. In the program implementation, the law is derived to relate an output signal in terms of % VV position command to an input in terms of counts of the input A/D converter. Also, coefficients X and Y are converted by scale factors so that the data internal to the microprocessor can be maintained accurately in integer form as is suitable for such processors. Both the control law coefficients and the scaling factors employed are stored in data tables in read-only memory (ROM) with a different table (including different scaling factors) for each separate control law. The appropriate data table is selected by the controller program according to the control law number entered via the thumbwheel on the controller front panel.

There is also a provision for incorporating an overall gain factor, K_G, as entered via the ten-turn potentiometer on the controller front panel and an offset, or bias command, can also be entered on the thumbwheel. The actual signal output is then

$$K_G*(u + BIAS) \qquad (5\text{-}2)$$

converted to D/A counts and finally (by the D/A) to an appropriate voltage.

Limits are also applied to the signal before outputting it to assure that commands for VV position below 5% open or above 95% open are not given; the upper limit may also be selected via the thumbwheel to lie anywhere in the range 5 to 95%. This serves to protect the VVs from any contact with the hardware stops.

The scale factors for each control law are generally selected on a compromise basis to satisfy the following principal criteria:

1. To avoid excessive overflows in the storage of computed control signals (these are stored in a double precision form such that 2**16 times the stored value is an integer).

2. To allow sufficient precision in the stored values of the control law coefficients. These are scaled to (a) not exceed the 16-bit word length, and (b) to have as many significant figures as possible within that word length.

3. To allow a sufficient number of significant figures in the stored computed control signals. Insufficient accuracy in the stored representation of these values can lead to undesirable wandering of the output signal when the input signal levels are low (for control laws having non-zero Xs).

For the proportional controller, the control law, Equation (5-1), reduces to simply

$$u = Y(0)*y(0) \tag{5-3}$$

The single coefficient was selected to achieve an overall gain for the controller installation of 7.5%/psf (in terms of % VV command per unit cushion pressure)at $K_G = 1$ with all four VVs active. This level was selected as appropriate on the basis of experience with the corresponding analog controller (References 1 and 2). The control law is in series with devices having the following gains:

Cushion Pressure Transducer	0.025 v/psf
A/D	409.4 counts/v

Therefore the internal gain is

$$Y(0) = 7.5/(0.025*409.4) = 0.7328 \text{ \%/count} \tag{5-4}$$

With the scale factors selected for this case, this value scales to 480 as the integer value stored in the ROM.

The implementation of the control law was checked by driving the controller A/D with a sine-wave generator at various frequencies and monitoring the D/A output with a gain-phase meter. This provides a direct end-to-end check using the actual hardware and ROM to be employed on the craft. The results are shown on Figure 5-2. Note that the simple proportional law performance is modified slightly by the digital implementation. This results in a phase lag arising from delays in the system due to the sample-and-hold effect of the sampled output signal and to computational delays in the microprocessor.

The sample-and-hold amounts to an effective delay of one-half sampling interval. The computational delay is the time required to acquire the input signal, compute the desired output signal (converted to proper units for the D/A) and output the signal through the D/A; this requires about 2 msec. At the selected sampling rate of 200 pps, the predicted lag is as shown on Figure 5-2 and is in good agreement with the test data.

The compensated control law was chosen to be of the same form used for the development of the classical control laws of Reference 1. These laws were composed of a serial connection of second order transfer functions of the form

$$H(s) = \frac{s^2 + 2\zeta_N\omega_n s + \omega_n^2}{s^2 + 2\zeta_D\omega_n s + \omega_n^2} \qquad (5\text{-}5)$$

where ω_n is the natural frequency of the component transfer function and ζ_N and ζ_D are damping ratios. Note that these transfer functions go to unity both at zero frequency and as the frequency approaches infinity. This is an improper transfer function (i.e., it does not to to zero at infinite frequency) and requires some special care in converting to digital form.

In Reference 1, the compensation laws employed used two or more such components in series. However, some experimentation with these forms showed that, by employing larger numerator damping ratios than used in Reference 1, satisfactory compensation could be achieved with a single term of the form of Equation (5-5). This is the compensation law selected with $\omega_n = 2\pi$, $\zeta_D = 0.2$ and $\zeta_N = 1.0$.

In order to convert this analog law to digital form, a modification of the usual technique is required. The customary approach is to expand the analog transfer function into partial fractions (unnecessary here, since we have but a single second-order term), then identify the corresponding z-transform for each term such that the analog transfer function and the discrete transfer function are, respectively, the Laplace and z-transforms of the same time function; namely, the desired controller impulse response. This assures that both the analog and digital laws have the same impulse response (at the sampling instants only).

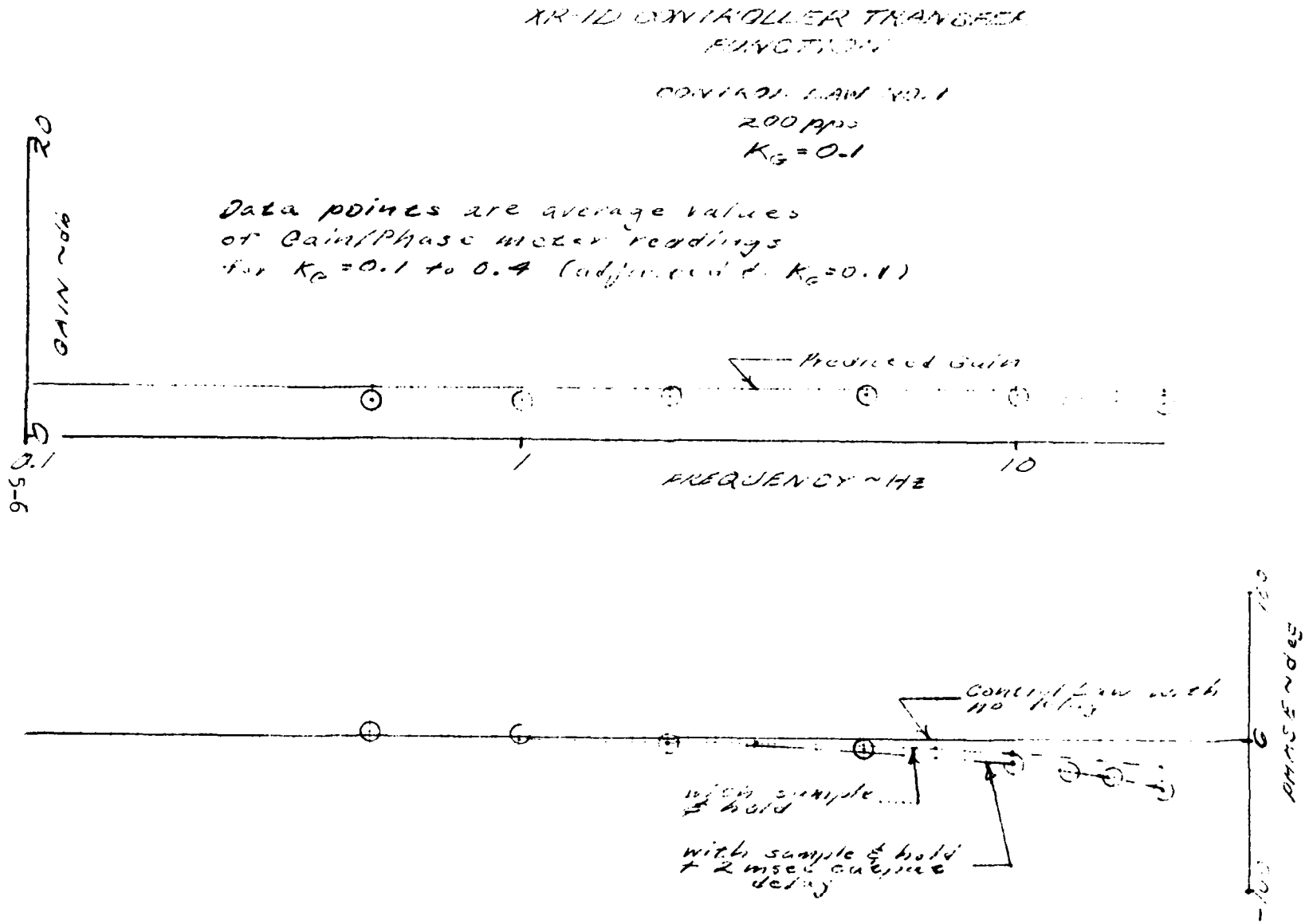
XR-10 CONTROLLER TRANSFER FUNCTION
CONTROL LAW NO. 1
200 pps
$K_G = 0.1$
Data points are average values of Gain/Phase meter readings for $K_G = 0.1$ to 0.4 (adjusted to $K_G = 0.1$)
GAIN ~db
20
0
-20
Predicted Gain
0.1
1
10
FREQUENCY ~ Hz
9-5-6
PHASE ~ deg
Control Law with no lag
With sample & hold
With sample & hold + 2 msec sample delay

Figure 5-2

In the case of an improper transfer function, however, this cannot be done because the impulse response of the analog law contains a delta function, i.e., an infinite spike in the response at time zero. A discrete transfer function cannot duplicate this behavior because its shortest response is of one sampling interval duration, i.e., the sharp spike is replaced by a flat-topped pulse of finite duration. This problem is circumvented by choosing to characterize the control law in the time domain by its step function response, rather than its impulse response. Rather than matching H(s) of Equation (5-5), we choose to match $H_1(s) = H(s)/s$. This assures that the digital and analog step function responses match. Of course, this matching occurs only at the sampling instants. At times between samples, the responses will generally be different.

To accomplish this, we first express H(s) in partial fraction form as

$$H_1(s) = \frac{1}{s} + \frac{10.053}{(s + 1.2566)^2 + (6.1562)^2} \tag{5-6}$$

The matching z-transform is readily found to be

$$H(z) = \frac{z-1}{z} + \frac{1.63296e^{-1.2566T} \sin(6.1526T)t_z}{z^2 - 2e^{-1.2566T} \cos(6.152(T)z + c^{-2(1.2566)T}} \tag{5-7}$$

where T is the sampling interval. The desired discrete transfer function is recovered by multiplication by $z/(z - 1)$ to convert the transform of the step function response to that of the impulse response. Substituting the delay operator $d = 1/z$, inserting numerical values for the a and b, and using T = 0.005 sec. (200 pps) gives the final law as

$$H(d) = \frac{1 - 1.93659d + 0.93757d^2}{1 - 1.98653d + 0.98751d^2} \tag{5-8}$$

This yields the coefficients of Equation (5-1) as

$$Y(0) = 1 \tag{5-9}$$
$$Y(1) = -1.93659 \tag{5-10}$$
$$Y(2) = 0.93757 \tag{5-11}$$
$$X(1) = 1.98653 \tag{5-12}$$
$$X(2) = -0.98751 \tag{5-13}$$

It may be noted that the denominator polynomial in Equation (5-8)

has poles at

$$d = 1.005828 + 0.030959i \tag{5-14}$$

lying perilously close to the stability boundary (the unit circle in the d-Plane). This is characteristic of discrete control laws at high sampling rates and it may be shown that all poles tend to converge on the point d = 1 as the sampling rate approaches infinity. To assure a stable control law then requires rather accurate placing of the roots. Some care is required in converting the coefficients to digital form lest the round-off errors move the poles into the unstable region. With the scale factors selected for this case, the integer coefficients corresponding to Equations (5-9) through (5-13) are

$$YC(0) = 12,006 \tag{5-15}$$
$$YC(1) = -23,251 \tag{5-16}$$
$$YC(2) = 11,257 \tag{5-17}$$
$$XC(1) = 32,547 \tag{5-18}$$
$$XC(2) = -16,179 \tag{5-19}$$

(there is an implied value of XC(0) = -16,384 corresponding to an implied value of X(0) = -1 with Equations (5-12) and (5-13) to complete the denominator polynomial). The poles for the integer coefficient polynomial are at

$$d = 1.00584 + 0.0309i \tag{5-20}$$

which agrees well with Equation (5-14). Additional checks on the accuracy of the integer coefficient representation were made by comparing the frequency plane transfer functions computed frequency-by-frequency with that for the non-integer case.

Finally, the law was inserted into the controller ROM and the resultant end-to-end transfer function was measured experimentally as was done for the proportional control law. The results are shown on Figure 5-3 and are considered a satisfactory match to the desired transfer function also shown on Figure 5-3. As for the proportional control law, some correction for the sample-and-hold and the computational delays is required on the phase data.

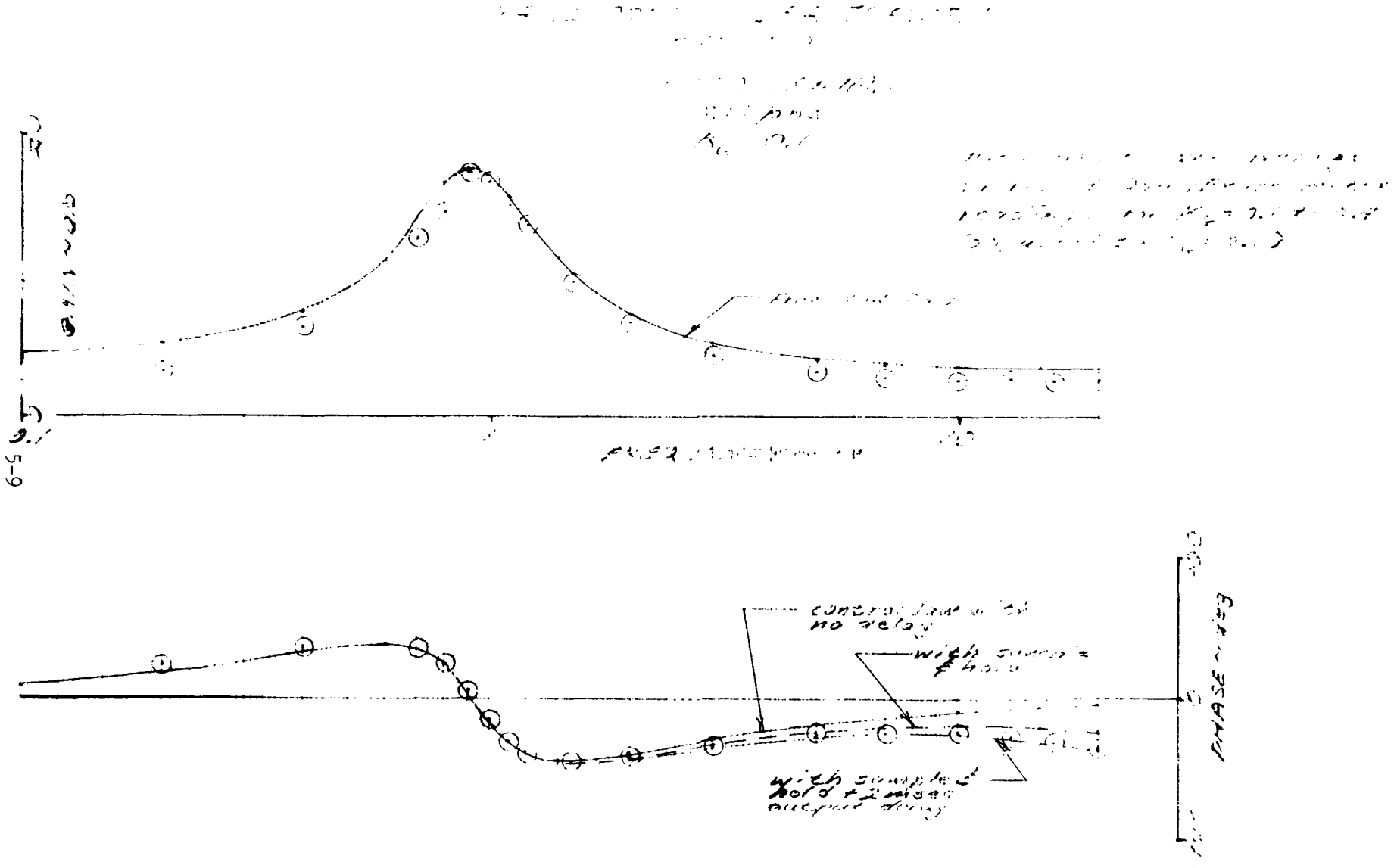

Figure 5-3

5.1.2 Digital RCS Operation

5.1.2.1 Power-Up

The digital RCS obtains power from the ship's 115 volt, 60 Hz, single-phase auxiliary power unit. Switch the front panel breaker to "ON". The RCS will illuminate and display the thumbwheel switch position. This indicates that power is on and that the system is ready to enter the self-check or operating mode. The display will flicker slightly which gives a visual indication of proper system power-up.

If possible, turn on the RCS prior to turning hydraulic power on and off. However, if this is not possible, ensure that no one is working on the vent valves prior to turning on and off RCS power with hydraulics running.

5.1.2.2 Self-Check

Prior to proceeding to the operating mode, the system should be sequenced through the self-check to ensure proper functioning of the hardware. Set the thumbwheel switches at "CL NO = 00" for entry of control law number "00". Press the ENTER pushbutton. Verify that the system responds by displaying "SELF CHECK OK". If this response is given, press the CLEAR pushbutton. This returns the system to the power-up mode and the display will flicker slightly.

If faults were detected during the self-check, the display will respond by displaying the fault number(s). The operator should then refer to Table 5-1 to identify the fault detected. After recording the number(s) of the fault(s) displayed, press the CLEAR pushbutton. If additional faults were detected, the system will display them. Continue to press the CLEAR pushbutton until all faults have been displayed and the system returns to the power-up mode.

5.1.2.3 Initialization

To initialize the digital RCS, place the desired VENT VALVE SELECT switches in the "ON" position. Select the desired control law (either "CL NO 01" or "CL NO 02".) using the thumbwheel switches and press the ENTER pushbutton. Select the desired vent valve bias using the thumbwheel switches and press the ENTER pushbutton. If no entry is made, the system will use a default value of 5% to prevent mechanical contact at the full closed position. The digital RCS smoothly sets the bias when a vent valve bias entry is made. It takes approximately 30 seconds for the vent valves to reach the commanded bias position. The craft may slow down or settle slightly during this period. If the speed loss is excessive, it will be necessary for the Ship Commander to increase the fan flow rate to compensate for dumping pressurized airflow overboard through the biased valves.

Table 5-1
Digital Ride Control System
Self-Check Diagnostics

Fault Number	Fault Description	RCS Card(s) Possibly Defective
1	Ram Memory Check Failed	40/41
2	9900 CPU Math Check Failed	3
3	No A/D's Started Conversion	39
4	A/D #1 Check Failed	38
5	A/D #2 Check Failed	37
6	A/D #3 Check Failed	36
7	A/D #4 Check Failed	35
8	MUX A/D Check Failed	34
9	9901 PSI I/O Check Failed	10
10	9901 PSI Timer Check Failed	10
11	9900 Interrupt Request Line Not Clear	3/10
12	D/A Check Failed	33
13	+5 Volts out of Range	Power Supply
14	-5 Volts out of Range	3
15	-15 Volts out of Range	Power Supply
16	+15 Volts out of Range	Power Supply
17	+28 Volts out of Range	Power Supply
18	±12 Volts out of Range	1/2
19	1010J MULT/ACCUM Check Failed	4

Select the desired limit using the thumbwheel switches and press the ENTER pushbutton. If no entry is made, the system will use a default value of 95% to prevent mechanical contact at the full open position. The RCS is now initialized for active control.

5.1.2.4 Active Control

Set the gain pot at the desired value and put the ACTIVE switch in the "ON" position. The RCS brings the gain up slowly, taking approximately 20 seconds for the full effectiveness of the RCS to be realized. If the operator sets a gain which is too high, the system will utilize the maximum value for the control law selected. This default value is equal to the gain limit for the selected control law. Once RCS operation has been initiated in this manner, it can be discontinued at any time by placing the ACTIVE switch in the "OFF" position. The system will bring the gain down slowly over a 20-second period. If it is necessary to discontinue active ride control and close the vent valves immediately, this can be done by placing the VENT VALVE SELECT switches in the "OFF" position.

!! Caution !!
When people are working on the vent valves, the VENT VALVE SELECT switches should never be moved from the "ON" position to the "OFF" position.

When the system is performing active ride control, the mean hydraulic pressure and cushion pressure can be displayed by selecting the appropriate thumbwheel switch position (PHYD or PC). Also, the standard deviation of cushion pressure and heave acceleration can be displayed by selecting the appropriate thumbwheel switch position (PC 1Σ or AZ 1Σ). It takes approximately 60 seconds for these values to stabilize after adjustments to the RCS or craft operating systems (propulsion and lift) have been made.

In the event that the RCS displays a warning message, the operator should press the CLEAR pushbutton. If the warning does not reappear, then it is likely that a false indication was received. However, if after pressing the CLEAR pushbutton one or more times the warning message is continually displayed, then it is likely a valid condition exists and the operator must take appropriate action. The warnings presently installed in the RCS are listed in Table 5-2.

Warnings 6, 7, 8 and 9 display SHDN which indicates a shutdown has occurred. This condition locks the vent valves at the bias position. The operator should then close the vent valves using either the thumbwheel switches (which close the vent valves slowly) or the VENT VALVE SELECT switches (which close the vent valves immediately). In order to restart the system after a shutdown, it is necessary to recycle power and enter the con trol law parameters again. If the system displays a warning which does not cause a shutdown, system operation will continue. It is advisable that active control be discontinued and the vent valves be closed until the warning can be properly investigated.

Table 5-2

Digital Ride Control System
Warning Messages

Message No.	Message	Description
1	PROG DELAY	Software Error Resulting in Processing Delay
2*	LOW HYD PR	Hydraulic Pressure less than 2000 psi
3*	BIAS SPRD	VV Bias Out of Range
4*	AMP SPRD	VV Amplitude Out of Range
5	MUX A/D	MUX A/D Failed During Conversion
6*	HYD SHDN	Hydraulic Pressure less than 1000 psi
7	TIMER SHDN	Control Law Cycle Timer Failed
8	A/D SHDN	Feedback A/D Failed During Conversion
9	CPU SHDN	CPU Attempted to Execute Invalid Instruction

* Not implemented for XR-1E testing.

5.1.3 Installation on the XR-1E

The digital RCS was mounted in the XR-1E Data Acquisition System (DAS) compartment on top of the instrumentation rack which houses the Data Logger and the Analog RCS. This location was selected because it simplified interconnection of the RCS with existing craft systems, e.g., the vent valves, the DAS and the Analog RCS. Figure 5-4 shows the cable interconnection between the digital RCS and these craft systems. Figures 5-5 and 5-6 show the wiring for the cables.

Prior to initiation of any testing it was necessary to adjust the actuator/LVDT linkages and calibrate the vent valve servo loops. This was accomplished by adjusting each linkage with hydraulic and electrical power on until the actual vent valve position matched the commanded vent valve bias. This adjustment was made at 5% bias and checked at 50% and 95% bias. It should be noted that this is the only adjustment required to make the digital RCS operational. There are no trim pots or scaling amplifiers in the digital RCS.

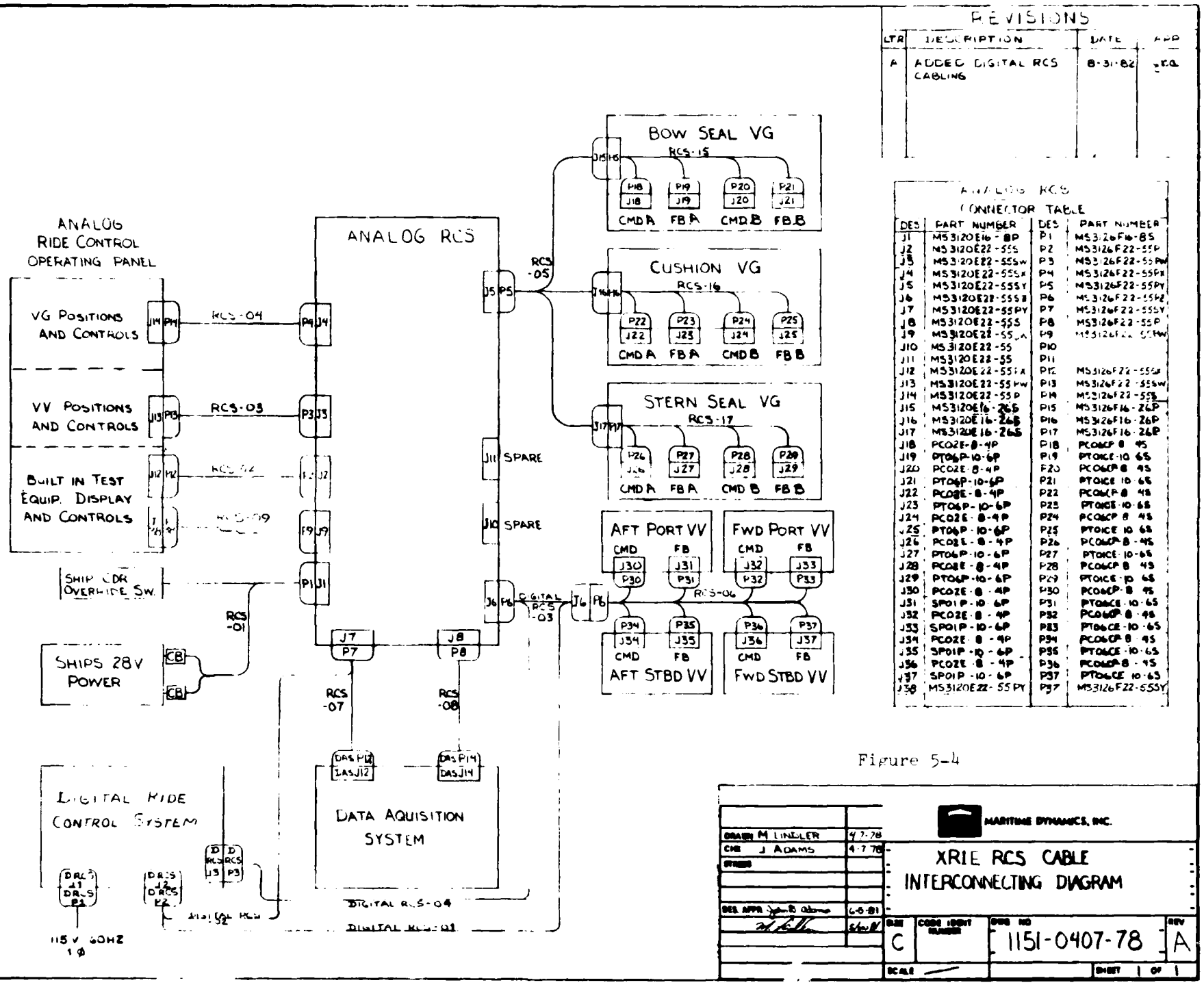

Figure 5-4

DRAWN M LINDLER	4-7-78	MARITIME DYNAMICS, INC.
CHK J ADAMS	4-7-78	XRIE RCS CABLE INTERCONNECTING DIAGRAM
ENGR		
DES APPR	6-8-81	
		SIZE C; CODE IDENT NUMBER; DWG NO 1151-0407-78; REV A
		SCALE; SHEET 1 OF 1

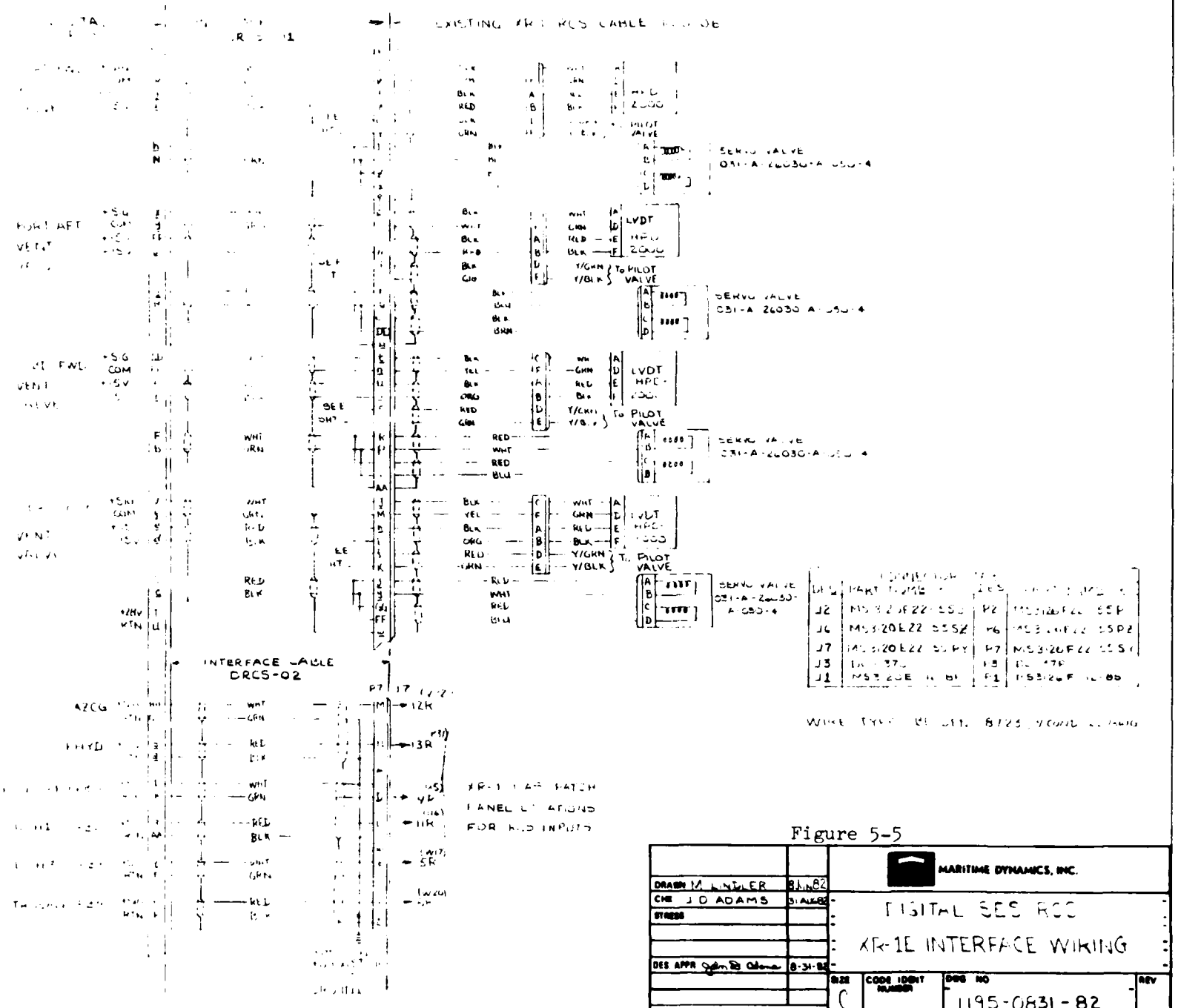

Figure 5-5

		MARITIME DYNAMICS, INC.
DRAWN M. KNEELER	8 JUN 82	
CHK J. D. ADAMS	31 AUG 82	DIGITAL SES RCS
STRESS		XR-1E INTERFACE WIRING
DES APPR	8-31-82	
SIZE C	CODE IDENT NUMBER	DWG NO 1195-0831-82 REV
SCALE		SHEET 1 OF 2

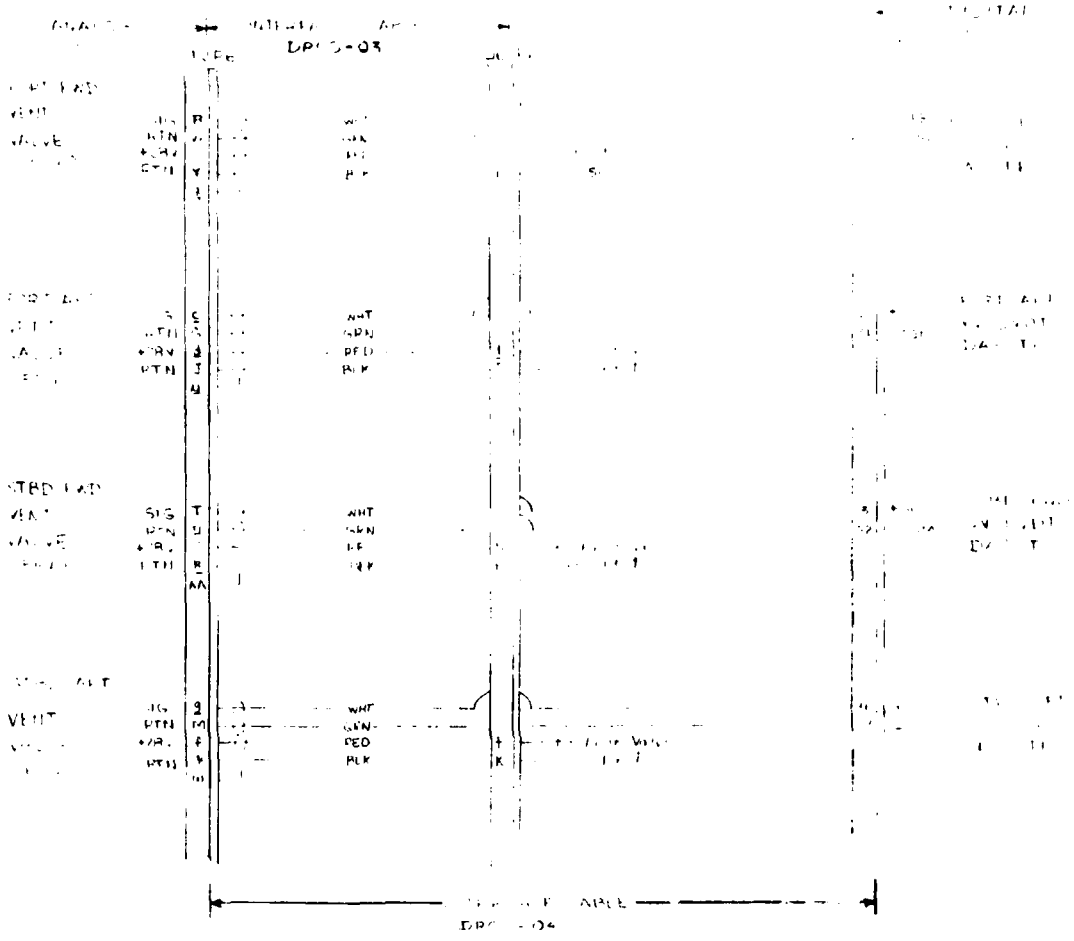

Figure 5-6

DRAWN J.D. ADAMS	9.2.82	MARITIME DYNAMICS, INC.
CHK		DIGITAL SES RCS
STRESS		XR-1E INTERFACE WIRING
DES APPR	9-2-82	
SIZE C	CODE IDENT NUMBER	DWG NO 1195-0831-82 REV
SCALE		SHEET 2 OF 2

5.2 TEST MISSIONS

Two types of tests were conducted to satisfy the test program objectives:

1. Open Loop Tests
2. Closed Loop Tests

The type of open loop tests discussed herein are standard practice in the development of feedback control systems. They are conducted by breaking the control loop at the feedback sensor (cushion pressure) input and inserting a sine wave generator at this point. These tests provide a straightforward means of checking the overall control system stability. In this case, the data was also used to compare the stability of the digital RCS with that of the previously developed analog RCS.

Closed loop tests are all-up tests of the digital RCS during craft operations in waves. In this program, the tests were conducted at Froude-scaled Sea Bird fan flow rates and speeds so the resultant data could be used to predict RCS performance on the Sea Bird Class. Both RCS-On and RCS-Off tests were run for comparison.

5.2.1 Open Loop Tests

Reference 2 describes in detail the test procedures, data reduction and analysis techniques used by MariDyne for RCS open loop testing. It is recommended that the reader review this reference in order to fully understand the material presented below.

During open loop testing the XR-1E was operated on-cushion while tethered in the SESTF syncrolift. The airflow is exhausted out the vent valves which makes the craft extremely stable. The control loop is broken and a sine wave generator is inserted in place of the cushion pressure feedback transducer. During testing, the generator drives the system at different amplitudes and frequencies which causes the vent valves to oscillate. The craft, in turn, responds by heaving. However, the heave amplitudes are limited such that the mooring lines do not affect the motions and the airflow cannot escape under the sidewalls and seals.

The open loop tests conducted had two principal objectives:

1. Verification of Digital RCS-Plus-Craft Open Loop Transfer Functions

2. Comparison of Digital RCS and Analog RCS Stability

The craft open loop responses were previously measured during tests of the analog RCS conducted on 3 January 1980. In order to satisfy test objectives, the craft was tested at exactly the same conditions (rpms, biases, frequencies, amplitudes, etc.) as those used for the 3 January tests.

Tables 5-3 and 5-4 list matrices of open loop tests completed for Control Laws 1 and 2, respectively. The table entries include fan speeds, vent valve bias, RCS gain and the test point duration at each frequency.

Figures 5-7 and 5-8 show the open loop gain and phase measured during tests of the analog RCS on 3 January 1980. Also shown are the predicted open loop gain and phase characteristics for Control Law 1. As shown, the digital sampling delays introduced reduce the predicted gain margin by approximately 5 db relative to the analog RCS. The ramifications of this are discussed in the next section.

5.2.2 Closed Loop Tests

As mentioned earlier, the primary purpose of the closed loop tests was to obtain data which could be used to predict RCS performance on the USCG Sea Bird Class SES. To accomplish this objective, the XR-1E was operated at Froude-scaled fan flow rates and speeds. As shown in Table 5-5, the XR-1E cushion dimensions approximate a 1/2-scale Sea Bird Class SES.

It is recognized that the test technique may be criticized for the following reasons:

1. The atmospheric pressure is not scaled as required for full dynamic similarity between the model (i.e., the XR-1E) and the full-scale craft (i.e., the Sea Bird).

2. The sidewalls and seals of the two craft are different. The XR-1E has thin sidewalls and is equipped with a transversely stiffened membrane (TSM) bow seal and a planing stern seal. Sea Bird SES have full displacement sidewalls and are equipped with finger bow seals and bag-type stern seals.

3. The lift air supply system and lift fan characteristics (i.e., the slope of the fan's pressure/flow curve) of the two craft are different.

Items 1 and 2 are not considered to be serious deficiencies in the test technique. Non-scaling of the atmospheric pressure means the XR-1E heave natural frequency is higher than desired. In this particular case, the scale ratio is so small ($\lambda = 2$) that the actual heave frequency (3.4 Hz) is only slightly greater than the frequency (2.8 Hz) required for full dynamic similarity.

Seals and sidewalls on an SES primarily serve to maintain the air cushion since over 90% of the lift is typically provided by the cushion. Since it is wave-induced fluctuations in cushion pressure which give rise to heave accelerations, it is not expected that seal and sidewall configuration differences play a significant role in the RCS's effectiveness.

TABLE 5-3

XR-1E Open Loop Hover Tests
Digital RCS - Control Law Number 1

Test Date 17 September 1982
Test Series I
RCS Gain 0.1
CL No. 01
Bow & Stern Seals Full Down

VV Bias 60% (3 VV's)
VG Bias 50%
Bow Fan Speed 3232
Stern Fan Speed 2570
Relief Valves Full Open

Test Point	Test Frequency	Test Point Start	Test Point Stop	(Sec.) ΔT	Gain (db)	Phase (deg)
1	0.0	10:07:45	10:08:45	60		
2	0.2	10:09:40	10:11:20	100		
3	0.4	10:11:35	10:12:25	50		
4	0.6	10:13:10	10:13:40	30		
5	0.8	10:14:20	10:14:50	30		
6	1.0	10:15:15	10:15:35	20		
7	1.4	10:16:00	10:16:20	20		
8	2.0	10:16:50	10:17:00	10		
9	2.4	10:17:25	10:17:35	10		
10	3.0	10:18:00	10:18:10	10		
11	3.2	10:18:25	10:18:35	10		
12	3.4	10:18:55	10:19:05	10		
13	3.6	10:19:20	10:19:30	10		
14	3.8	10:19:50	10:20:00	10		
15	4.0	10:20:25	10:20:30	5		
16	6.0	10:21:00	10:21:05	5		
17	7.0	10:21:35	10:21:40	5		
18	8.0	10:24:05	10:24:08			
19	9.0	10:24:35	10:24:38	3		
20	10.0	10:25:05	10:25:08	3		
21	11.0	10:25:30	10:25:33	3		
22	12.0	10:25:50	10:25:53	3		
23	13.0	10:25:05	10:26:07	2		
24	14.0	10:25:20	10:26:22	2		
25	15.0	10:26:35	10:26:37	2		
26	16.0	10:26:50	10:26:52	2		
27	17.0	10:27:12	10:27:14	2		
28	18.0	10:27:35	10:27:37	2		
29	19.0	10:27:45	10:27:47	4		
30	20.0	10:28:20	10:28:22	2		
31	0.0	10:29:10	10:30:10	60		

TABLE 5-4

XR-1E Open Loop Hover Tests
Digital RCS - Control Law Number 2

Test Date 17 September 1982
Test Series II
RCS Gain 0.1
CL No. 01
Bow & Stern Seals Full Down

VV Bias 60% (3 VV's)
VG Bias 50%
Bow Fan Speed 3232
Stern Fan Speed 2570
Relief Valves Full Open

Test Point	Test Frequency	Test Point Start	Test Point Stop	(Sec.) ΔT	Gain (db)	Phase (deg)
32	0.0	10:33:20	10:34:20	60		
33	0.2	10:34:55	10:36:35	100		
34	0.4	10:36:55	10:37:45	50		
35	0.6	10:38:20	10:38:50	30		
36	0.8	10:39:15	10:39:45	30		
37	1.0	10:40:10	10:40:30	20		
38	1.4	10:41:00	10:41:20	20		
39	2.0	10:41:45	10:41:55	10		
40	2.4	10:42:25	10:42:35	10		
41	3.0	10:43:00	10:43:10	10		
42	3.2	10:43:35	10:43:45	10		
43	3.4	10:44:05	10:44:15	10		
44	3.6	10:44:45	10:44:55	10		
45	3.8	10:45:15	10:45:25	10		
46	4.0	10:45:45	10:45:50	5		
47	6.0	10:46:10	10:46:15	5		
48	7.0	10:46:30	10:46:35	5		
49	8.0	10:47:00	10:47:03	3		
50	9.0	10:47:30	10:47:33	3		
51	10.0	10:47:55	10:47:58	3		
52	11.0	10:48:15	10:48:18	3		
53	12.0	10:48:35	10:48:38	3		
54	13.0	10:48:55	10:48:57	2		
55	14.0	10:49:20	10:49:22	2		
56	15.0	10:49:40	10:49:42	2		
57	16.0	10:50:00	10:50:02	2		
58	17.0	10:50:20	10:50:22	2		
59	18.0	10:50:45	10:50:47	2		
60	19.0	10:51:10	10:51:12	2		
61	20.0	10:51:30	10:51:32	2		
62	0.0	10:52:20	10:53:20	60		

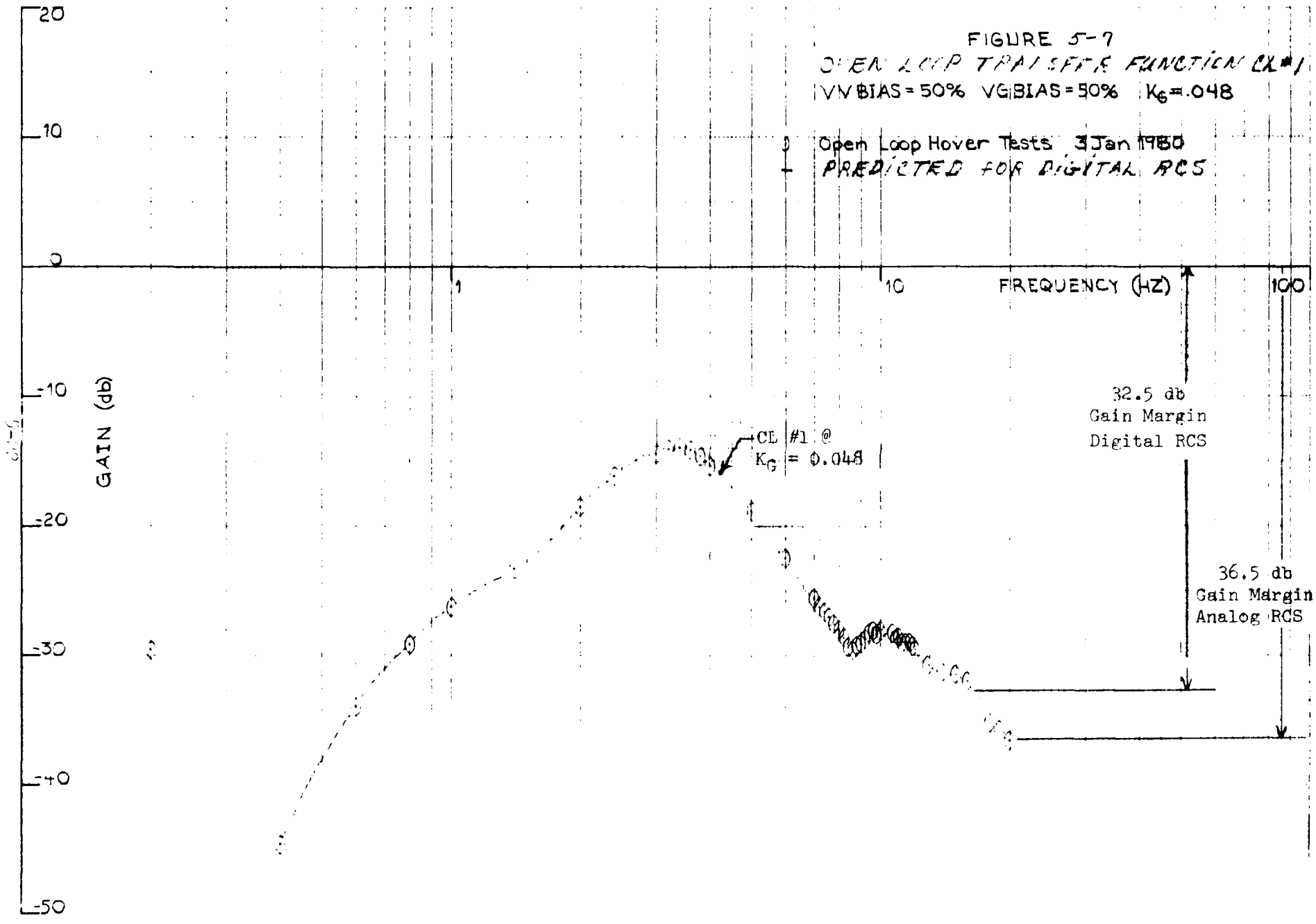
FIGURE 5-7
OPEN LOOP TRANSFER FUNCTION CL #1
VV BIAS = 50% VG BIAS = 50% K_G = .048
Open Loop Hover Tests 3 Jan 1980
PREDICTED FOR DIGITAL RCS
20
10
0
-10
-20
-30
-40
-50
GAIN (db)
1
10
100
FREQUENCY (HZ)
CL #1 @
K_G = 0.048
32.5 db
Gain Margin
Digital RCS
36.5 db
Gain Margin
Analog RCS

FIGURE 5-8

VVBIAS=50% VGBIAS=50% K_G=.048

◊ Open Loop Hover Tests 3 Jan 1980 ANALOG RCS

— PREDICTED FOR DIGITAL RCS

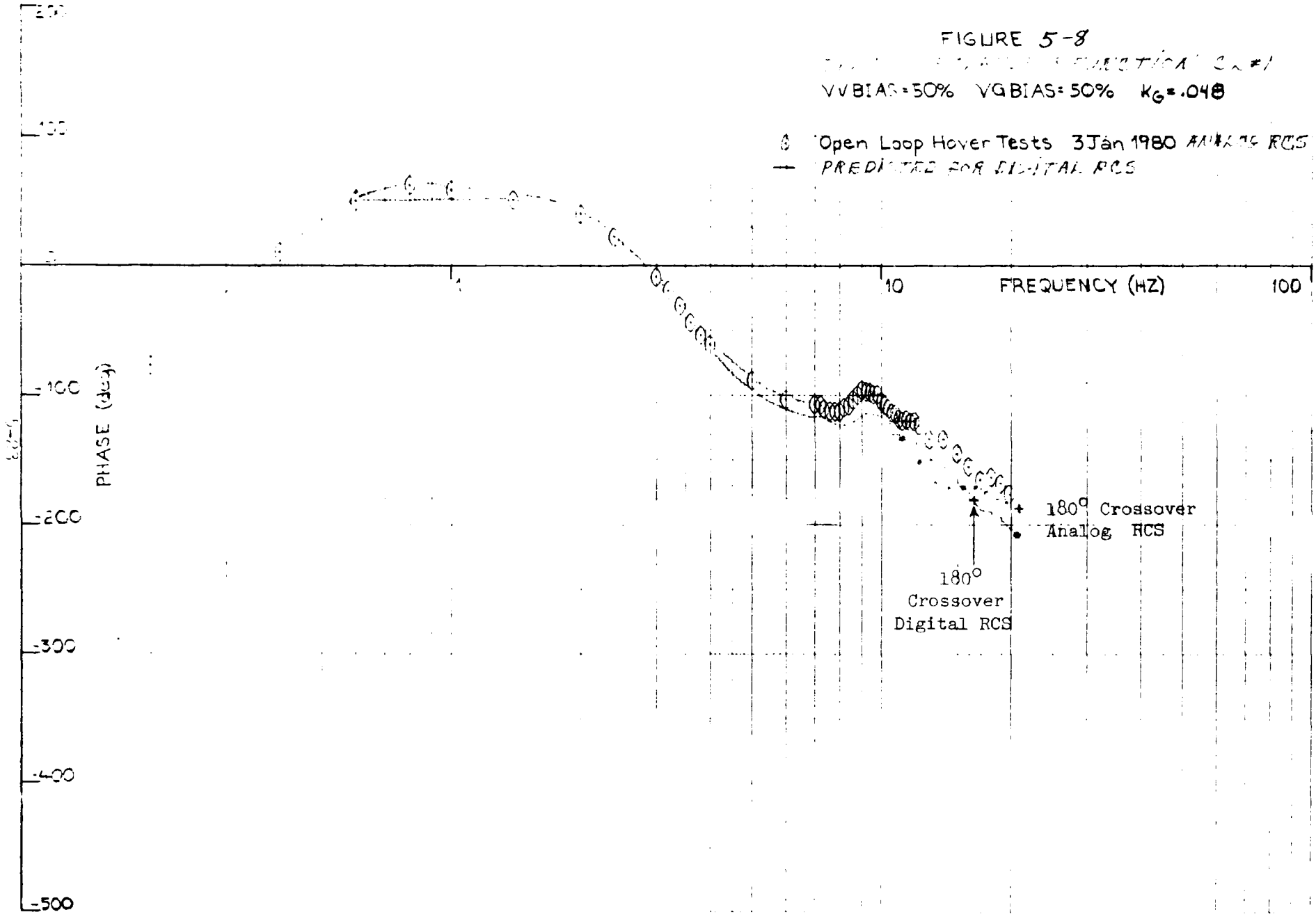

TABLE 5-5

Comparison of XR-1E and Sea Bird
Principal Characteristics

Parameter	Units	XR-1E	BH-110	Froude Scale Ratio
Displacement, Δ	lb	52,000	313,600	1.8
Cushion Length, l_c	ft	40	83.3	2.1
Cushion Beam, b_c	ft	15	31.6	2.1
Cushion Area, A_c	sq.ft	600	2,632	2.1
Loading $P_c/\sqrt{A_c}$	lb/cu.ft	2.9	2.1	-
Cushion Height:				
a. Bow	ft	3.25	7.5	2.3
b. Stern	ft	3.25	5.0	1.5
Flow Rate, Q_c	cfs	370*	2,100	2.0
Cushion Pressure, P_c	psf	67	110	1.6

*Flow rate selected for closed loop tests
Maximum XR-1E flow rate exceeds 1200 cfs

Proper modeling of the lift fan's pressure/flow curve is important because this parameter influences damping of the heave mode. Damping to a large extent determines the severity of the RCS-OFF heave acceleration. Since the fan slope is not properly scaled, we would not expect the RCS-OFF heave acceleration levels for the XR-1E and the Sea Bird to be identical for a given set of operating conditions.

The cushion dimensions (length, beam, height), the operating conditions (displacement, lift flow rate, speed) and the environment (wave heights, periods) are Froude scaled. Therefore, we would expect that the percent reduction in heave acceleration relative to RCS-OFF levels measured on the XR-1E could also be obtained on the Sea Bird. This is all that is of interest because there is an adequate data base on the Sea-Bird heave acceleration without ride control from USCG and USN tests (References 5, 6 and 7). By reducing these RCS-OFF levels by the percent reduction measured during the XR-1E tests, it will be possible to make RCS-ON preductions for the Sea Bird Class SES.

The closed loop tests were run at XR-1E speeds of 14 - 17 kts and 19 - 22 kts in head seas. These speed ranges correspond to 20 - 24 kts and 27 - 31 kts on the Sea Bird and cover the range of cushionborne operations for which ride control would be needed.

The testing was initiated by establishing the heading, fan rpms and ship speed. Then a one (1) minute RCS-OFF data point was recorded. Next the vent valve bias and RCS gain were set and a one (1) minute RCS-ON data point was recorded. This was followed by a second one (1) minute RCS-OFF data point. No adjustments to lift or propulsion power were made after the initial settings were established. It would have been desirable to run longer test points, but this was not considered feasible because the seas in Chesapeake Bay rarely remain stationary and it was desirable to keep the craft close to the Wave Rider Buoy.

Each RCS-ON data point recorded was run at a progressively larger vent valve bias to systemmatically investigate RCS effectiveness and power requirements. The RCS power is equivalent to the change in speed that results from dumping pressurized air overboard through the vent valves.

The test conditions and technique are significantly different from those used to test the Analog RCS during the XR-1D RCS Program (see References 1 and 2). The speeds and fan flows were higher in the Analog RCS tests because the intent was to model USN 3KSES design conditions. The XR-1D test technique was also different because the fan flow was increased to compensate for the mean flow rate exhausted through the valves. When this technique is employed, ship speed usually remains constant and the RCS power is equivalent to the increase in fan horsepower. This technique was not employed in the XR-1E tests because the intent was to model the Sea Bird SES. The Sea Bird does not have significant excess fan capacity and therefore the best technique is to measure the RCS power requirement in terms of the associated speed change.

Missions 345, 346 and 348 conducted on 27 September, 30 September and 8 October 1982, respectively, were devoted to closed loop tests of the digital RCS. Tables 5-6, 5-7 and 5-8 list the tests completed during these missions. All RCS-ON tests were conducted using Control Law Number 2 since it maintains a higher gain over the wave encounter frequency range than Control Law Number 1 (see Section 5.1.1). The overall RCS gain was set at the maximum value used for the Analog RCS (see Reference 1). The test program was intended to cover Sea State I, II and III conditions (equivalent Sea States II-IV for the Sea Bird). However, SESTF terminated testing without getting Sea State III coverage because of schedule commitments on the SES-200.

TABLE 5-6
XR-1E MISSION 345
TEST CONDITIONS

TEST POINT	TEST CONDITION/REMARKS	BOW FAN RPM	STERN FAN RPM	VG BIAS	VV BIAS	RCS GAIN	DATA ON	DATA OFF
1	RCS OFF	2800	2800	50%	0%	OFF	11:02:15	11:04:15
2	RCS ON/Two VVs	2800	2800	50%	5%	1.0	11:05:45	11:07:45
3	RCS OFF	2800	2800	50%	0%	OFF	11:23:45	11:25:45
4	RCS ON/Two VVs	2800	2800	50%	10%	1.0	11:[illegible]	11:[illegible]
5	RCS OFF	2800	2800	50%	0%	OFF	11:43:00	11:45:00
6	RCS ON/Two VVs	2800	2800	50%	15%	1.0	11:46:00	11:48:00
7	RCS OFF	2800	2800	50%	0%	OFF	11:59:00	12:01:00
8	RCS ON/Two VVs	2800	2800	50%	20%	1.0	12:02:00	12:04:00
9	RCS OFF	2800	2800	50%	0%	OFF	12:17:00	12:19:00
10	RCS ON/Two VVs	2800	2800	50%	25%	1.0	12:20:00	12:22:00
11	RCS OFF	2800	2800	50%	0%	OFF	12:33:00	12:35:00
12	RCS ON/Two VVs	2800	2800	50%	30%	1.0	12:37:00	12:39:00
13	RCS OFF	2800	2800	50%	0%	OFF	12:50:00	12:52:00
14	RCS ON/Two VVs	2800	2800	50%	35%	1.0	12:54:00	12:56:00
15	RCS OFF	2800	2800	50%	0%	OFF	13:08:00	13:10:00
16	RCS ON/Two VVs	2800	2800	50%	40%	1.0	13:11:00	13:13:00

TABLE 5-7
XR-LF MISSION 5A
TEST CONDITIONS

TEST POINT	TEST CONDITIONS/REMARKS	ROW FAN RPM	STBD FAN RPM	VI BIAS	VV BIAS	RCS GAIN	DATA ON	DATA OFF
1	RCS OFF	2800	2800	50%	0%	OFF	11:28:10	11:30:10
2	RCS ON/Two VVs	2800	2800	50%	5%	1.0	11:31:45	11:33:45
3	RCS OFF	2800	2800	50%	0%	OFF	11:34:15	11:36:15
4	RCS ON/Two VVs	2800	2800	50%	10%	1.0	11:37:30	11:39:30
5	RCS OFF	2800	2800	50%	0%	OFF	11:55:00	11:57:00
6	RCS ON/Two VVs	2800	2800	50%	15%	1.0	[illegible]	11:59:45
7	RCS OFF	2800	2800	50%	0%	OFF	12:00:30	12:02:30
8	RCS ON/Two VVs	2800	2800	50%	20%	1.0	12:03:15	12:05:15
9	RCS OFF	2800	2800	50%	0%	OFF	12:05:45	12:07:45
10	RCS ON/Two VVs	2800	2800	50%	25%	1.0	12:08:30	12:10:30
11	RCS OFF	2800	2800	50%	0%	OFF	12:27:30	12:29:30
12	RCS ON/Two VVs	2800	2800	50%	30%	1.0	12:30:30	12:32:30
13	RCS OFF	2800	2800	50%	0%	OFF	12:33:00	12:35:00
14	RCS ON/Two VVs	2800	2800	50%	35%	1.0	12:36:00	12:38:00
15	RCS OFF	2800	2800	50%	0%	OFF	12:38:30	12:40:30
16	RCS ON/Two VVs	2800	2800	50%	40%	1.0	12:41:30	12:43:30
17	RCS OFF	2800	2800	50%	0%	OFF	13:01:00	13:03:00
18	RCS ON/Two VVs	*2700	2800	50%	45%	1.0	13:04:00	13:06:00
19	RCS OFF	2800	2800	50%	0%	OFF	13.06:45	13:08:45
20	RCS ON/Two VVs	2700	2800	50%	50%	1.0	13:10:00	13:12:00
21	RCS OFF	2800	2800	50%	0%	OFF	13:12:30	13:14:30

---

* Forward lift engine RPM decreased as VV Bias increased.

TABLE 5-8
XR-1E MISSION 348
TEST CONDITIONS

TEST POINT	TEST CONDITION REMARKS	BOW FAN RPM	STERN FAN RPM	VG BIAS	VV BIAS	RCS GAIN	DATA ON	DATA OFF
1	RCS OFF	2800	2800	50%	0%	OFF	11:03:30	11:05:30
2	RCS ON/Two VVs	2800	2800	50%	5%	1.0	11:06:30	11:08:30
3	RCS OFF	2800	2800	50%	0%	OFF	11:12:45	11:14:45
4	RCS ON/Two VVs	2800	2800	50%	35%	1.0	11:16:00	11:18:00
5	RCS OFF	2800	2800	50%	0%	OFF	11:20:00	11:22:00
6	RCS ON/Three VVs	2800	2800	50%	5%	1.0	11:23:00	11:25:00
7	RCS OFF	2800	2800	50%	0%	OFF	11:47:00	11:49:00
8	RCS ON/Two VVs	3100	2800	50%	35%	1.0	11:52:30	11:54:30
9	RCS OFF	2800	2800	50%	0%	OFF	11:56:45	11:58:45
10	RCS OFF	3100	2800	50%	25%	1.0	12:00:45	12:02:45
11	RCS OFF	2800	2800	50%	0%	OFF	12:22:00	12:24:00
12	RCS ON/Three VVs	3400	3000	50%	40%	1.0	12:28:00	12:30:00
13	RCS OFF	2800	2800	50%	0%	OFF	12:31:30	12:33:30
14	RCS ON/Two VVs	2800	2800	50%	5%	1.0	12:34:30	12:36:30
15	RCS OFF	2800	2800	50%	0%	OFF	12:39:15	12:41:15
16	RCS OFF	3100	2800	50%	0%	OFF	12:44:00	12:46:00
17	RCS ON/Two VVs	3100	2800	50%	5%	1.0	12:47:15	12:49:15
18	RCS ON/Three VVs	3100	2800	50%	5%	1.0	12:49:45	12:51:45

5.3 DATA ACQUISITION SYSTEM

When the Analog RCS was tested on the XR-1D, a new Data Acquisition System (DAS) was designed and installed on the testcraft by SESTF and Mari-Dyne personnel. This system was also used to measure and record craft parameters during testing of the digital RCS.

The DAS (Figure 5-9) utilizes PCM multiplexing to record 72 main frame and 20 sub-frame measurements on magnetic tape. Main frame measurements (accelerations, cushion and seal pressures) are filtered using 40 Hz low pass Butterworth filters and recorded on tape at 200 pps. Sub-frame measurements (torques, rpms, angles, rates) are filtered at 20 Hz and recorded at 100 pps. The low pass filters prevent aliasing high frequency noise into the data band during PCM multiplexing or subsequent digitizing of the data. A more complete description of the DAS is given in Reference 1.

The list of measurements continuously recorded during digital RCS testing is given in Table 5-9. Prior to the initiation of testing, SESTF recalibrated the critical measurements (i.e., the pressures, accelerometers and vent valve positions).

Wave height was measured by a Datawell Wave Rider Buoy during all closed loop tests. The buoy signal was transmitted to a receiver located on a 26 ft Bertram which is used to support test operations. The receiver output is recorded on an FM recorder and on a two (2)-channel strip chart for quick-look analysis of the sea state during testing.

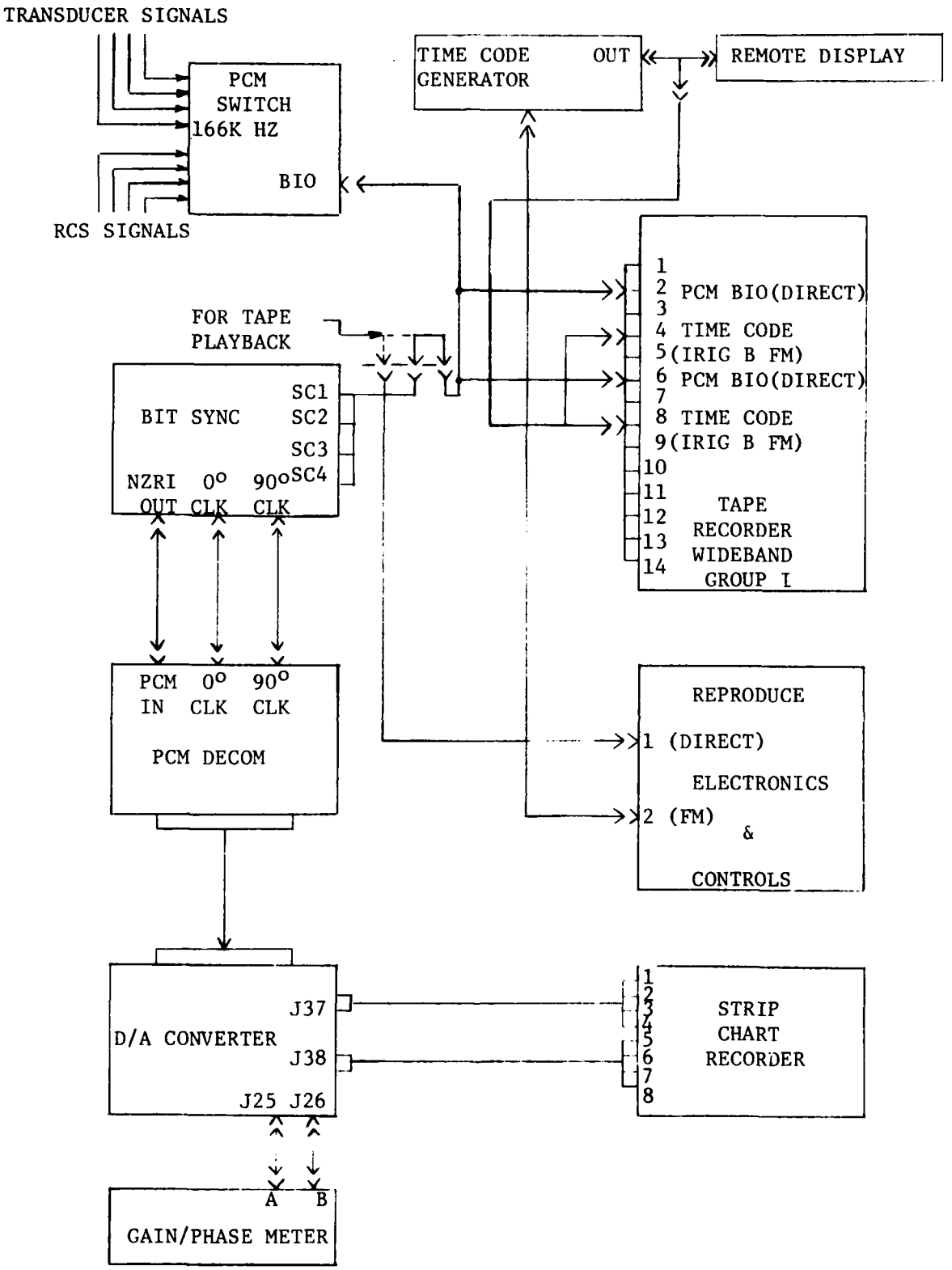

Figure 5-9 XR-1E Data Acquisition System Block Diagram

Table 5-9
XR-1E MEASUREMENT LIST
FOR
DIGITAL RIDE CONTROL SYSTEM TESTS

PCM/DATALOGGER CHANNEL NUMBER	MNEUMONIC	MEASUREMENT DESCRIPTION	DAS RANGE
P-01-0			
P-02-0			
P-03-0	X11/25	Parasol Batten 1 Acceleration	±250 G's
P-04-0			
P-05-0	X21/51	Parasol Batten 2	±250 G's
P-06-0			
P-07-0			
P-08-0			
P-09-0	BVGPOSA	Bow VG Sleeve Position, Side A	0-100%
P-10-0	BVGPOSB	Bow VG Sleeve Position, Side B	0-100%
P-11-0	CVGPOSA	Cushion VG Sleeve Position, Side A	0-100%
P-12-0	CVGPOSB	Cushion VG Sleeve Position, Side B	0-100%
P-13-0	SVGPOSA	Stern VG Sleeve Position, Side A	0-100%
P-14-0	SVGPOSB	Stern VG Sleeve Position, Side B	0-100%
P-15-0	FVVPOSP	FWD VV Effective Area, Port Side	0-1.5 ft^2
P-16-0	FVVPOSS	FWD VV Effective Area, STBD Side	0-1.5 ft^2
P-17-0			
P-18-0			
P-19-0	BVGCL	Bow VG Control Law Output	±10 v.
P-20-0	CVGCL	Cushion VG Control Law Output	±10 v.
P-21-0	SVGCL	Stern VG Control Law Output	±10 v.
P-22-0	PVVCL	Port VV Control Law Output	±10 v.
P-23-0	SVVCL	STBD VV Control Law Output	±10 v.
P-24-0	FUNGEN	Test Function Generator	±10 v.
P-25-0	AVVPOSP	Aft VV Effective Area, Port Side	0-1.5 ft^2
P-26-0	AVVPOSS	Aft VV Effective Area, STBD Side	0-1.5 ft^2
P-27-0/1	BOWFANSP	Bow Fan Exit Static Pressure	0-200 psf
P-28-0/2	CUSFANSP	Cushion Fan Exit Static Pressure	0-200 psf
P-29-0/3	STRFANSP	Stern Fan Exit Static Pressure	0-200 psf
P-30-0/4	BOWSEALP	Bow Seal Pressure, Port	0-200 psf
P-31-0/5	BOWSEALS	Bow Seal Pressure, STBD	0-200 psf
P-32-0/6	CUSH1	FWD Cushion Pressure, Port	0-144 psf
P-33-0/7	CUSH2	FWD Cushion Pressure, STBD	0-200 psf
P-34-0/8	CUSH3	Mid Cushion Pressure, Port	0-200 psf
P-35-0/9	CUSH4	Mid Cushion Pressure, STBD	0-200 psf
P-36-0/10	CUSH5	Aft Cushion Presusre, Port	0-200 psf
P-37-0/11	CUSH6	Aft Cushion Pressure, STBD	0-200 psf
P-39-0/12	STRSEALP	Stern Seal Pressure, Port	0-200 psf
P-40-0/13	STRSEALS	Stern Seal Pressure, STBD	0-200 psf
P-41-0			
P-42-0			
P-44-0/15	AZCG	Vertical Acceleration, CG	-1 to +3 G's
P-45-0/16	AZSTR	Vertical Acceleration, Stern	
P-46-0			
P-47-0/17	AYCG	Lateral Acceleration, CG	±1 G
P-48-0/18	AXCG	Longitudinal Acceleration, CG	±1 G
P-49-0			
P-50-0	X13	TFG	0-5 v.
P-51-0			
P-52-0/50	CUSFANTQ	Cushion Fan Torque	0-250 ft-lb
P-53-0/25	X14	Parasol Geometry Strap #3 Tension	0-1400 lb
P-54-0/26	X15	Retract Strap #3 Tension	0-1400 lb
P-55-0/27	X16	Retract Strap #4 Tension	0-1400 lb
P-56-0			
P-57-0/23	PNZSTATP	Port Nozzle Discharge Static Press.	0-100 psi
P-58-0	X3		
P-59-0	X4		
P-60-0	X5		
P-61-0	X6		
P-62-0	X7		
P-63-0	X8		
P-64-0	X9		
P-65-0/28	PNZSTATS	STBD Nozzle Discharge Static Press.	0-1400 lb
P-68-0/40	SGT	Parasol Geometry Strap #4 Tension	0-1400 lb
P-69-1/29	PITCH	Pitch Attitude	±10°
P-70-1/30	ROLL	Roll Attitude	±10°
P-71-1/31	PITRATE	Pitch Rate	±20°/sec.
P-72-0/32	ROLLRATE	Roll Rate	±20°/sec.
P-73-1/33	YAWRATE	Yaw Rate	±20°/sec.
P-74-1/34	NOZP	Port Nozzle Angle	±35°
P-75-1/35	NOZS	STBD Nozzle Angle	±35°
P-76-1/35	BSACTPOS	Bow Seal Actuator Position	0-100%
P-77-1			
P-78-1			
P-79-1			
P-80-1			
P-81-2/35	BOERPM	Boeing Turbine N2 RPM	0-5k RPM
P-82-2/39	SFANRPM	Stern Fan Speed	0-5k RPM
P-83-2			
P-84-2			
P-85-2/42	PPUMPRPM	Port Pump RPM	0-2857 RPM
P-86-2/43	SPUMPRPM	STBD Pump RPM	0-2857 RPM
P-87-2/44	PPUMPTQ	Port Pump Torque	0-15k ft-lb
P-88-2/45	SPUMPTQ	STBD Pump Torque	0-15k ft-lb
P-89-2	EVENT	Event Marker	-5 v.
P-90-2/47	PHYD	Hydraulic System Pressure	0-4k psi
P-91-2/48	PITOTP	Port Pitot Pressure	0-30 psi
P-92-2/49	PITOTS	STBD Pitot Pressure	0-30 psi

5.4 DATA REDUCTION

Data recorded on magnetic tape was digitized on the NATC Real-Time Processing System (RTPS) and then reduced by SESTF on their PDP-11 computer. Figure 5-10 shows the types of data that were supplied to MariDyne for the open and closed loop tests conducted.

5.4.1 Open Loop Test Data Reduction

Means, standard deviations and Fourier Series Coefficients for selected measurements were reduced from the open loop test data. The principal quantities of interest were the Fourier Series Coefficients which were obtained by deriving the Cs and ϕs of the following series for each measurement and test condition:

$$x(t) = C_o + C_1 \sin(2\pi wt + \phi_1) + C_2 \sin(2\pi wt + \phi_2) + C_3 \sin(2\pi wt + \phi_3)$$

The procedures employed by SESTF to derive these coefficients from sinusoidal open loop test data are documented in Reference 8. Phases (ϕ_1, ϕ_2 and ϕ_3) were all adjusted relative to the fundamental frequency of the sine wave generator which served as the input or driving signal for the open loop tests. The coefficients C_1 and ϕ_1 were used to obtain the gain and phase of the transfer function for each channel.

5.4.2 Closed Loop Test Data Reduction

Means, standard deviations, power spectra and 1/3 octave band data for selected measurements were reduced from the closed loop test data. The mean values and standard deviations were computed using all samples recorded during each 60-second test point, i.e., the data were not decimated.

Power spectra were computed by applying the following processing parameters to each test segment:

Record Length	T_R = 50 sec
Bandwidth	β_e = 0.2 Hz
Sampling Interval	Δ_t = 0.01 sec
Nyquist Frequency	f_c = 50 Hz

It should be noted that the short test points and small bandwidth result in a ±22% standard ordinate error. This results in a fairly large spread in the 90% confidence bounds of the power spectra. Unfortunately it was not considered feasible to run longer test points because the seas rarely remain

Figure 5-10
Data Reduction Chart
Digital RCS Tests on XR-1E SES

Measurement	Open Loop Tests					Closed Loop Tests			
	Means & Std. Dev.	Fourier Series Coeff.	Power Spectra	Histograms	1/3 Octave Band	Means & Std. Dev.	Power Spectra	Histograms	1/3 Octave Band
Accelerations	X	X				X	X		X
Attitude Gyros	X					X	X		
Fan Pressures	X					X			
Hydraulic Pressure	X					X			
Seal & Cushion Pressures	X	X				X	X		
Rate Gyros	X					X			
RPMs	X					X			
Speed						X			
Torques	X					X			
Vent Valve Positions	X	X				X	X		
VG Fan Positions	X					X			
Wave Rider Buoy						X	X		
WJ Nozzle Position						X			
WJ Nozzle Pressure						X			

spatially consistent in the Chesapeake Bay. Also, it was not possible to relax the 0.2 Hz bandwidth requirements because the acceleration and pressure spectra have sharp peaks which would lose definition.

The 1/3 octave band data were reduced over the same 50-second interval as the power spectra. The primary reason for obtaining this information was to compare it with habitability criteria which are presented in the 1/3 octave format.

Wave height information recorded on the FM tape recorder was also digitized and processed. Power spectra were computed for time segments during which the RCS tests were conducted. The following processing parameters were used:

Record length	T_R = 500 sec.
Bandwidth	β_e = 0.04 Hz
Sampling Interval	ΔT = 0.10 sec.
Nyquist Frequency	f_c = 5 Hz

The standard ordinate error of each spectra computed is $\pm 22\%$. Each time segment was selected to cover 2 or 3 of the one (1) minute RCS test points.

6. DIGITAL RCS PERFORMANCE ON XR-1E SES

This section is devoted to presenting and analyzing the test results in terms of the XR-1E SES. The section which follows will then apply the test results to the Sea Bird Class SES for purposes of making RCS performance predictions.

6.1 STABILITY

6.1.1 Comparision of Measured and Predicted Stability

Figure 6-1 shows the measured and predicted gain and phase from the open loop tests of Control Law 1 summarized in Table 5-3. Figure 6-2 shows similar data for Control Law 2 tests listed in Table 5-4.

Mean values of primary parameters for these tests are shown below along with similar data from open loop tests of the analog RCS.

Parameter	Digital RCS Tests 17 September '82	Analog RCS Tests 3 January 1980
Bow Fan Speed	3232 rpm	3155 rpm
Cushion Fan Speed	2815 rpm	2748 rpm
Stern Fan Speed	2570 rpm	2615 rpm
Bow Seal Pressure	72.4 psf	65.3 psf
Cushion Pressure	61.4 psf	60.8 psf
Stern Seal Pressure	65.3 psf	65.3 psf
Vent Valve Bias	60% (3 VVs)	50% (4 VVs)
Total Fan Flow Rate	525 cfs	570 cfs

The mean values of the two data sets are in close agreement which means a good comparison of digital and analog RCS stability should be possible. However, there is a difference in the number of vent valves used for the tests. During the digital RCS open loop tests, one vent valve was inoperative due to a failed louver shaft bushing. Therefore the tests were conducted by using three valves and adjusting the bias to obtain the same total flow rate used in the analog RCS tests. This difference is not significant since the mean operating conditions are the same.

As illustrated in Figure 6-1, the measured gain and phase for Control Law 1 are in good agreement with the predictions. The gain is slightly higher (approximately 3 db) in the low frequency end and also in the region above 10 Hz where the acoustic modes are important. The phase angle data (which are considered most important for RCS design purposes) compare very closely even in the range of the acoustic frequencies. In view of the fact that the phase data agrees so well, the differences in the measured and predicted open loop gain are not considered serious.

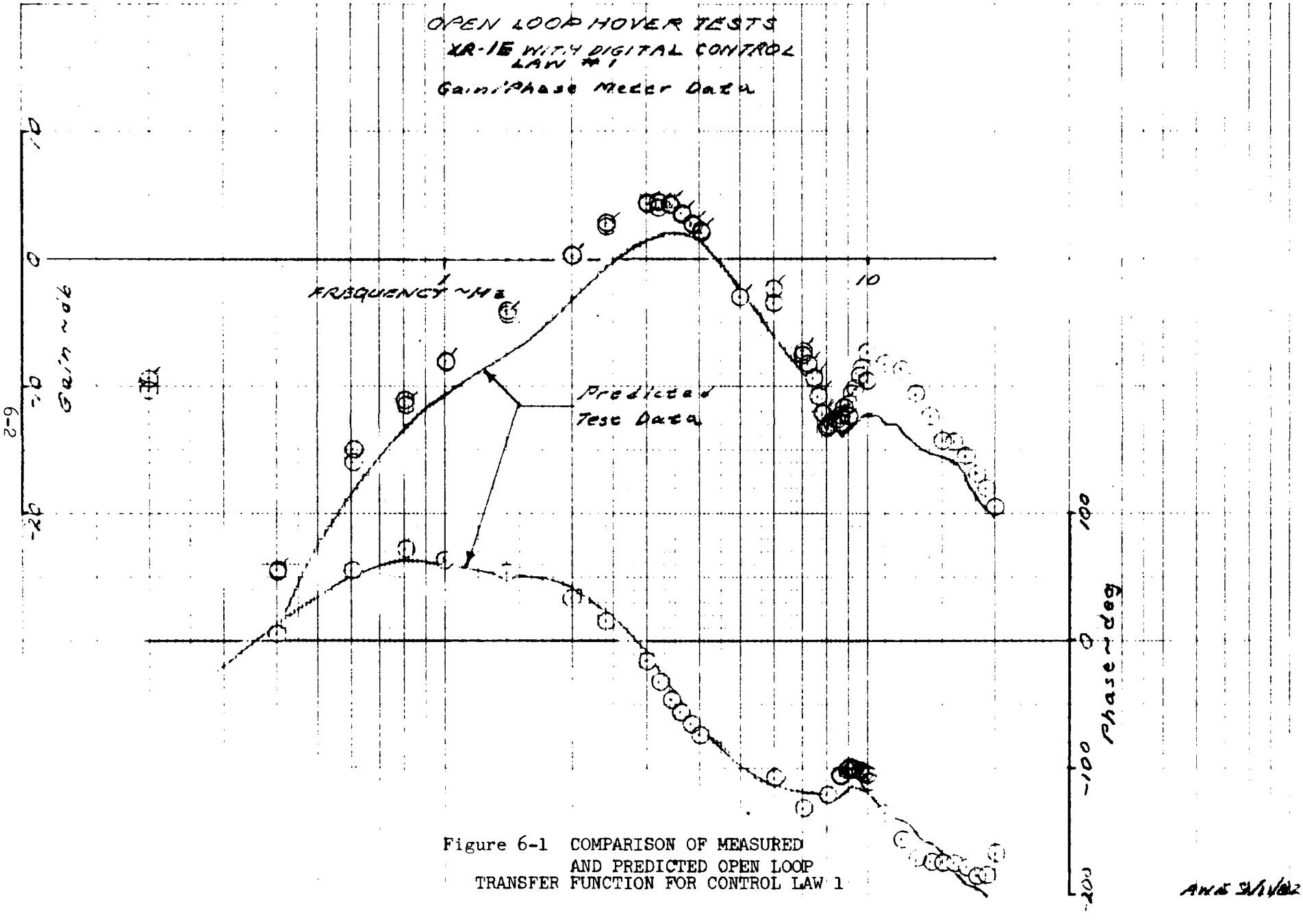

Figure 6-1 COMPARISON OF MEASURED AND PREDICTED OPEN LOOP TRANSFER FUNCTION FOR CONTROL LAW 1

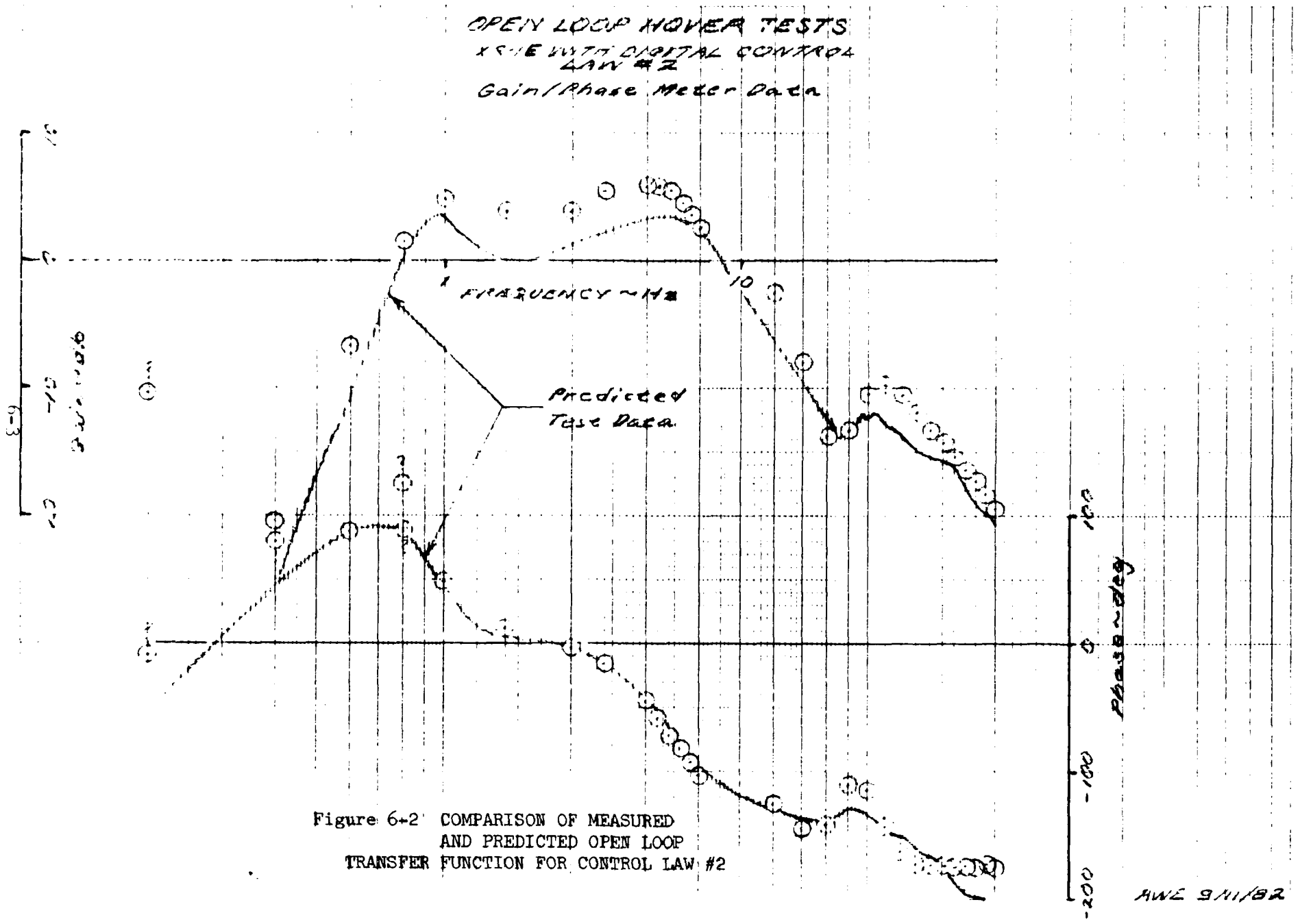

Figure 6-2 COMPARISON OF MEASURED AND PREDICTED OPEN LOOP TRANSFER FUNCTION FOR CONTROL LAW #2

The difference may simply be due to the fact that the data plotted were obtained in real-time from a Hewlett-Packard Gain/Phase meter instead of from Fourier Series data (see Section 5.4.1). The Gain/Phase meter simply ratios the RMS (root mean square) of the output signal to the RMS of the input to obtain a gain reading. This procedure overestimates the true linear gain of the system if harmonics of the driving frequency are excited.

Figure 6-2 illustrates that the above discussion of measured and predicted open loop responses for Control Law 1 applies equally well to Control Law 2. Therefore, it is concluded that the overall dynamics of the digital RCS-plus-craft are in good agreement with the predicted values. This serves to validate the RCS hardware and software plus its integration with the XR-1E SES.

6.1.2 Comparison of Digital and Analog RCS Stability

Figure 6-3 compares Control Law 1's measured open loop gain and phase characteristics for both digital and analog implementation. The gain curves for both controllers are identical; however, the phase characteristic differs at the high frequency end due to the sampling delays resulting from digital implementation. These lags (see Section 5.1.2) shift the 180° phase crossover from 20 Hz for the analog RCS to 17.5 Hz for the digital RCS. This, in turn, reduces the digital RCS gain margin relative to the analog system. The actual reduction in gain margin is 1 db less than predicted (see Section 5.2.1). This difference is well within the accuracy of the data.

The reduction in the control system's gain margin is small but not insignificant. It means the digital RCS must operate with less margin against high frequency instability or limit cycling to employ the same overall closed loop gain as the analog RCS. This could have been avoided by developing a digital system which utilizes a much higher sample rate. Because the gain characteristic changes so rapidly in the vicinity of the 180° phase crossover, the sample rate would probably have to be increased from 200 pps (the present rate) to 600 pps to make the digital and analog RCS gain margins equivalent. Higher sample rates were considered during design of the digital RCS. They would have required a much faster CPU than was readily available or a significant amount of hard wired logic to replace slower software operations. It was decided that the potential benefits of such high sample rates did not warrant the required increase in cost and complexity.

The fact that the digital RCS stability and sample rate are adequate was demonstrated during closed loop testing. In these tests, the digital RCS was operated at the same overall gain utilized during tests of the analog RCS. There was no evidence of instability, limit cycling or excessive amplification of pressures in the acoustic frequency range (10 - 20 Hz) due to the 3 - 5 db reduction in gain margin.

Figure 6-3

COMPARISON OF DIGITAL AND ANALOG RCS
OPEN LOOP TRANSFER FUNCTIONS
FOR CONTROL LAW #1

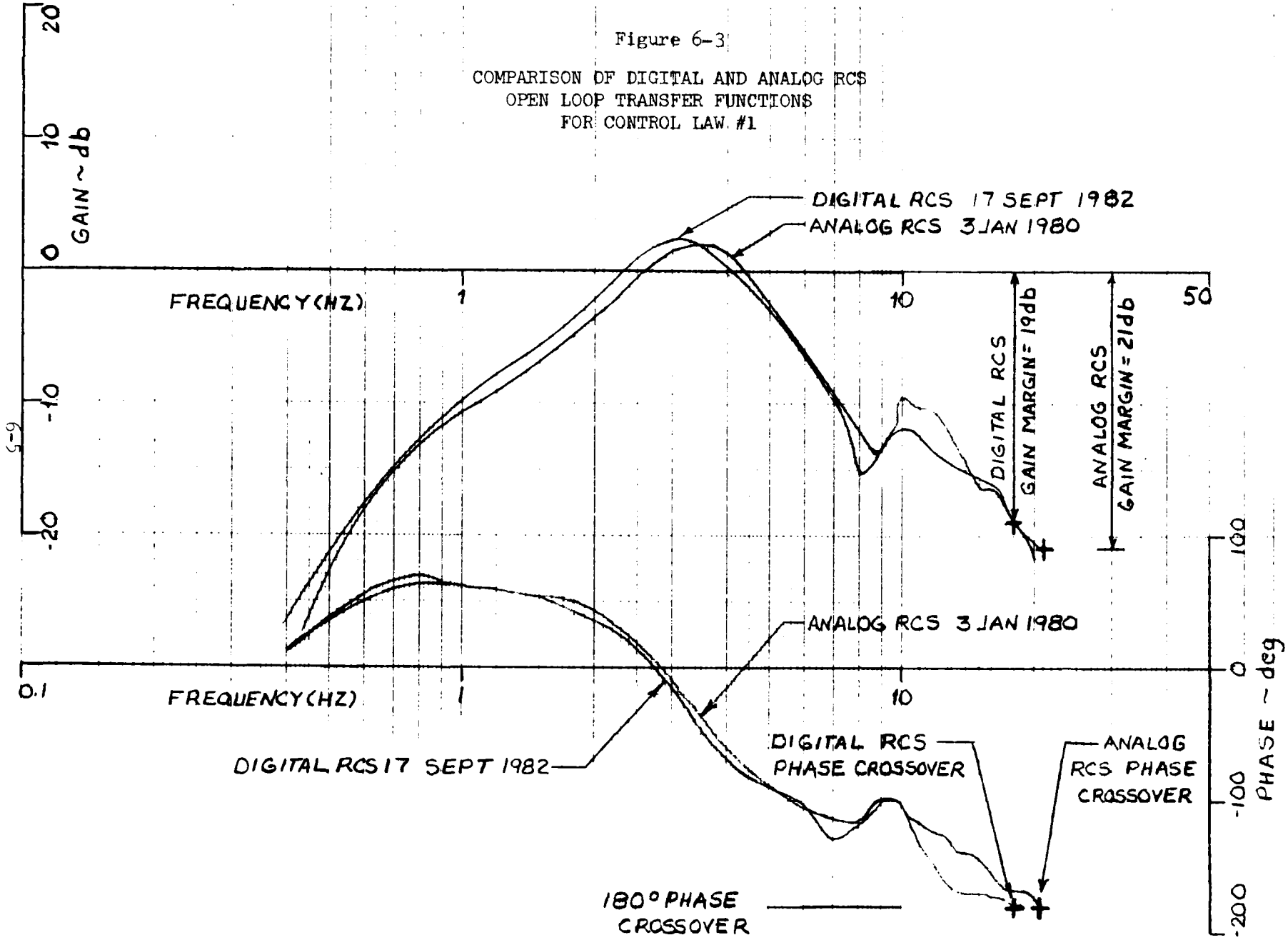

6.2 SYSTEM PERFORMANCE EVALUATION

6.2.1 Closed Loop Test Conditions

Figure 6-4 illustrates the range of sea state and speed over which the digital RCS was tested. In Figure 6-4(a) the heave acceleration standard deviations are plotted versus the significant wave height for all RCS-Off tests conducted. The data fall into two distinct groups which correspond to the two speed ranges (14 - 17 kts and 19 - 22 kts) in which tests were conducted. This division of the data is also illustrated in Figure 6-4(b) where speed is plotted versus significant wave height for all RCS-Off tests.

Since the data fall into these categories, all points plotted are identified by speed and mission number throughout the remainder of this section. Shaded symbols identify speeds between 19 and 22 kts while open symbols designate speeds between 14 and 17 kts. The symbols used to identify the various missions are shown on the figures. All data points plotted are taken from the data qualification tables for Missions 345, 346 and 348 contained in Appendix A. Wave height power spectra for these missions are included in Appendix B.

The closed loop tests were set up to investigate RCS effectiveness and power requirements as a function of vent valve bias. The bias is the mean opening about which the vent valves are controlled. Five percent (5%) bias was the lowest bias at which tests were conducted. At 5% bias, the vent valves are only driven in response to increases in cushion pressure, i.e., positive heave accelerations. This results in a pure one-sided type of control as illustrated in Figure 6-5. One-sided control is effective on SES because it provides some damping of positive and negative heave mode accelerations and it attenuates the pressure spikes which result from cushion venting in large waves (see Reference 1 for additional discussion).

For biases greater than 5%, the vent valves are driven in response to both positive and negative cushion pressure fluctuations and the control is two-sided as illustrated in Figure 6-6. This type of control is typically more effective than one-sided control; however, there may be an increase in power requirements because more pressurized air is exhausted overboard.

For bias settings below 50%, more flow control is used for attenuation of positive accelerations than for negative accelerations. It is expected that the optimum bias from the standpoint of effectiveness and power will actually be less than 50%. This is due to the fact that in large waves the positive accelerations typically exceed the negative accelerations, therefore more flow control is needed in the direction of increasing vent valve opening.

6.2.2 RCS Reduction of Heave Acceleration

6.2.2.1 Standard Deviations

RCS performance analyses typically utilize the standard deviation of heave acceleration as the fundamental measure of RCS effectiveness.

Figure 6-4(a) XR-1E RCS-Off Heave Acceleration Vs. Wave Ht, Head Seas

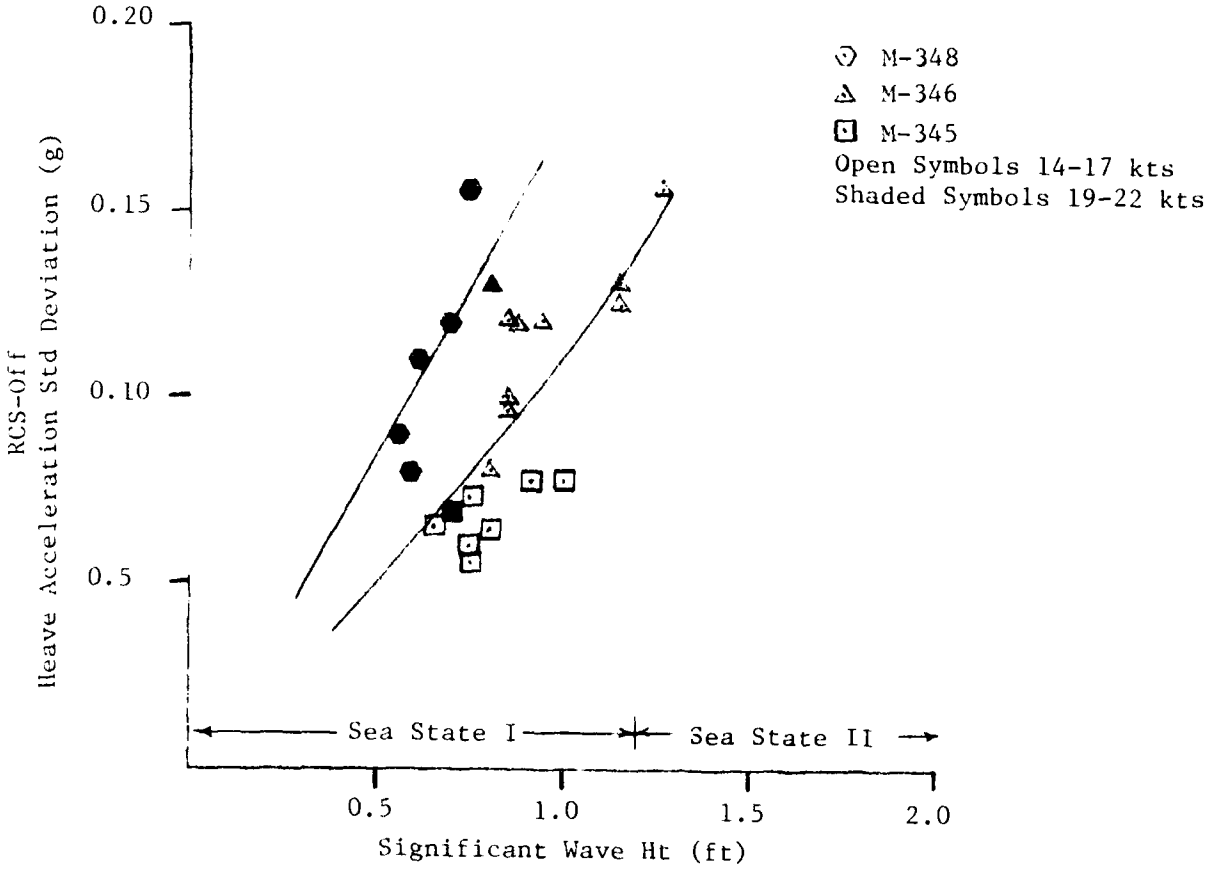

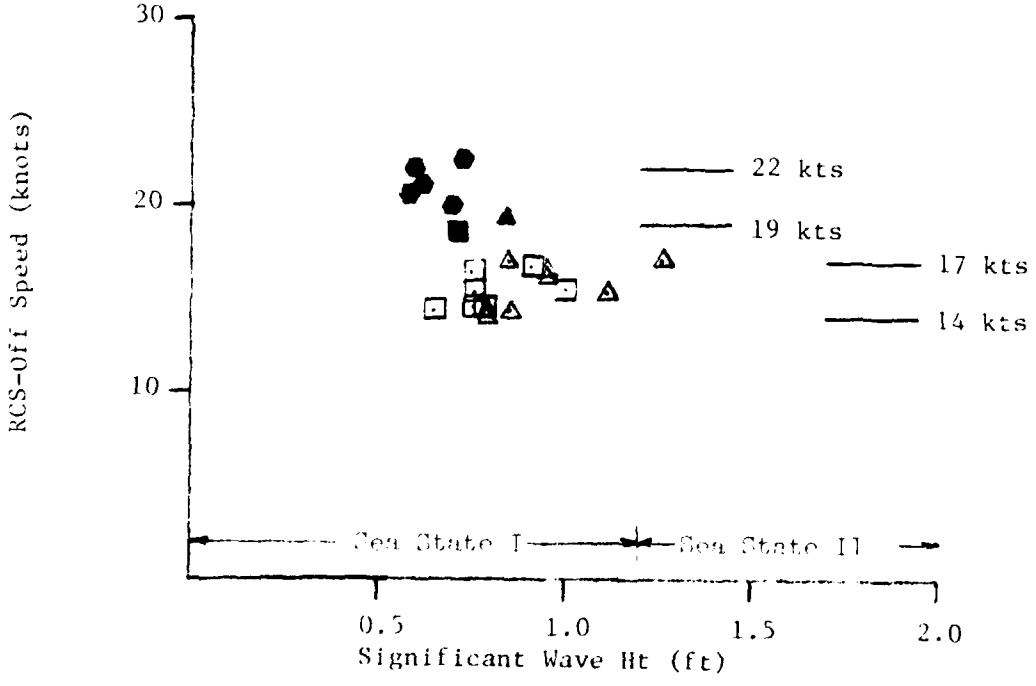

Figure 6-4(b) XR-1E RCS-Off Speed Vs. Wave Ht, Head Seas

Figure 6-5 ILLUSTRATION OF ONE-SIDED CONTROL

Operation

-VVs set at the minimum (5% bias) position

-VVs cycle open/closed intermittently as cushion pressure rises/falls

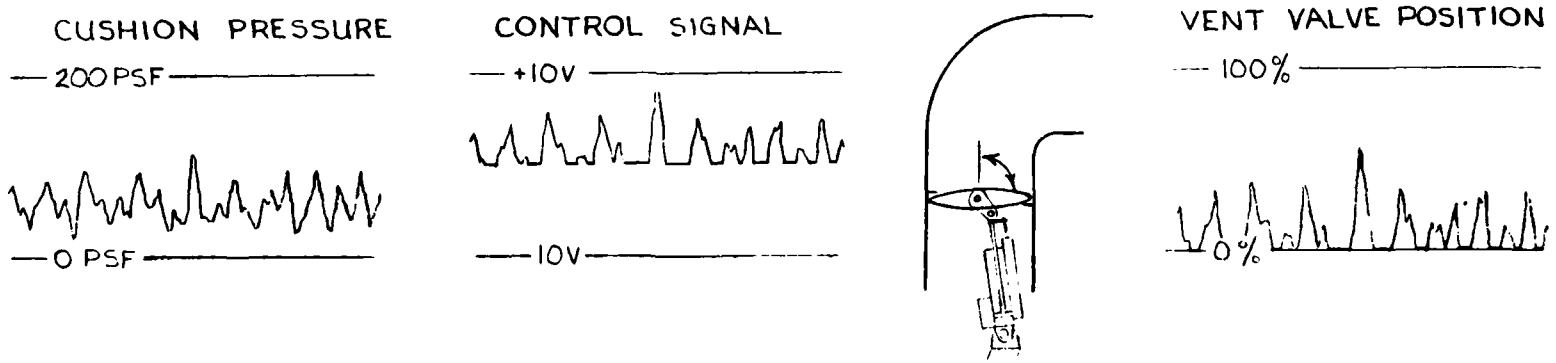

Figure 6-6 ILLUSTRATION OF TWO-SIDED CONTROL

Operation

- -VVs set at an intermediate bias position
- -fan flow may need to be increased to maintain speed
- -VVs cycle open/closed continuously as pressure rises/falls

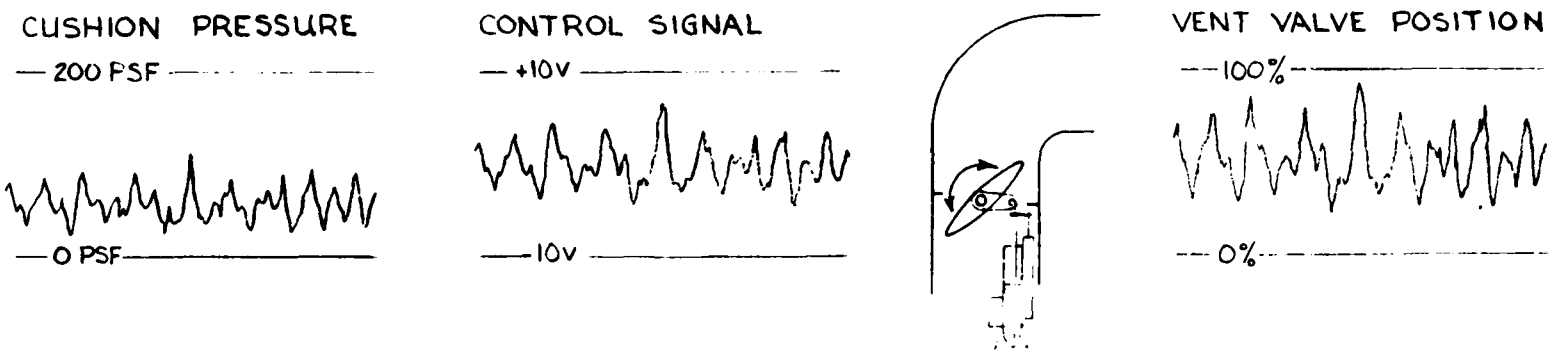

Vertical acceleration has been found to be the parameter which most significantly degrades SES habitability and it is the heave component of vertical acceleration which the RCS is designed to regulate. The standard deviation is used because it has become recognized as a rule-of-thumb measure of ride quality for advanced marine vehicles.

In Figure 6-7(a) the percent reduction in the RCS-Off heave acceleration standard deviation is plotted versus the RCS-On vent valve bias. The percent reduction in the heave acceleration standard deviation was calculated using the following equation:

$$\% \text{ Reduction } \sigma_{\ddot{z}}(\text{off}) = \left[1 - \frac{\sigma_{\ddot{z}}(\text{on})}{\frac{\sigma_{\ddot{z}}(\text{off}) + \sigma_{\ddot{z}}(\text{off})}{2}}\right] \times 100 \qquad (6\text{-}1)$$

Averaging of two RCS-Off values in the above equation results from the fact that RCS-Off test points were recorded before and after each RCS-On test point. This procedure attempts to average out any changes in sea condition which may have occurred during the time interval covered by the test points.

The data indicate that the RCS's effectiveness is fairly linear for bias values between 5% and 35%. Heave acceleration reduction varies from 40% at 5% bias to 60% at 35% bias. Above 35% bias, the effectiveness starts to level off. This is due to excessive saturation, i.e., the vent valve travel is being limited by the RCS at 5% and 95% a significant fraction of the time. This reduces the linear gain of the RCS which causes the system's effectiveness to level off.

Overall the consistency of the data is quite good. The data represent two sea state conditions (I and II) and two speeds (14-17 kts and 19-22 kts). The 60% ride quality improvement obtained is considered excellent. It should be noted that this level of ride quality improvement was obtained using only two (2) of the ship's four (4) vent valves. Also the fan flow was not increased to compensate for dumping pressurized air overboard through the vent valves.

In the previous higher speed tests of the analog RCS reported in Reference 1, 80% reduction in the RCS-Off heave acceleration was obtained in similar sea states. However, this was accomplished at the expense of using four (4) vent valves and roughly doubling the fan flow rate which, in turn, doubles the lift system power.

6.2.2.2 Power Spectra

Figure 6-8 shows representative heave acceleration spectra for the RCS-On condition and the RCS-Off tests conducted immediately before and after. The test conditions represent head sea operation in Sea State II at 15 knots.

Figure 6-7(a) REDUCTION IN XR-1E RCS-OFF HEAVE ACCELERATION STANDARD DEVIATION VS. VENT VALVE BIAS

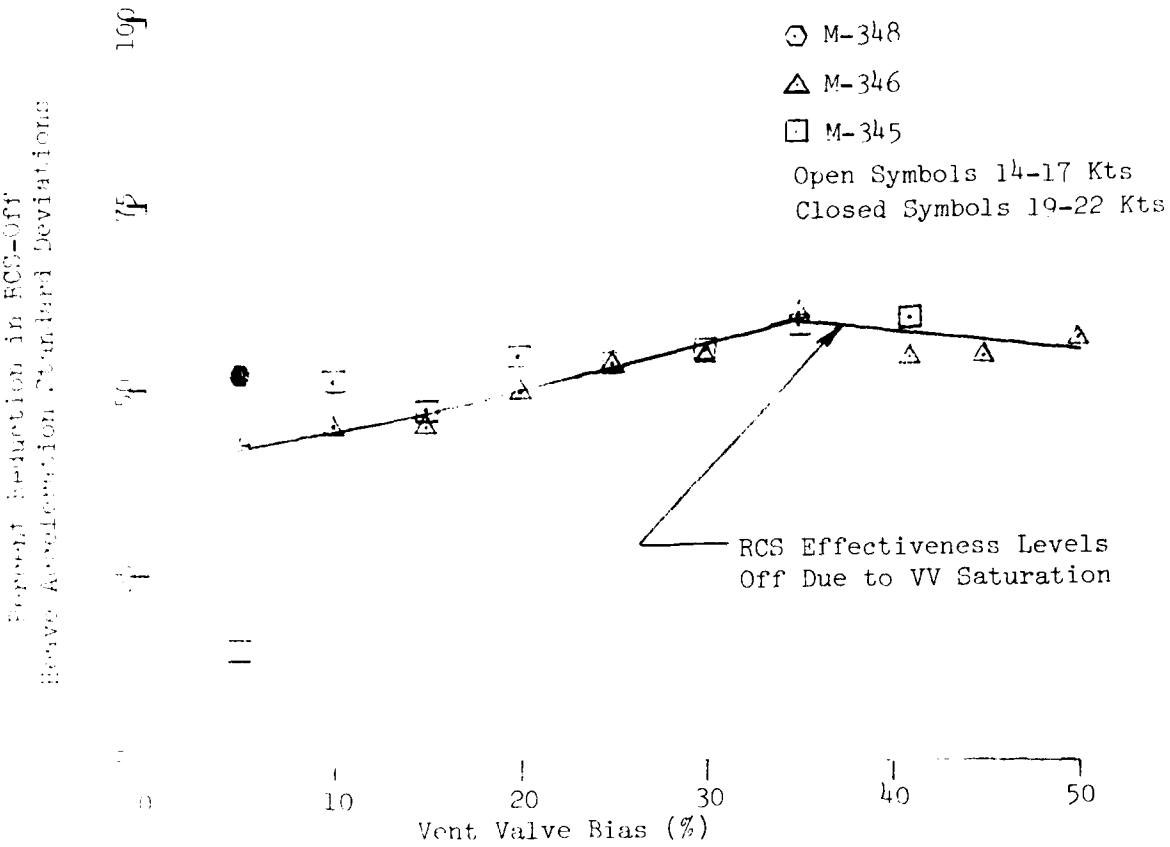

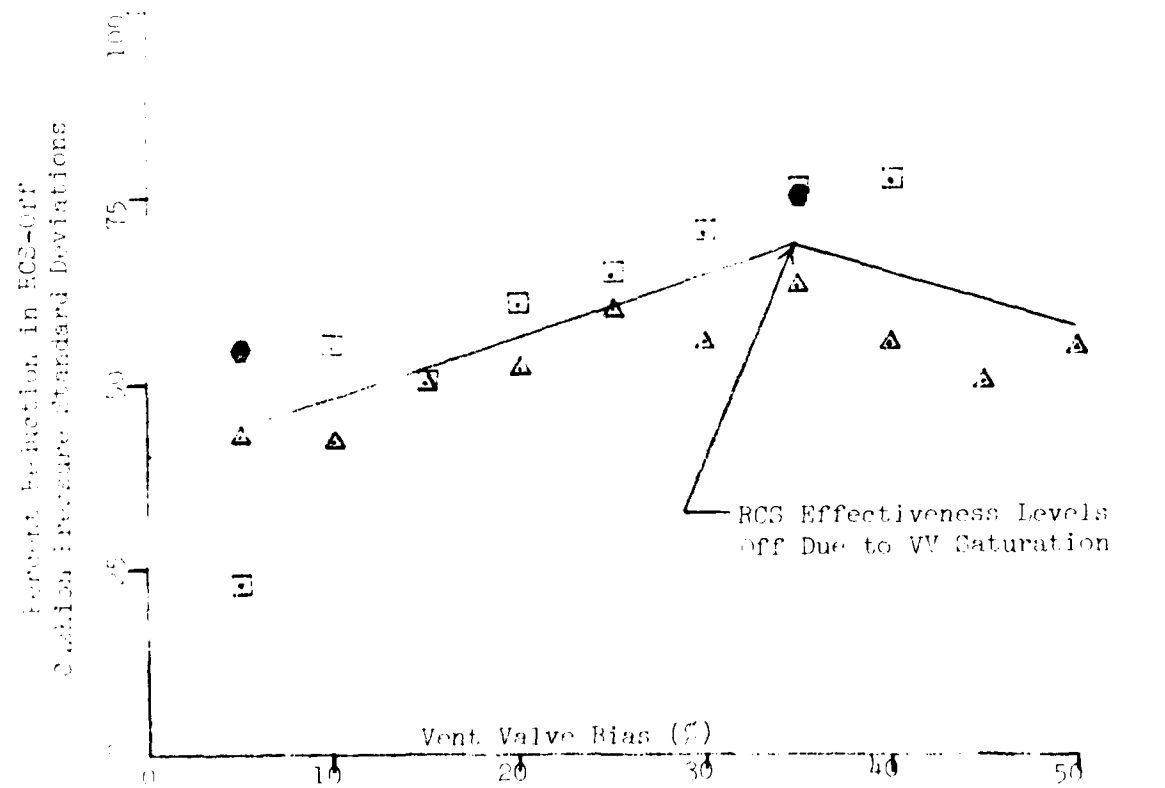

Figure 6-7(b) REDUCTION IN XR-1E RCS-OFF HEAVE ACCELERATION STANDARD DEVIATION VS. VENT VALVE BIAS

Standard Ordinate Error = 22.4%
Bandwidth = 0.2 Hz
Delta Time = 0.01 sec.
Nyquist Frequency = 50 Hz

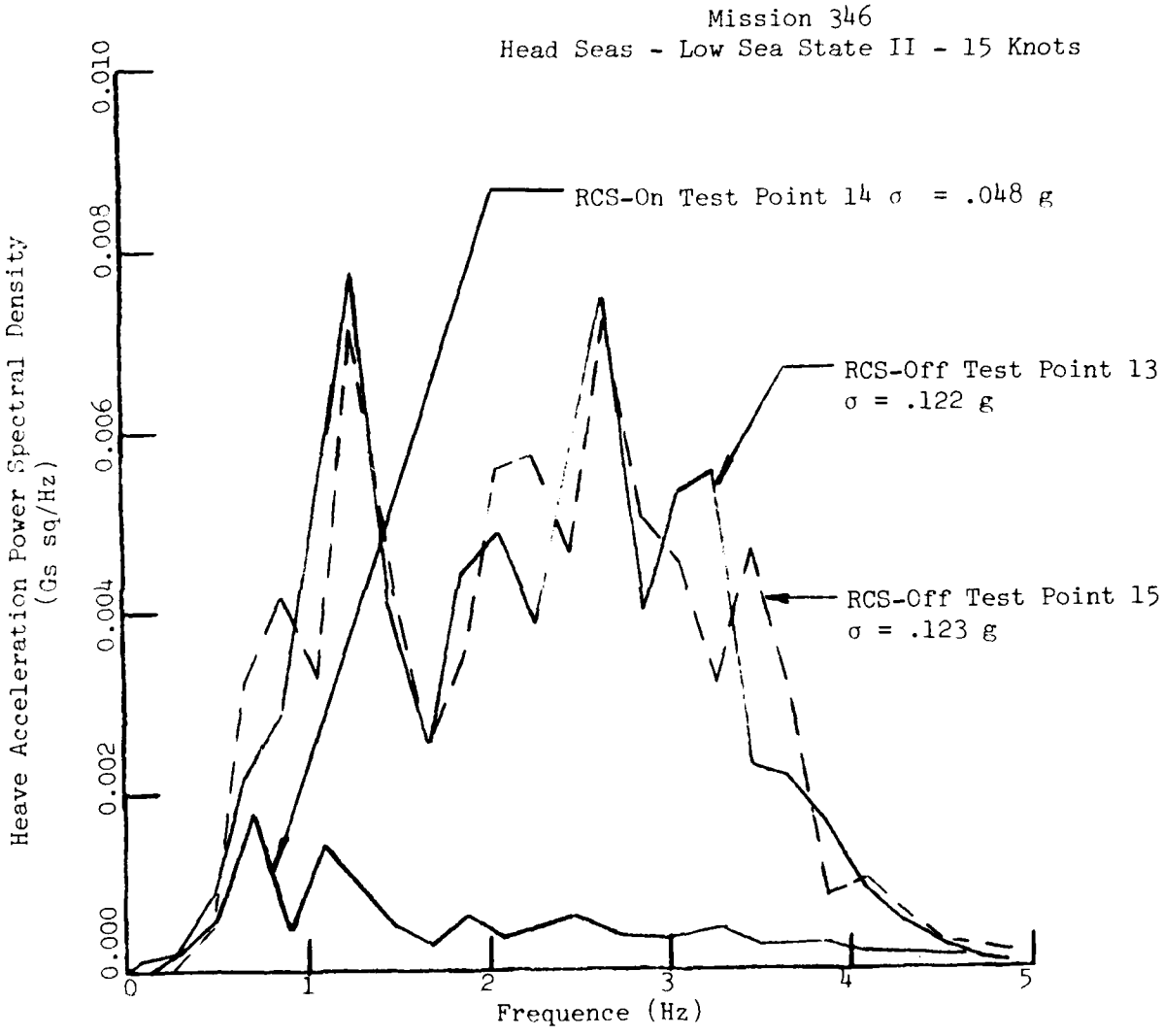

Figure 6-8 XR-1E HEAVE ACCELERATION POWER SPECTRA, RCS-OFF AND RCS-ON

RCS operation significantly reduces the spectral levels over the entire frequency range. RCS-Off spectral peaks occur at frequencies of 1.2, 2.7 and 3.4 Hz. The peak at 3.4 Hz occurs at the heave natural frequency of the XR-1E. Peaks at the lower frequencies are associated with waves pumping the cushion volume. The deep notch in the spectra at 1.7 Hz is located at a cushion wave pumping minima. The minima correspond to frequencies at which an integer number of wave lengths just fit into the cushion and therefore (for a platforming craft) produce no forced volume changes.

6.2.2.3 1/3 Octave Band Data

Figure 6-9 shows RCS-Off and RCS-On heave acceleration data plotted in 1/3 octave band format. Also shown are maximum vertical acceleration levels which have been proposed for multi-thousand ton SES mission scenarios (Reference 9). The data plotted are from the same test points as the spectral data shown in Figure 6-8, i.e., 15 knots, head seas, Sea State I.

The four different habitability levels plotted considered a number of different missions that were appropriate for the 3KSES. Therefore, it may not necessarily be entirely appropriate to apply these same criteria to the 26-ton XR-1E. However, since the criteria do cover the XR-1E frequency range, the comparison illustrates the RCS effectiveness in terms of human body tolerance limits.

Reference 9 defines the four habitability levels as follows:

Habitability Level A, Brief Exposure, refers to conditions encountered under emergency conditions. Relevant limits are those for physical safety, in terms of: throwing the crew about the ship; impacting limbs on nearby objects; or causing complete loss of locomotion (e.g., zero or negative g's for more than a second). Statistically, the duration of such situations will seldom exceed a few minutes, hence the term "brief exposures". A "characteristic time" limit of 5 minutes is specified.

Habitability Level B, "Short Mission Phases", is applied to a wide range of operationally important mission phases wherein the focus of attention is on military weapon or rescue operations, during which all secondary functions such as eating, sleeping, etc., may be suspended. In terms of SES scenarios, this would include: dash maneuvers, ASW chase operations, escape maneuvers, and rescue operations. The crew could remain strapped down, if necessary, and there is high motivation among crew members. Such mission phases can normally be expected to last no more than one-half hour or so. Hence, 30 minutes was designated as the appropriate time characteristic for Habitability Level B. Under battle conditions, Level B may extend from 1 to 4 hours.

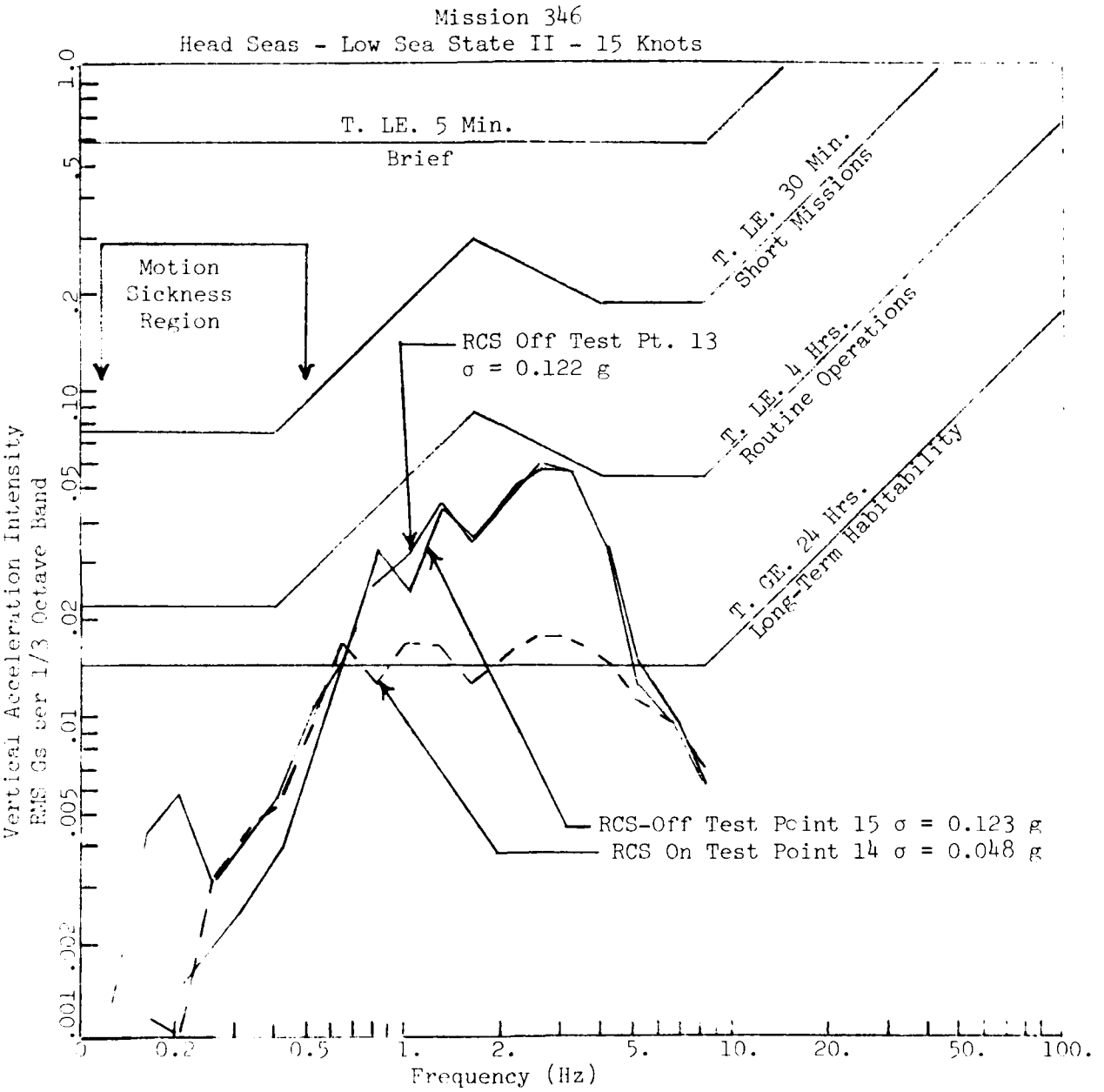

Figure 6-9 COMPARISION OF XR-1E HEAVE ACCELERATION WITH SEC HABITABILITY CRITERIA, RCS-OFF AND RCS-ON

Habitability Level C, "Routine Operations", is applied to the major fraction of time spent aboard a long SES cruise. Routine operations include: moving about the ship, eating, sleeping and making repairs with minor task interference. A great majority of the crew is not strapped in place. Such operations would typically be limited to less than four hours by virtue of change in watch, mission accomplishment, fuel limitation or traversing an area where sea conditions would be rough. We have set a limit of four hours as a characteristic time for Habitability Level C. Routine operations can extend for several hours in a small percentage of situations.

Finally, Habitability Level D, "Long-Term Habitability", covers the desirable limit for minimal impairment of normal functions such as sleeping, walking, eating, resting and routine maintenance with a negligible degree of impairment. Such conditions should be habitable for several days in succession, thus the time limit is set as greater than 24 hours.

The criteria are primarily applicable to pure sinusoidal or narrowband random vibration where the top-tenth peak accelerations do not exceed the RMS levels by more than a factor of 2-3. In evaluating wideband motion typical of SES, one accepted scheme is to consider only the peak which intercepts or penetrates the highest curve. This concept is based on the psycoacoustic phenomenon that the most intense tone masks a less intense tone. Another procedure used is to apply a frequency weighted criterion. This is accomplished by multiplying the actual acceleration levels by a weighting function and summing the resultant values. The resulting weighted RMS acceleration is then compared with the criterion level at a reference frequency.

This latter method is probably technically more accurate; however, for simplicity, we choose to employ the former method. With the RCS off, the highest peak nearly exceeds the limit for Routine Operations which has a characteristic time of four hours duration. With the RCS on, the highest peak barely exceeds the limit set for long-term habitability.

An increase in crew fatigue sufficient to reduce proficiency in performing skilled tasks associated with the mission is likely to occur when the habitability criteria are exceeded. This is known as fatigue-decreased proficiency or FDP. The RCS in the case illustrated in Figure 6-9 is able to decrease the heave accelerations to levels that should be tolerable for several days without physical impairment of normal functions.

6.2.3 RCS Power Requirements

Power required to operate the RCS on the XR-1E can be divided into two categories:

1. Hydraulic power required to move the vent valve louvers.
2. Speed lost due to dumping pressurized air overboard.

Hydraulic power requirements are modest because the louvers have low rotational inertia and are lightly loaded by the air flow. During two vent valve operation, hydraulic power should not exceed 5 hp which is only 0.4% of the total installed lift and propulsion power.

Speed loss due to dumping pressurized air overboard will be explained with the aid of Figures 6-10(a), -(b) and -(c). As the mean vent valve opening (or bias) is increased, the mean vent valve flow rate and the amount of vent valve activity both increase. These characteristics are illustrated in Figures 6-10(a) and 6-10-(b), respectively.

Figure 6-10(a) is a plot of the mean or time-averaged vent valve flow rate over the test point versus the vent valve bias. Figure 6-10(b) is a plot of the standard deviation of vent area versus bias. This second plot illustrates the amount of vent valve activity at each test condition. Data points in Figures 6-10(a) and -(b) follow two separate curves which correspond to the two sea conditions in which tests were conducted.

As the sea state increases, the severity of the RCS-Off cushion pressure fluctuations and heave accelerations increases. This, in turn, increases the RCS-On vent valve activity in the higher sea state as shown in Figure 6-10(b). This increase in vent activity with sea state is greater in the opening direction than the closing direction. Therefore, the time-averaged vent valve flow rate also increases with sea state (see Figure 6-10(a)).

In the higher of the two sea conditions, the mean vent flow rates are very high relative to the total fan flow rate (see Figure 6-10(a)). Above 35% bias, nearly 2/3 (two-thirds) of the fan flow is being exhausted through the vent valves on a time-averaged basis. It would probably not be possible to dump this much flow overboard on a continuous basis and still maintain speed above the primary wave drag hump at 12 knots. However, the RCS modulates the air flow as opposed to a continuous overboard discharge. This action reduces the heave accelerations and motions which in turn must reduce air leakage under the seals and sidewalls. It is this reduction in leakage which permits the use of high vent airflows without excessive speed loss.

In Figure 6-10(b), the line labeled "Excessive Vent Valve Saturation" corresponds to a standard deviation of vent area equal to 35% of the total vent area (3 sq.ft). For comparison, the standard deviation of a sine wave equals 70.7% of the amplitude or 35% of the double amplitude. Excessive saturation is present for all HSSI/LSSII tests at biases greater than 25%. This explains the leveling off of RCS effectiveness shown in Figure 6-7(a) and 6-7(b), i.e., vent valve travel is being limited a large fraction of the time.

The speed change associated with RCS operation is shown in Figure 6-10(c). It does not display a consistent variation with vent valve bias. There is an initial 1-knot speed loss at 5% bias which, surprisingly, gets smaller with increases in bias up to 20%. At 20% bias, the speed loss is essentially negligible. Above 20% bias, the speed loss starts to increase and reaches 2.5 knots at 35% bias. The data seem to support another reduction in the speed loss for biases greater than 35%. However, in this region we suggest not trusting the data too much due to the limited number of points.

Figure 6-10(a)

MEAN XR-1E VV FLOW RATE VS. VV BIAS

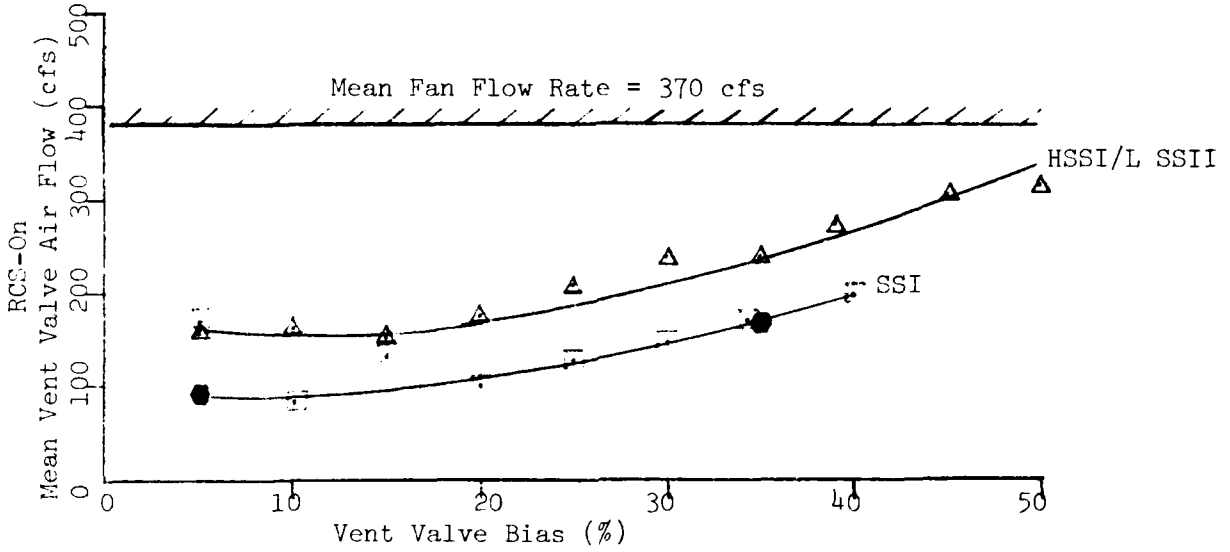

Figure 6-10(b)

STD. DEV. OF XR-1E
VENT AREA VS. VV BIAS

Open Symbols 14 - 17 knots
Closed Symbols 19 - 22 Knots

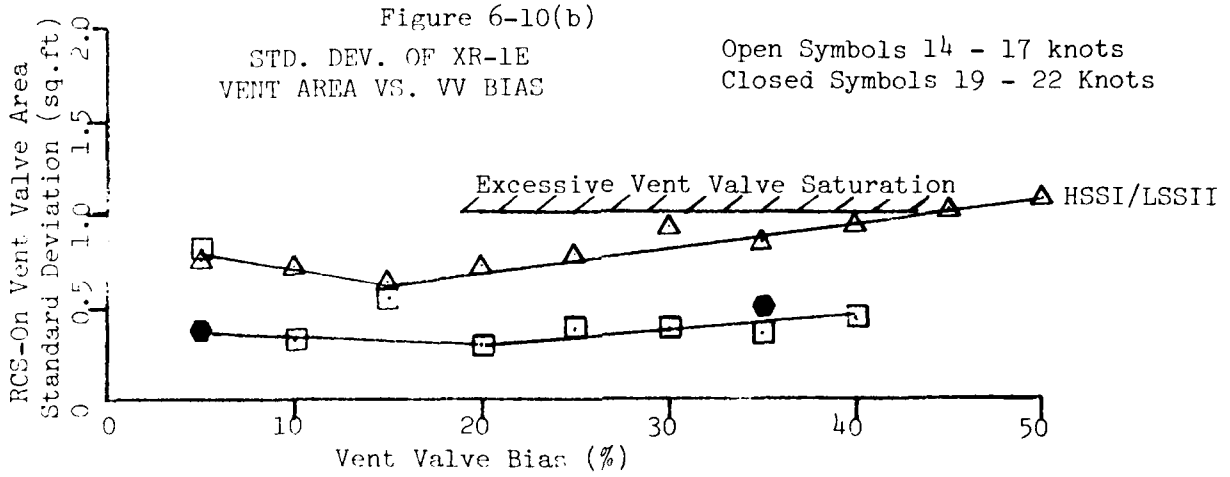

Figure 6-10(c)

XR-1E RCS-ON SPEED CHANGE VS. VV BIAS

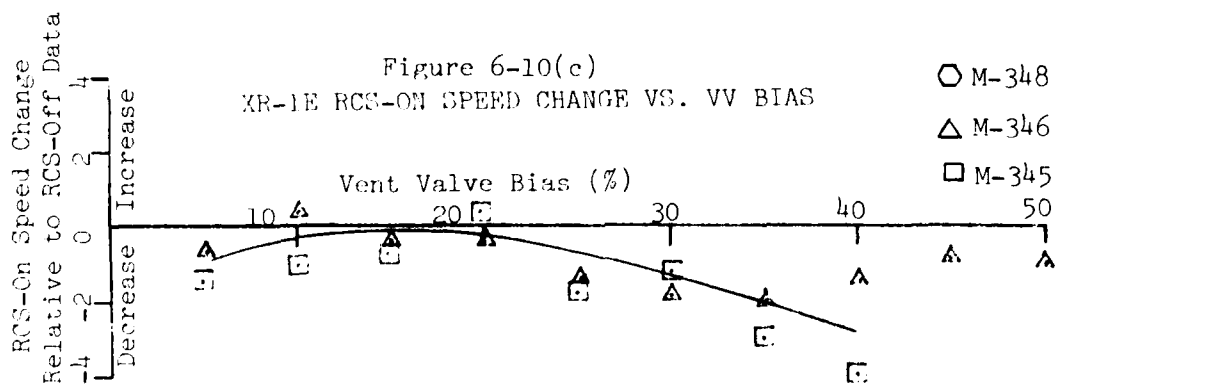

The data shown in Figure 6-7(a) and 6-10(c) suggest that XR-1E RCS operation in Sea States I and II is most efficient at 20% bias. At this bias, a 50% reduction in the standard deviation of heave acceleration was obtained without any loss of speed. Therefore, for RCS operation under these conditions only, a small amount of additional power is required to run the hydraulics.

6.2.2.4 RCS Reduction of Cushion and Seal Pressures

Heave acceleration in the frequency range between 0 and 5 Hz primarily arises from changes in cushion pressure caused by wave pumping. This means the heave acceleration and cushion pressure signals have a high degree of coherency. Between 0 and 5 Hz, these two parameters are related by the following simple relationship which ignores sidewall buoyancy effects:

$$\Delta\ddot{z} = \frac{A_c}{m} \Delta P_c$$

where

A_c = Cushion Area

m = Mass of Craft

ΔP_c = Change in Cushion Pressure

$\Delta\ddot{z}$ = Change in Heave Acceleration

Because cushion pressure and heave acceleration are so highly correlated, it is theoretically possible to use either signal as the feedback parameter. However, to date, only cushion pressure feedback has been successful. This is due to the fact that accelerometers contain energy from structural modes and machinery vibration that is impossible to filter out without destroying the low frequency effectiveness of the system.

As expected, the RCS reduces the RCS-Off cushion pressure standard deviation as much as it did the heave acceleration (see Figure 6-7(b)). The cushion pressure data are a bit more scattered but the general trend is the same.

Figure 6-11 shows cushion pressure power spectra for the RCS-On condition and for the RCS-Off tests conducted immediately before and after. These power spectra were selected from the same test points used to compute the heave acceleration power spectra plotted in Figure 6-8. Notice that the spectra in Figures 6-8 and 6-11 are remarkably similar due to the high degree of coherency between heave acceleration and cushion pressure. All comments made in Section 6.2.2.2 regarding RCS reduction of the heave acceleration spectral levels apply equally well to these cushion pressure spectra.

Standard Ordinate Error = 22.4% Delta Time = 0.01 sec.

Bandwidth = 0.2 Hz Nyquist Frequency = 50 Hz

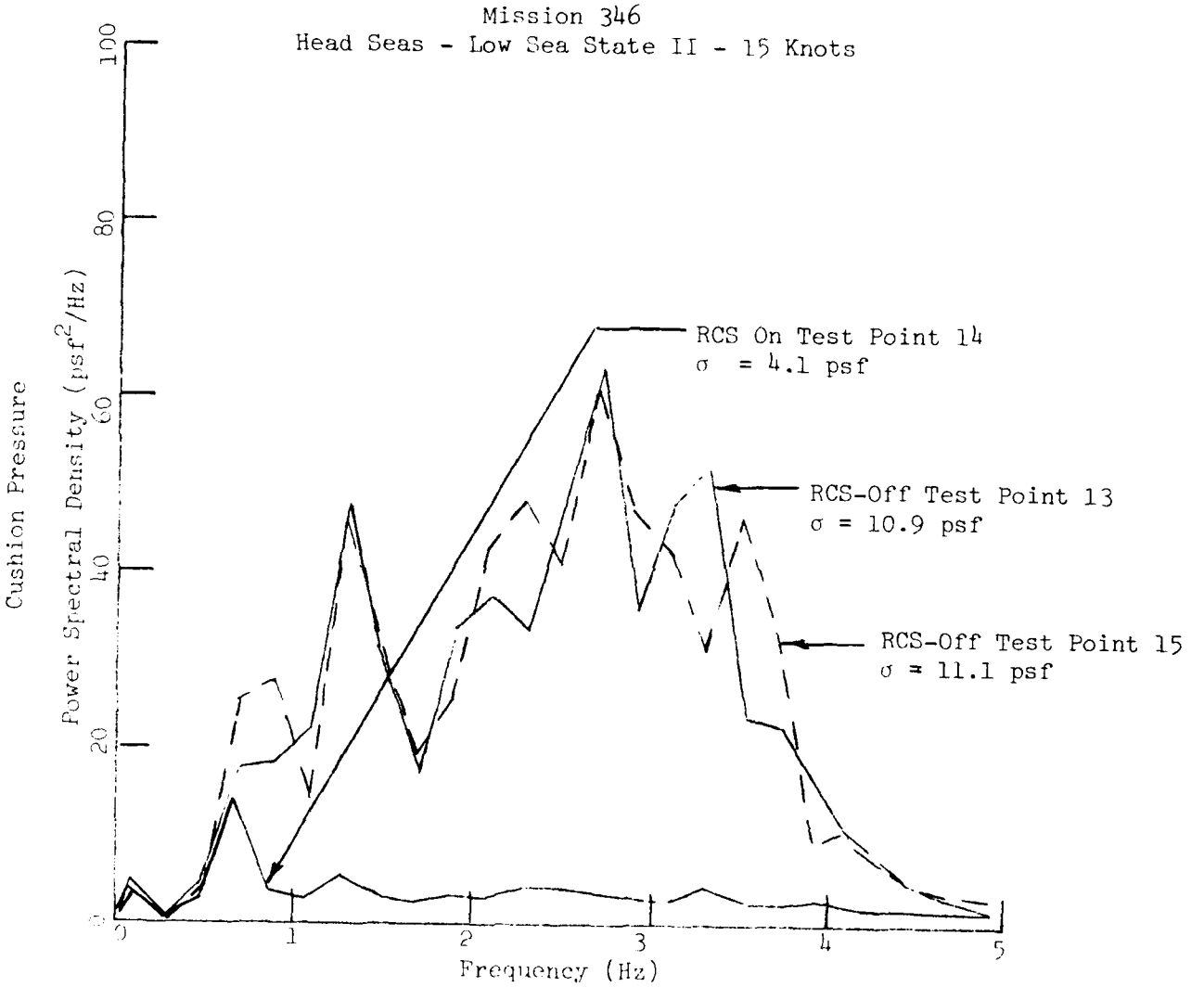

Figure 6-11 XR-1E CUSHION PRESSURE POWER SPECTRA, RCS-OFF AND RCS-ON

Standard Ordinate Error = 22.4% Delta Time = 0.01 sec.

Bandwidth = 0.2 Hz Nyquist Frequency = 50 Hz

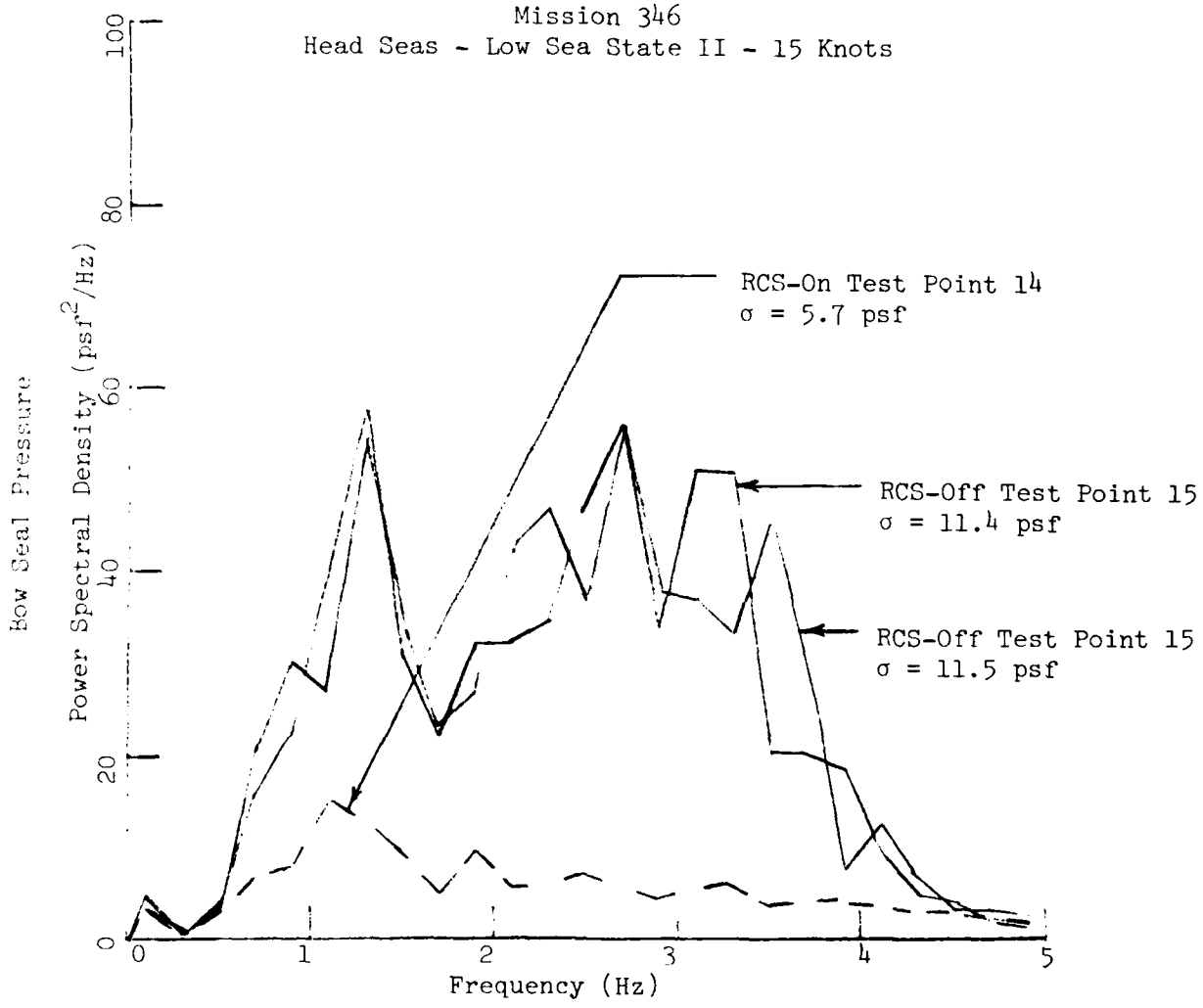

Figure 6-12 XR-1E BOW SEAL PRESSURE POWER SPECTRA, RCS-OFF AND RCS-ON

Standard Ordinate Error	= 22.4%	Delta Time	= 0.01 sec.
Bandwidth	= 0.2 Hz	Nyquist Frequency	= 50 Hz

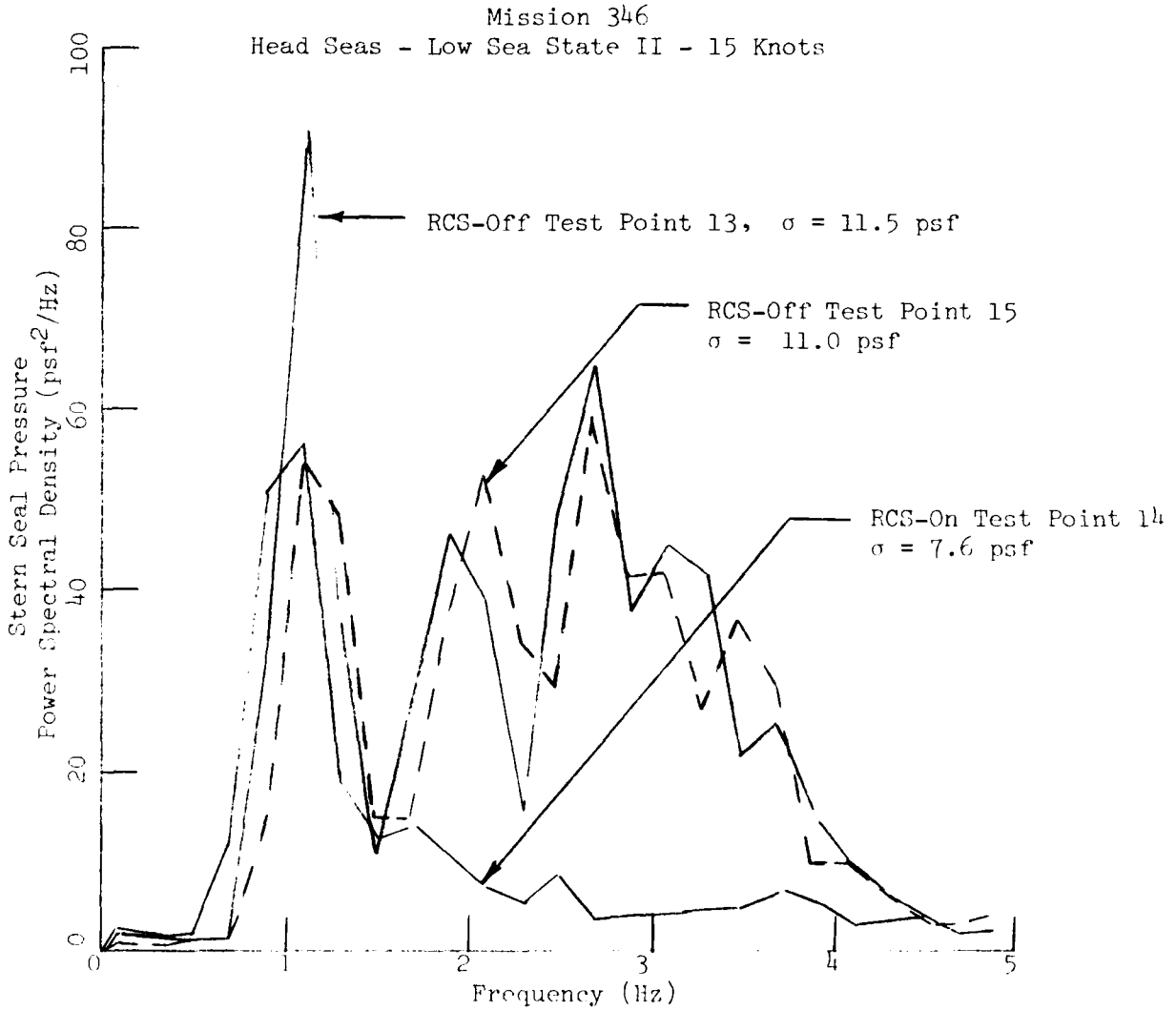

Figure 6-13 XR-1E STERN SEAL PRESSURE POWER SPECTRA, RCS-OFF AND RCS-ON

Since the seal and cushion volumes are interconnected, RCS attenuation of cushion pressure also has the secondary benefit of reducing pressures in the seal bags. This could reduce the peak cyclic loads enough to improve life of SES seals. Figure 6-12 shows bow seal pressure power spectra and Figure 6-13 shows stern seal pressure power spectra for RCS-On and RCS-Off tests. These power spectra correspond to the same test conditions as the heave acceleration and cushion pressure power spectra shown in Figure 6-8 and 6-11, respectively.

6.2.5 RCS Effect on Pitch Motion

Previous tests of the analog RCS did not demonstrate any significant RCS effect on pitch motion (see References 1 and 2). This is due to the fact that the RCS primarily affects the heave plane. There is no significant pitch/heave coupling which would cause the RCS to amplify or attenuate the pitch motion.

The digital RCS tests were conducted at significantly lower speeds (14-17 and 19-22 knots) than the previous tests (25-30 knots). Therefore it is desirable to examine this new data to see if the RCS affects pitch motion at the slower speeds.

Figure 6-14(a) is a plot of RCS-On versus RCS-Off pitch standard deviations for all test points. Figure 6-14(b) presents a similar comparison for pitch rate data. The general method of testing was to run an RCS-Off test before and after each RCS-On test. RCS-On data shown in Figures 6-14(a) and 6-14(b) are plotted versus an interpolated value for the RCS-Off case obtained by averaging the preceding and succeeding RCS-Off runs. Actual values for the RCS-Off runs used in each instance are indicated by vertical bars connected by a horizontal line to show any spread in the data.

The pitch and pitch rate data tend to cluster about the RCS-On - RCS-Off lines, thus indicating that the RCS does not affect pitch motion. There is some scatter which is most likely due to the use of short one (1) minute data segments.

Figure 6-14(a) XR-1E RCS-ON VERSUS RCS-OFF PITCH ANGLE STANDARD DEVIATION

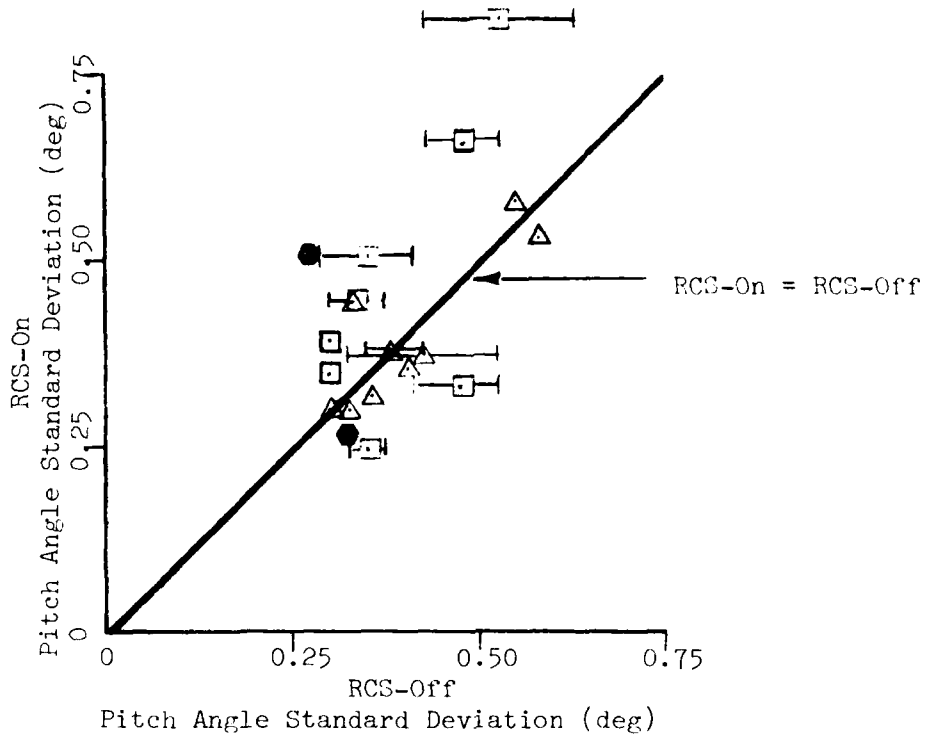

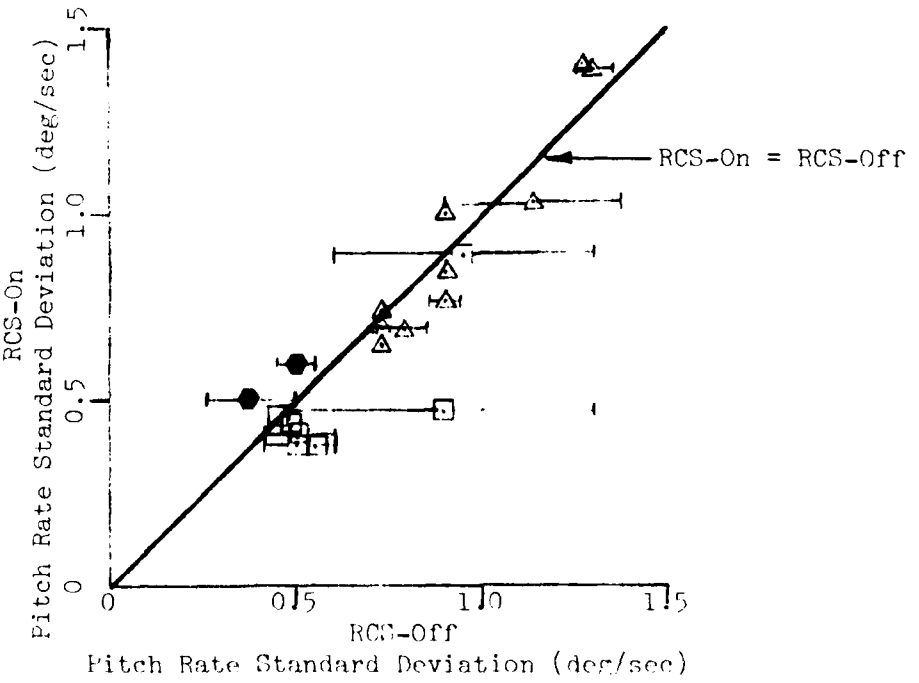

Figure 6-14(b) XR-1E RCS-ON VERSUS RCS-OFF PITCH RATE STANDARD DEVIATION

7. PREDICTED RCS PERFORMANCE FOR USCG SEA BIRD CLASS SES

In this section, data from USCG and USN tests of the Bell-Halter 110 and data from the XR-1E Digital RCS tests are used to predict RCS performance and power requirements for the Sea Bird SES. These predictions are made for head sea operation at maximum speed, since heave accelerations are largest under these conditions.

7.1 HEAVE ACCELERATION AND SHIP SPEED WITHOUT RIDE CONTROL

7.1.1 General Characteristics of Sea Bird Heave Motion

The principal dynamic characteristics of the Sea Bird Class SES were investigated in Reference 10. For 1700 lift fan rpm, the natural frequency and damping ratio of the heave mode are 2 Hz and 0.3, respectively. Critical damping which has a ratio of 1.0 allows a displaced system to return to its original position without oscillation. The Sea Bird is considered fairly lightly damped relative to a critically damped system, i.e., if displaced, it will oscillate for several cycles prior to returning to the original position.

Manned SES typically have low heave damping because the only significant source of damping is the slope of the lift fan pressure/flow curve. As fan rpm is increased to improve performance, the fan curve slope increases and this reduces heave damping, i.e., at 1900 rpm the damping ratio is lower than at 1700 rpm. RCS modulate cushion airflow in a manner which increases heave damping and the heave resonant frequency.

SES heave accelerations arise from waves pumping the cushion volume. Accelerations are maximum in head and bow seas due to the high frequency of encounter. In quartering and following seas, the Sea Bird operating speeds (20 - 30 kts) are close to wave speed (for Sea States I - IV) so the encounter frequency is fairly low. In pure beam seas, the encounter frequency and the forced cushion volume changes are both low.

Over hump operations in small waves ($H_{1/3}$ < 30% of cushion height) primarily excite the lightly damped 2 Hz heave resonance. This produces a bouncy ride (known as the cobblestone effect) which results in an appreciable amount of whole body vibration.

In larger waves the 2 Hz heave resonance continues to be excited and there is response at lower frequencies as well. The peak responses occur at wave pumping maxima, i.e., frequencies at which the wave profile inside the cushion cause significant displacement of the cushion volume.

When the significant wave height starts to exceed 60% of cushion height, a phenomenon referred to as cushion venting begins. The cushion vents under the bow seal during a pitch-up excursion on a wave crest. When this happens, cushion pressure may drop to atmospheric. As the craft starts to pitch down into the next wave trough, sudden recompression of the cushion causes a sharp rise or spike in the pressure. These spikes can reach as high as 3 times cushion pressure or 3 g's of vertical acceleration. Frequency of venting increases with the severity of the sea condition.

This brief discussion shows that the heave motions of an SES change significantly with sea state. Except in calm water, it is clear that an RCS would be desirable to reduce heave acceleration levels in virtually all sea conditions.

7.1.2 Heave Acceleration Without Ride Control

In Figure 7-1(a) the standard deviation (1σ) of heave acceleration for the Sea Bird Class SES is plotted versus significant wave height for head sea operation at maximum speed. Data points are from Navy and USCG tests of the original Bell-Halter 110 ft demonstration craft reported in References 5 through 7.

Sea Bird data points are plotted for Sea States II through IV. No Sea Bird data was reported for high Sea State I/low Sea State II conditions in any of the referenced reports. Therefore XR-1E data from the tests conducted at scaled Sea Bird flow rates and speeds is plotted for the lower sea states. The XR-1E data are Froude-scaled to represent the Sea Bird. It is recognized that the scaling technique may be criticized for reasons discussed in Section 5.2.2. However, the scaled data follow the trend of the measured Sea Bird data and will be treated as representative of low sea state conditions.

As shown, the 1σ heave acceleration increases linearly with increases in wave height through high Sea State II. It starts to level off at 0.2 g RMS in the higher sea states because the craft speed is decreasing due to power limitations. This characteristic is shown in Figure 7-1(b) and is discussed in the next subsection.

The Sea Bird heave acceleration data were available in 1/3 octave band format for only one test point. Figure 7-2 shows this data plotted against the four different habitability levels discussed in Section 6.2.2.3. As shown, the Sea Bird heave acceleration for Sea State II head sea operation exceeds the habitability limit for routine operations between 0.4 and 0.6 Hz. It comes close to exceeding the limit again at the 2 Hz heave resonance. The figure is similar to the XR-1E RCS-Off 1/3 octave band data plotted in Figure 6-9. The main difference is that, since it is a larger vessel, the Sea Bird data peaks at lower frequencies.

Using the simple technique of treating only the highest peak, Figure 7-2 would suggest that in Sea State II fatigue decreased proficiency in the crew could be expected in about 2 hours for head sea operation. Sea Bird SES typically operate in the Gulf of Mexico where Sea State II conditions are common. This illustrates that, even in typical low sea states, fatigue due to heave acceleration can be expected.

7.1.3 Ship Speed Without Ride Control

In Figure 7-1(b), speed is plotted versus significant wave height for the same test points plotted in Figure 7-1(a). These data points represent operation at maximum speed in head seas. Figure 7-1(b) also shows Bell-Halter's predicted V_{max} boundary for the Sea Bird SES (Reference 11).

Figure 7-1(a) SEA BIRD CLASS SES - 1σ HEAVE ACCELERATION VERSUS WAVE HEIGHT, MAXIMUM SPEED, HEAD SEAS, NO RCS

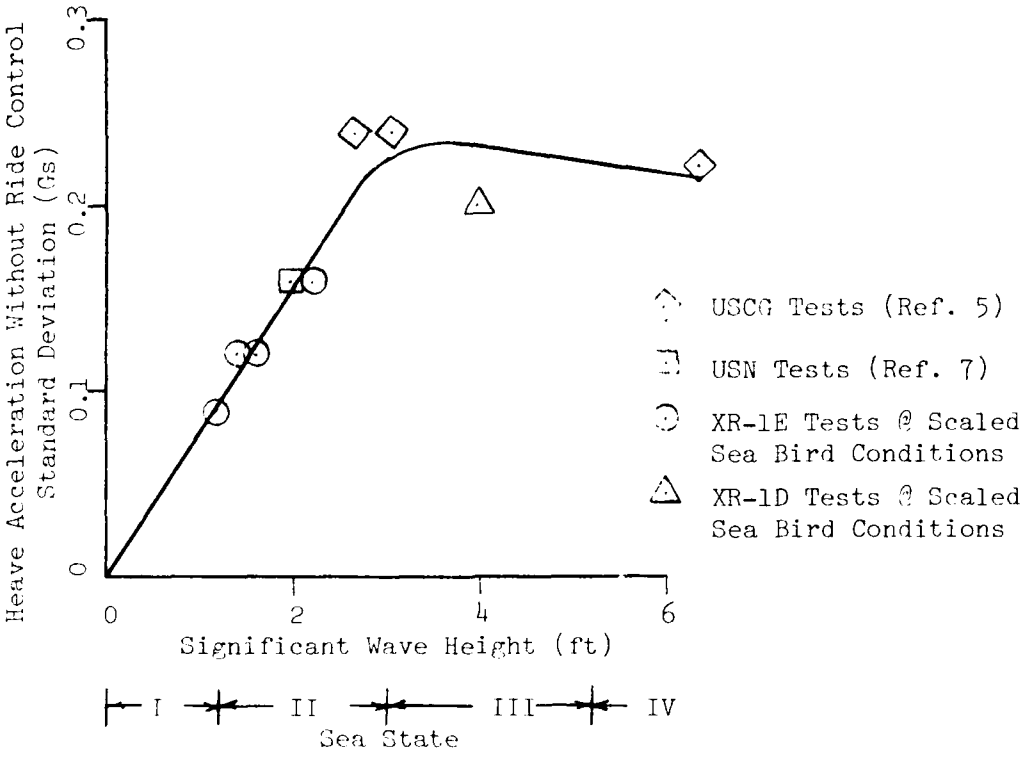

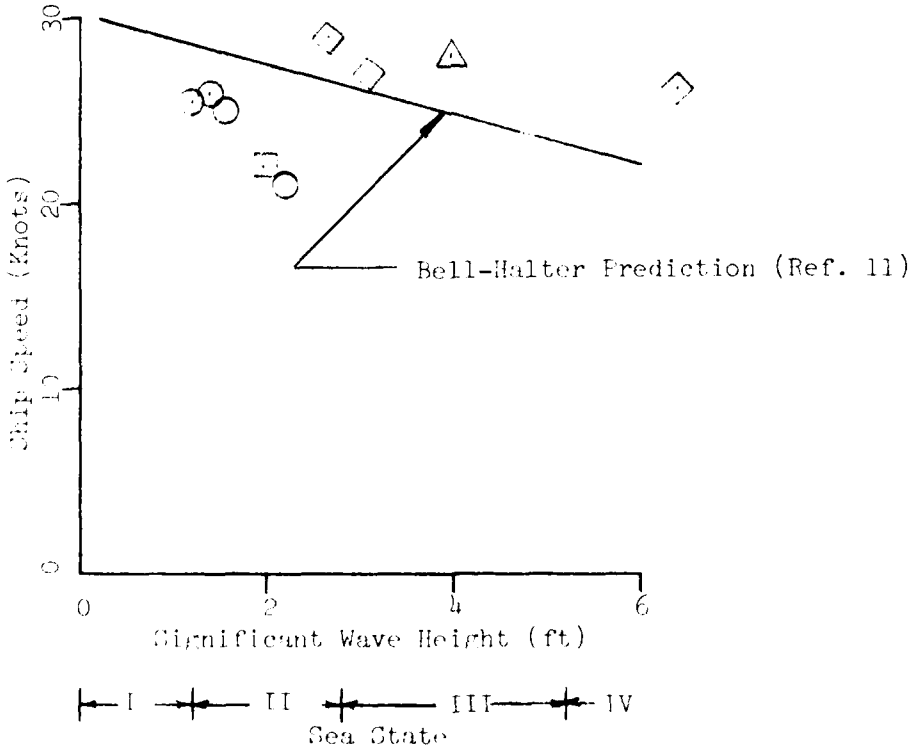

Figure 7-1(b) SEA BIRD CLASS SES - SPEED VERSUS WAVE HEIGHT, MAXIMUM SPEED, HEAD SEAS, NO RCS

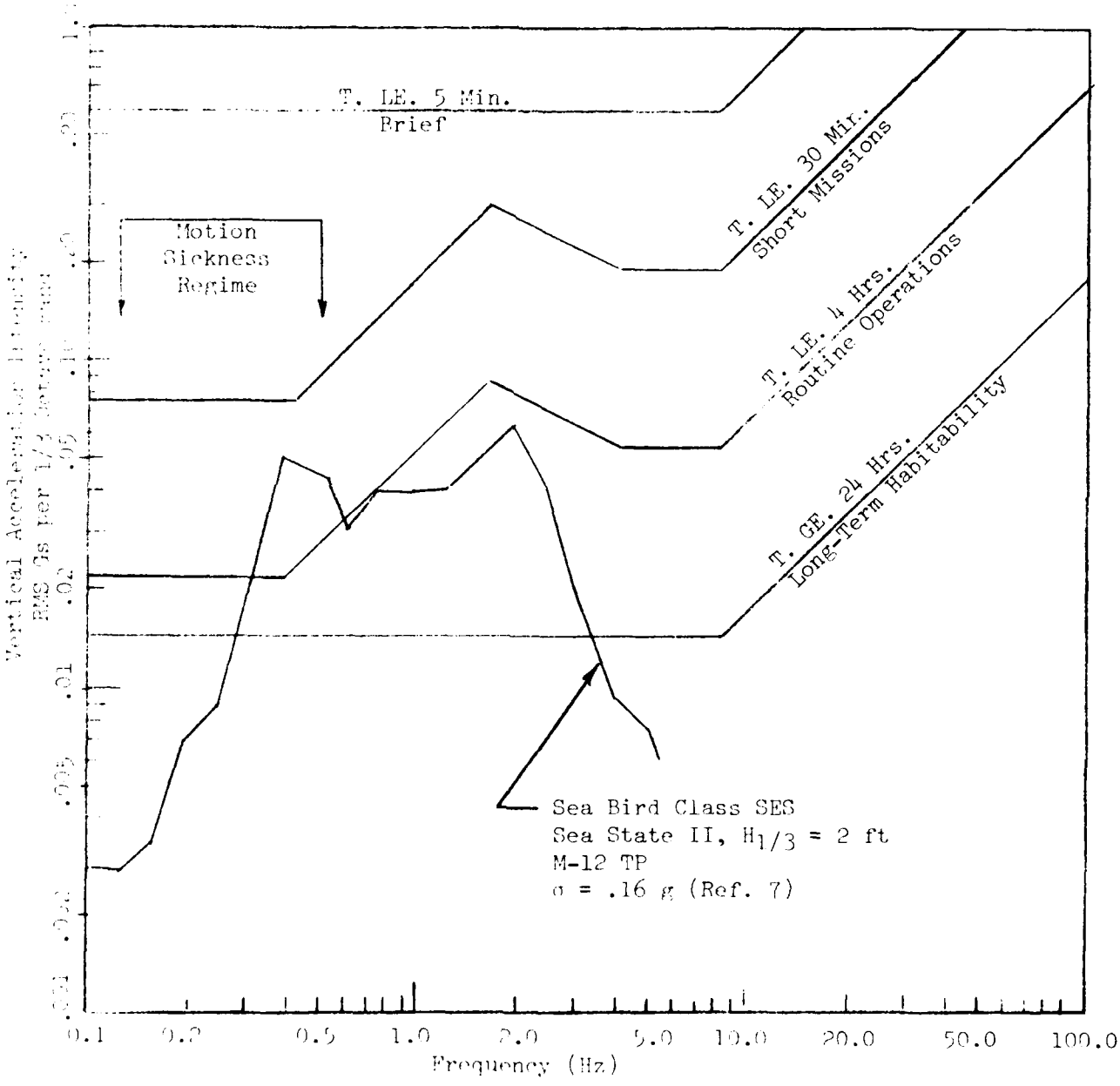

Figure 7-2 COMPARISON OF SEA BIRD CLASS SES HEAVE ACCELERATION WITH SES HABITABILITY CRITERIA, 20 KCS

Speed decreases linearly with increases in sea state from 30 knots in calm water to 22 knots in Sea State IV. The USCG data appear to confirm the Bell-Halter predictions. Scaled XR-1E data is shown to illustrate the scaled speeds at which these tests were run.

7.2 PREDICTED HEAVE ACCELERATION AND SHIP PERFORMANCE WITH RIDE CONTROL

7.2.1 Predicted Heave Acceleration With Ride Control

In order to make RCS-On heave acceleration predictions for the Sea Bird Class SES, a simple analytic technique was devised. This technique makes the assumption that the percent reduction in RCS-Off 1σ heave acceleration measured during XR-1E testing can be achieved on the Sea Bird Class SES using ride control. The analytical justification for applying this technique is that the XR-1E cushion dimensions (length, beam, height), displacement, lift flow rate, speed and sea state all approximate a 1/2-scale Froude model of the Sea Bird Class SES. Therefore, we predict that an RCS could be designed for the Sea Bird which would be as effective as the RCS on a 1/2 scale model.

Figures 7-3(a), -(b) and -(c) illustrate application of the technique to the Sea Bird Class SES. In Figure 7-3(a) the measured 1σ heave acceleration without ride control is plotted versus significant wave height. This plot is identical to Figure 7-1(a).

In Figure 7-3(b), the ratio of RCS-On to RCS-Off 1σ heave acceleration is plotted versus significant wave height. This figure was compiled using the XR-1E test data plotted in Figure 6-7(a), plus one XR-1D data point which was obtained at scaled Sea Bird conditions (see Reference 12). Significant wave height in this case has been scaled-up by a factor of 2 so that it represents the equivalent Sea Bird sea condition. The ratio of RCS-On to RCS-Off 1σ heave acceleration is non-dimensional and therefore was not scaled.

By multiplying the 1σ RCS-Off heave acceleration (from Figure 7-3(a)) by the ratio of RCS-On/RCS-Off from Figure 7-3(b), a plot of predicted 1σ RCS-On heave acceleration versus wave height is obtained. This plot is shown in Figure 7-3(c). It represents Sea Bird operation at maximum speed in head seas for Sea States I through IV.

Note that the prediction for Sea State IV is based on SES-200 data because there was no equivalent XR-1D or XR-1E data point. Use of SES-200 data may be criticized on the basis that the SES-200 and Sea Bird SES are not geometrically similar and they operate at different Froude numbers. These differences are not considered serious because the prediction is probably conservative. In Sea State IV, we would expect an RCS to perform better on the Sea Bird than on the SES-200 because of its smaller cushion volume relative to the installed fan capacity.

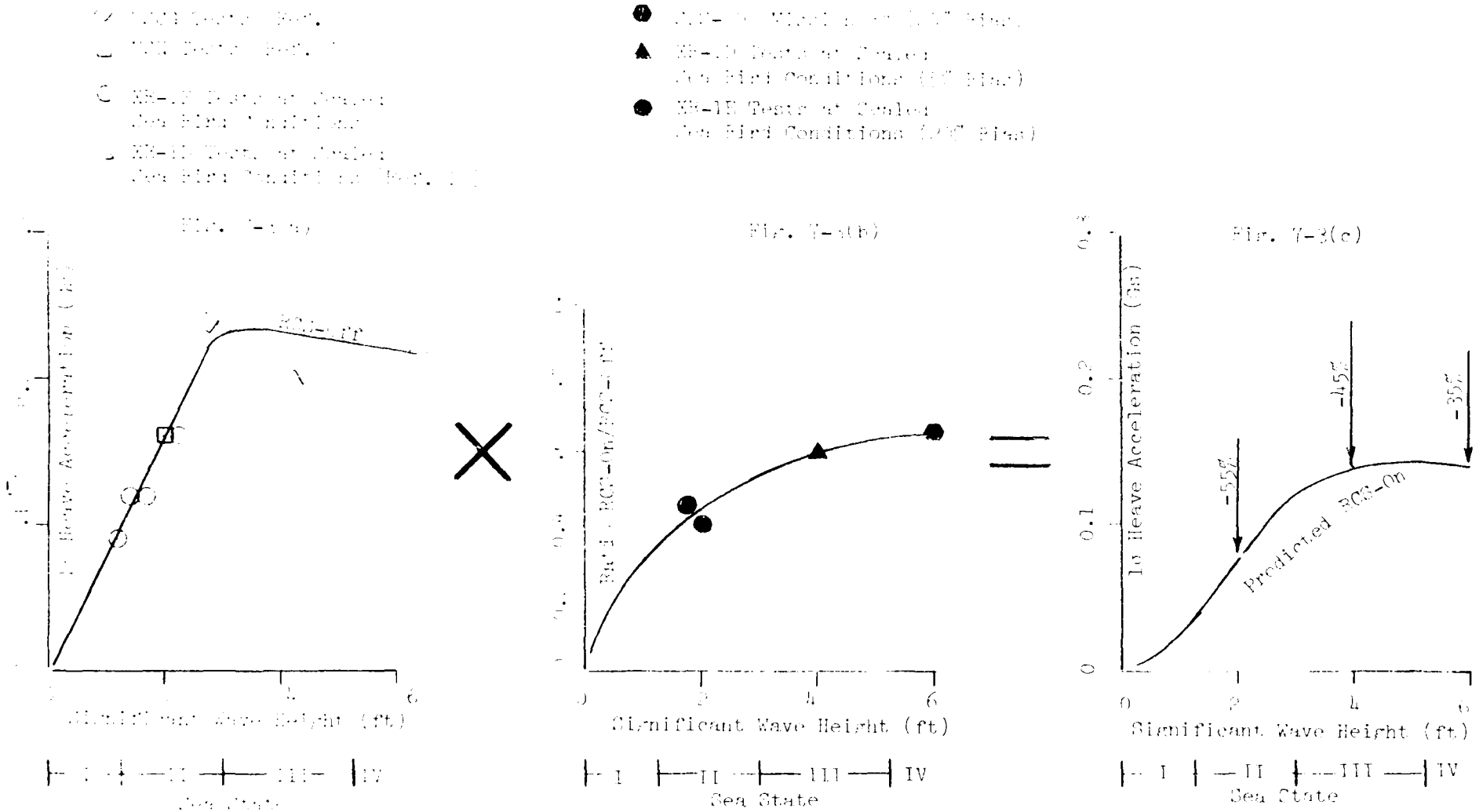

Figure 7-3 PREDICTION OF SEA BIRD CLASS SES HEAVE ACCELERATION WITH RIDE CONTROL
MAXIMUM SPEED, HEAD SEAS

Comparing Figures 7-3(a) and 7-3(c) shows that the RCS is predicted to reduce the 1σ heave accelerations by 50 to 60% in Sea States I and II, 40 to 50% in Sea State II and 35% in Sea State IV. This much reduction can significantly extend mission duration without crew fatigue. For the typical Sea State II head sea condition shown in Figure 7-2(a), the 1σ heave acceleration would be reduced by 60% from .16 g's to .06 g's. If the 1/3 octave RMS levels shown in Figure 7-2(a) are reduced 60%, they will cluster just above the Long Term Habitability line in the wave encounter frequency range (.3 - 4 Hz). This means with ride control, the onset of fatigue decreased proficiency will be extended from approximately 2 hours to at least 1 day and possibly longer. Crew efficiency and morale would be significantly improved during long transits, sweep and search and rescue operations. In higher sea states, the RCS still will be effective in delaying the onset of fatigue. System operation will be very noticeable in the larger seas due to attenuation of the pressure spikes associated with cushion venting.

In off head sea conditions the RCS is expected to reduce heave accelerations by the same percentages as those shown in Figure 7-3(c). Fatigue is caused by cumulative effects of acceleration level and mission duration. Therefore, it is expected that a Sea Bird crew would want to operate the RCS at all times during over hump operations in Sea States I - IV.

7.2.2 Ship Speed With Ride Control

As discussed in Section 6.2.3, RCS power requirements can be divided into the following categories:

1. Hydraulic power required to move the vent valve louvers.

2. Speed lost due to dumping pressurized air overboard through the vent valves.

Hydraulic power requirements are modest. A 19 gpm constant pressure variable flow pump has been selected for the proposed Sea Bird RCS hydraulic system (see Section 8.2.2). Under normal RCS operation, this pump will operate at 50% capacity and will absorb 20 hp or 0.6% of the total installed lift and propulsion power. This appears to be a very small price to pay considering the potential benefits. The excess flow capacity will be required only during initial dockside open loop tests to support control law development.

Predicted loss of speed due to RCS operation will be explained with the aid of Figures 7-4(a) and (b). In Figure 7-4(a), the change in speed following activation of the RCS is plotted versus significant wave height for XR-1E and SES-200 Head Sea Tests. XR-1E data points have been Froude-scaled using a ratio of 2 to represent the equivalent Sea Bird condition. SES-200 data has not been scaled. RCS heave acceleration predictions shown in Figure 7-3 were made using this same data base.

Figure 7-4(a) XR-1E AND SES-200 SPEED CHANGE AFTER RCS ACTIVATION, MAXIMUM SPEED, HEAD SEAS

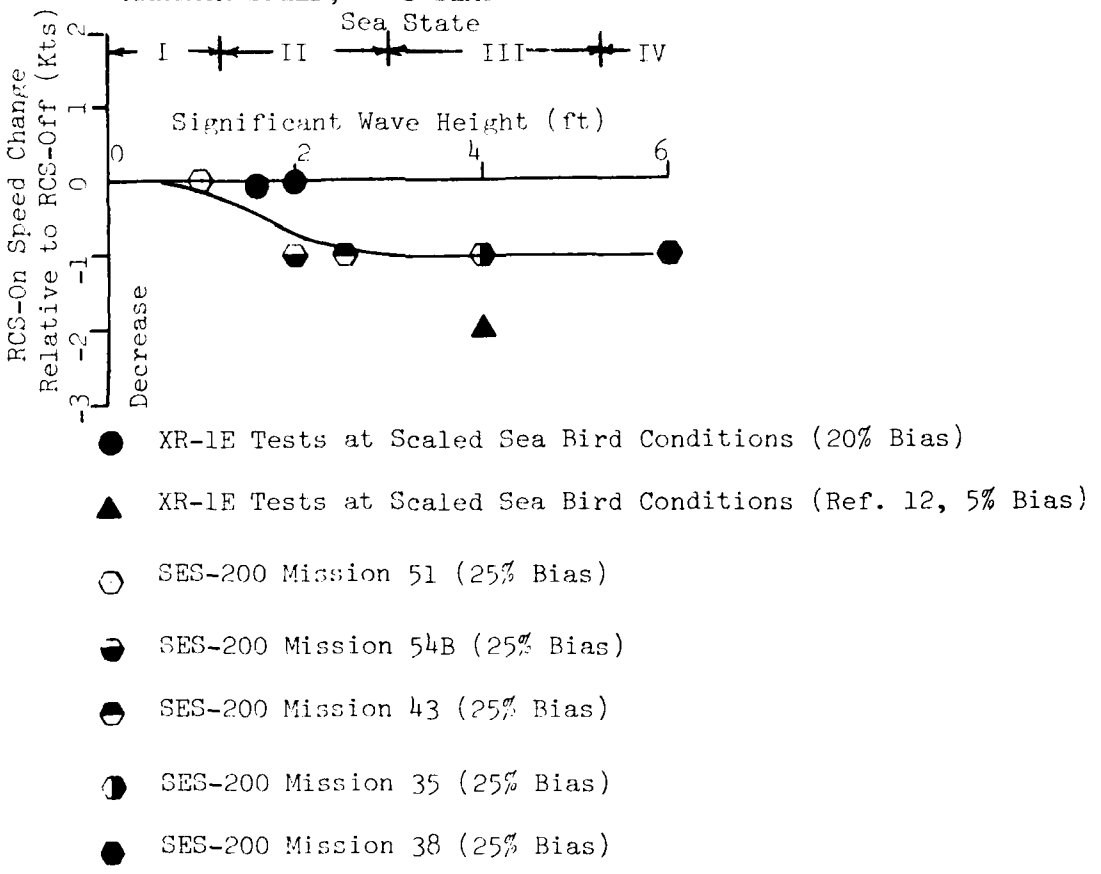

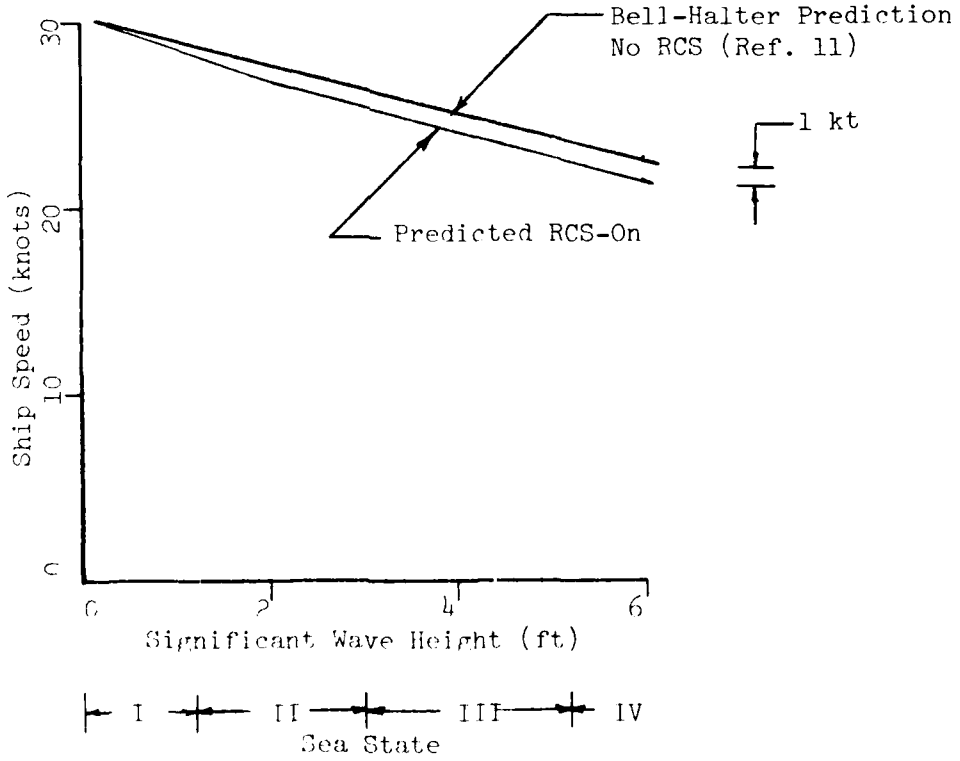

Figure 7-4(b) SEA BIRD CLASS SES, SPEED VERSUS WAVE HEIGHT, WITH AND WITHOUT RCS, MAXIMUM SPEED, HEAD SEAS

Based on Figure 7-4(a), it is predicted that the RCS reduction of heave acceleration illustrated in Figure 7-3 can be achieved with a 1 knot loss of speed. This would appear to be acceptable considering the appreciable reduction in heave acceleration which can be obtained (50% - 60% in Sea States I and II, 40% - 50% in Sea State III and 35% in Sea State IV). It should be noted that this speed loss is considerably less than predicted earlier (Reference 13) because the SES-200 data base was available to establish speed loss in the higher sea states. Figure 7-4(b) illustrates the predicted V_{max} boundary for head sea operation with and without ride control.

Impact of this 1 knot speed loss on the Sea Bird's range can be illustrated by considering an extended cruise in Sea State II. The following assumptions are made:

Fuel Capacity	=	7000 gallons
Fuel Consumption	=	160 gallons/hr.
Speed	=	28 knots

Present range at this cruise condition is:

$$\text{Present Range} = \frac{7000 \text{ gal.}}{160 \text{ gal./hr.}} \times 28 \text{ nm/hr.} = 1225 \text{ nm.}$$

With the RCS-On, the speed is 1 knot slower, so the new range is:

$$\text{RCS Range} = \frac{7000 \text{ gal.}}{160 \text{ gal./hr.}} \times 27 \text{ nm/hr.} = 1180 \text{ nm.}$$

The vessel's range has been reduced by 45 nm., or 3.7% for this extended cruise. In practice the range penalty would be even lower since it would not be normal for the vessel to operate at maximum speed until the fuel tanks are depleted.

The RCS configuration selected for the Sea Bird SES includes the installation of new port and starboard fuel tanks aft of Frame 13 (see Section 8). These tanks will reduce the present requirement to carry ballast aft in order to maintain an optimum LCG. The added fuel capacity (10%) will more than compensate for the range penalty associated with RCS operation.

8. CANDIDATE RIDE CONTROL SYSTEM INSTALLATION FOR SEA BIRD CLASS SES

The RCS installation selected for the Sea Bird Class SES is similar to the installation on the SES-200. This choice did not result from trying to duplicate the SES-200 installation. Instead, a tradeoff study which considered a variety of vent valve configurations showed this to be the best arrangement. This tradeoff study is summarized in Appendix C in case program sponsors wish to review the other configurations which were considered and eliminated.

Figure 8-1 illustrates the basic vent valve configuration and Figure 8-2 illustrates the spaces within the vessel which will be affected by retrofitting the RCS. The vent valve installation will involve installing two 3 ft by 5 ft flow trunks inside the Number 2 Centerline Fuel Tank. Vent Valve modules will be bolted to short trunk stacks which extend approximately 2 ft above the weather deck. This is similar to the SES-200 arrangement except that the number of modules has been reduced from four (4) to two (2). This considerably simplifies the mechanical and hydraulic portions of the ride control system.

Two non-integral fuel tanks (designated Number 3 Port and Starboard) will be installed in the unused spaces aft of Frame 13 to replace the volume of fuel removed from the Number 2 tank. This results in a favorable aft shift in the vessel's LCG because it is presently necessary to carry ballast in the aft (Number 3 ballast) tanks to maintain the LCG in the range required for best performance (1.5 ft aft of amidships).

At full load displacement the vessel nominally carries 7515 gallons of fuel, 1390 gallons of ballast water and weighs 323,700 lb for an LCG location 1.5 ft aft of amidships. Following retrofit of the RCS and the new fuel tanks, the vessel will carry 8242 gallons of fuel and will weigh 319,800 lb at full load displacement with a -1.5 ft LCG. The Sea Bird Class SES therefore will carry approximately 10% more fuel and weigh 3900 lb less at FLD after the RCS is installed. This favorable situation reduces the requirement to carry ballast water at FLD to maintain an optimum LCG position. At less than full load displacement, the modified craft also requires less ballast than the present configuration.

The hydraulic system will be located between Frames 9 and 10 in the lift engine compartment. Since the vent valve modules are located just aft of Frame 9, the plumbing requirements are minimal and all components are in proximity to one another. The hydraulic pump will be driven via a clutch which engages a belt-drive connected to the PTO pulley on the aft end of the starboard lift engine. A similar arrangement has proved satisfactory on the SES-200. The electronic control unit will be mounted on the bridge and interconnected with the various feedback sensors via a junction box located at Frame 10.

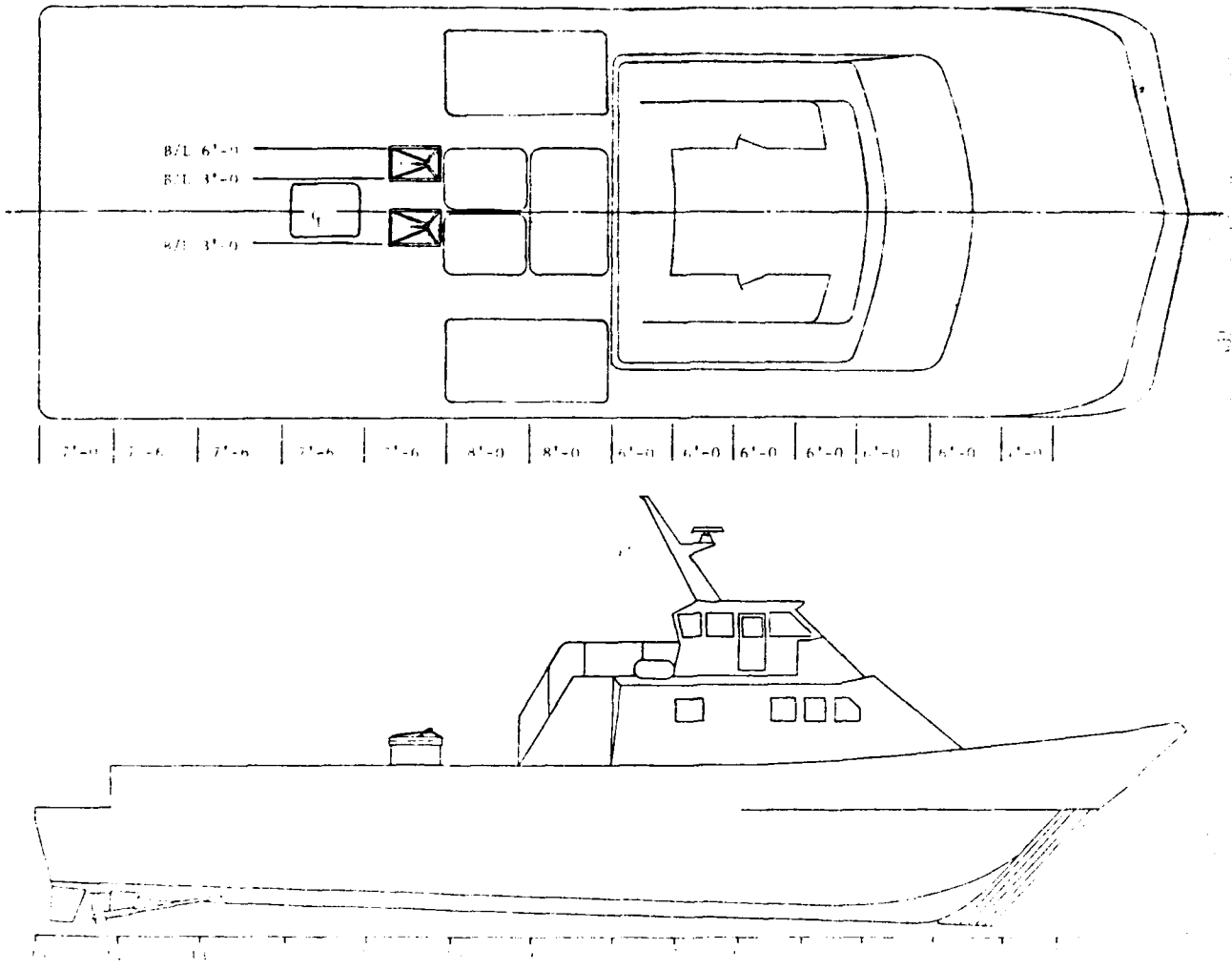

Fig. 1 Plan and Profile views of [illegible] configuration

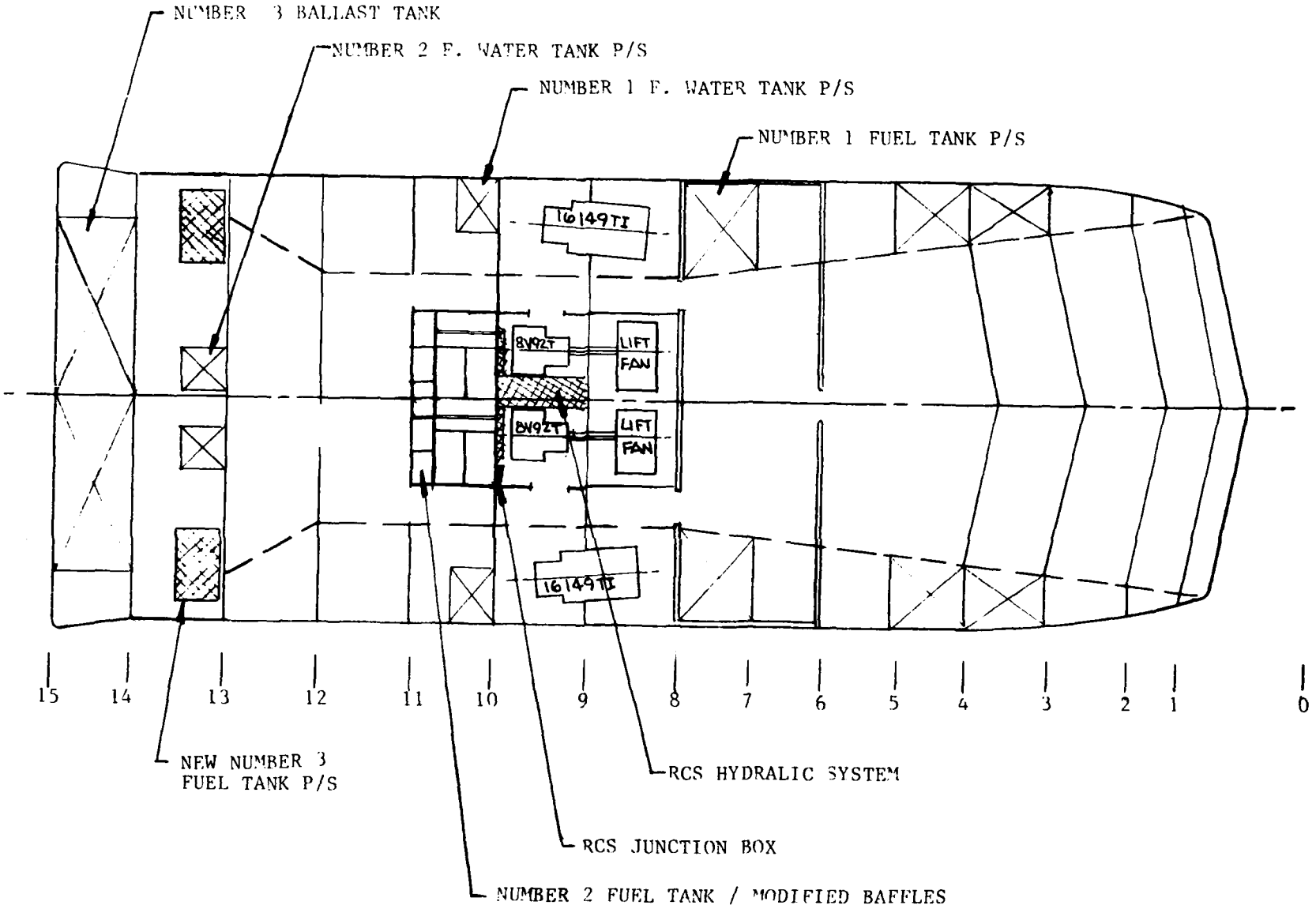

Figure 8-2 Sea Bird Class SES - Plan View at Second Deck of RCS Installation and Craft Modifications

8.1 IMPACT OF RCS INSTALLATION ON SEA BIRD CONFIGURATION AND OPERATION

In the following subsections the impact of installing the selected RCS configuration on the Sea Bird Class SES is examined in detail. Specifically discussed is the impact on the vessel's structure, weight, stability, machinery and operation.

8.1.1 Impact on Hull Structure and Arrangements

8.1.1.1 Flow Trunk Installation

Figure 8-2 illustrates the portion of the Number 2 Centerline Fuel Tank which must be modified to install the flow trunks. The structural changes primarily involve making penetrations through the various decks and modifying the fuel tank bulkheads and baffles as shown in Figure 8-3.

Cushion air inlets to the trunks will be located between wet deck longitudinals which are not presently used for seal air ducting. The starboard trunk inlet is located between the centerline and buttock line 3 ft 0 in. and the trunk is erected vertically. On the port side, the inlet is located between buttock lines 4 ft 6 in. and 7 ft 6 in. The port trunk slants inboard 18 inches between the second deck and weather deck. This distance corresponds to the spacing between longitudinal stringers. The slanted arrangement is considered good structural design practice because it places the port weather deck cutouts within the shadow of the lift engine and fan cutouts (see Figure 8-1).

The flow trunk installation would be accomplished by first removing the longitudinal fuel tank bulkhead at port buttock 7 ft 6 in. for access into the fuel tank. Weather deck, second deck and wet deck penetrations would also be made at this time to gain access to the remainder of the fuel tank. The deck cutouts would be reinforced with 3/8 inch doublers to preserve the hull section modulus and prevent cracking in the corners. Longitudinal Tee stiffeners inside the flow trunks at the wet deck (port buttock 6 ft and starboard buttock 1 ft 6 in) and the weather deck (port buttock 4 ft 6 in. and starboard buttock 1 ft 6 in.) would be converted to box beams and faired with half-rounds. This maintains longitudinal continuity of the hull structure.

The starboard trunk installation requires removing part of the longitudinal baffle at starboard buttock line 1 ft 6 in. and sections of the two transverse baffles between the ℄ and starboard buttock line 3 ft 0 in. Framing on the aft side of Bulkhead 10 will be modified to form the forward trunk wall (see view in upper right corner of Figure 8-3). Then solid bulkheads will be erected on the ℄ and on starboard buttock line 3 ft 0 in. to make the longitudinal trunk walls (see Section C-C of Figure 8-3). The trunk is enclosed by adding a solid transverse bulkhead between these two longitudinal walls. Horizontal stiffeners will be installed on the trunk walls to stiffen the plate so it can carry design pressure loads. Baffles which are modified will be rewelded to the trunk walls after the stiffener installation is complete.

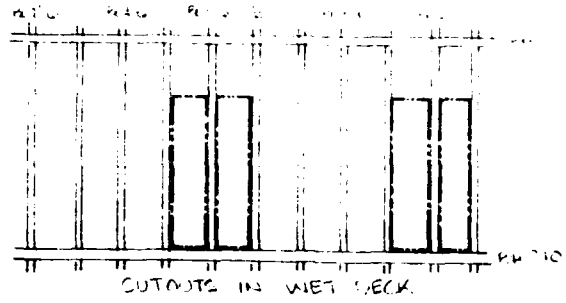

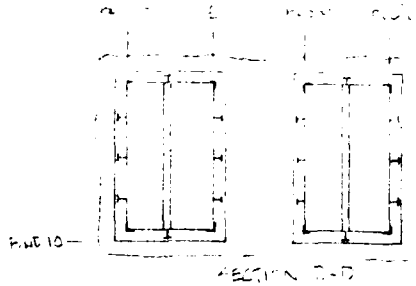

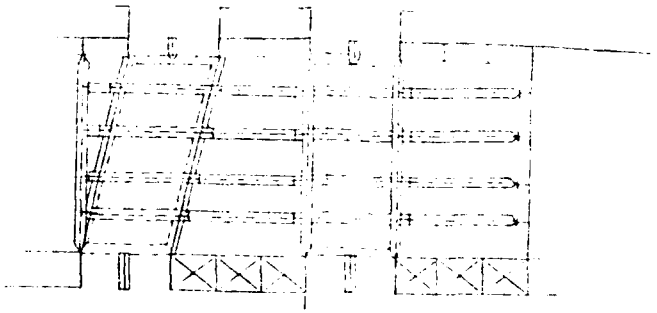

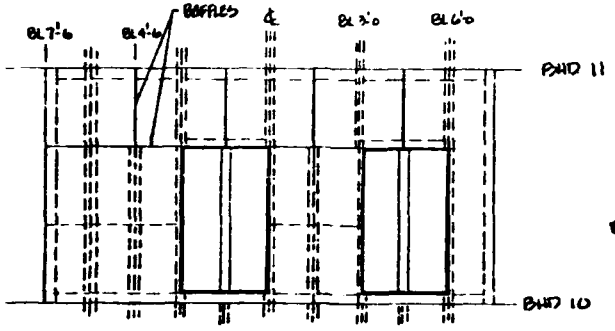

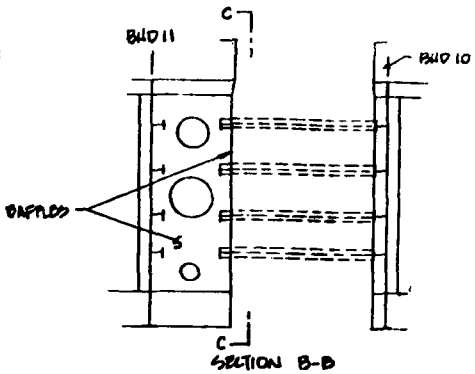

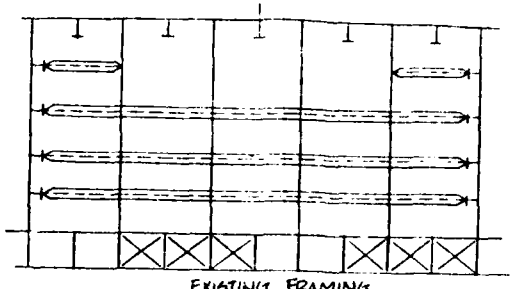

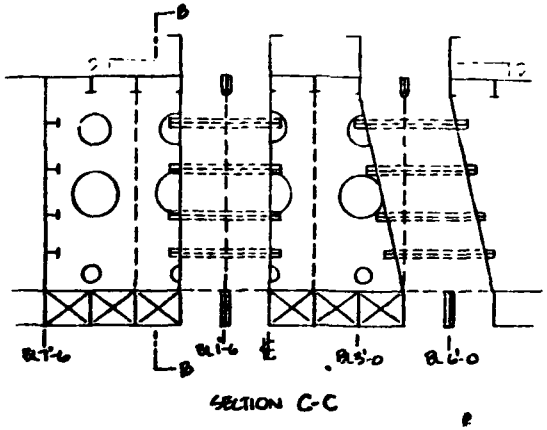

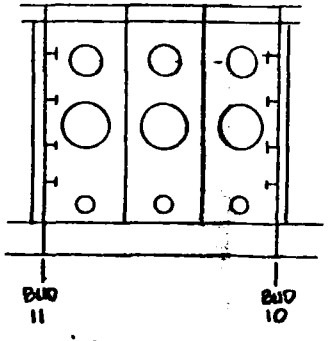

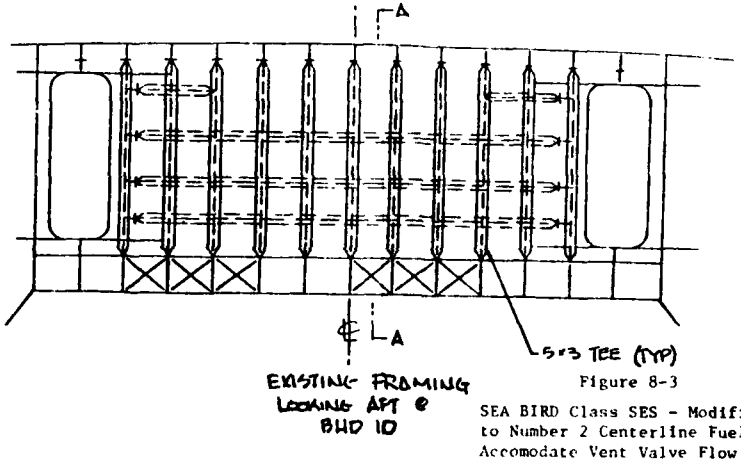

Figure 8-3

SEA BIRD Class SES - Modifications to Number 2 Centerline Fuel Tank to Accomodate Vent Valve Flow Trunks

Installation of the port trunk is similar to that of the starboard trunk except the longitudinal walls slant inboard 18 inches as previously discussed. The longitudinal fuel tank bulkhead at port buttock line 7 ft 6 in., which was removed for access, will be replaced with a slanted bulkhead as illustrated in Section C-C of Figure 8-3. This slanted bulkhead will serve as both a the fuel tank and trunk outboard wall.

Above the weather deck, the trunks terminate in short vertical stacks. The stack plating is stiffened vertically to withstand air pressure loads and provide an adequate foundation for the vent valve modules.

One definite advantage of installing the trunks in the fuel tank is that the entire installation is a structural modification. It will not be necessary to relocate existing machinery or electrical systems. This should help hold down costs since only one labor category (welders) will be required.

8.1.1.2 Fuel Tank Installation

The new Number 3 Port and Starboard Fuel Tanks, which must be installed to compensate for the volume of fuel removed from the center tank, will be located in unused spaces aft of Frame 13. These spaces are located over the sidewalls as illustrated in Figure 8-4(a). The proposed style and construction for these non-integral tanks would be identical to that used for the existing Number 2 Fresh Water Tanks which also are installed in this compartment (see Figure 8-4(b)).

Each tank would have a maximum height of 5 ft at Bulkhead 13 and would be 5 ft long by 7.5 ft wide. On the port side, installation of the fuel tank would necessitate moving the rope basket. This is considered minor since there is sufficient space on the port side between Frames 12 and 13 to relocate the basket.

Each tank will hold 1192 gallons and will have a 1-1/4 inch suction line with a reach rod to the main deck and a sediment/water trap. The return fuel lines will be 1 inch diameter and equipped with gate valves. Sight gauges will be installed on the inboard side of each tank so soundings can be taken. Suction and return lines will be connected into the existing fuel system such that the new Number 3 Tanks can supply all engines and the return fuel can be routed to any tank. These new tanks will be connected to the fuel transfer/filtration system.

8.1.2 Impact on Weight and LCG

The USCG SES squadron at Key West and the Office of Research and Development supplied MariDyne with draft readings for the Sea Hawk. These measurements were made during the Week of 11 April after the vessel's voids, bilges and ballast tanks had been pumped out and a full load of fuel and fresh water were on-board. The drafts measured 7 ft 8 in. forward and 9 ft 3 in. aft. Using the draft tables in Reference 14, the weight and LCG location for this condition are 311,810 lb and 0.07 ft forward of amidships, respectively. These values were used as a baseline for assessing the impact of the RCS installation on the vessel's weight and LCG.

Figure 8-4(a) View Looking Outboard Between Frames 13 and 14, Starboard Side, Proposed Location for Installation of Non-Integral Number 3 Port and Starboard Fuel Tanks.

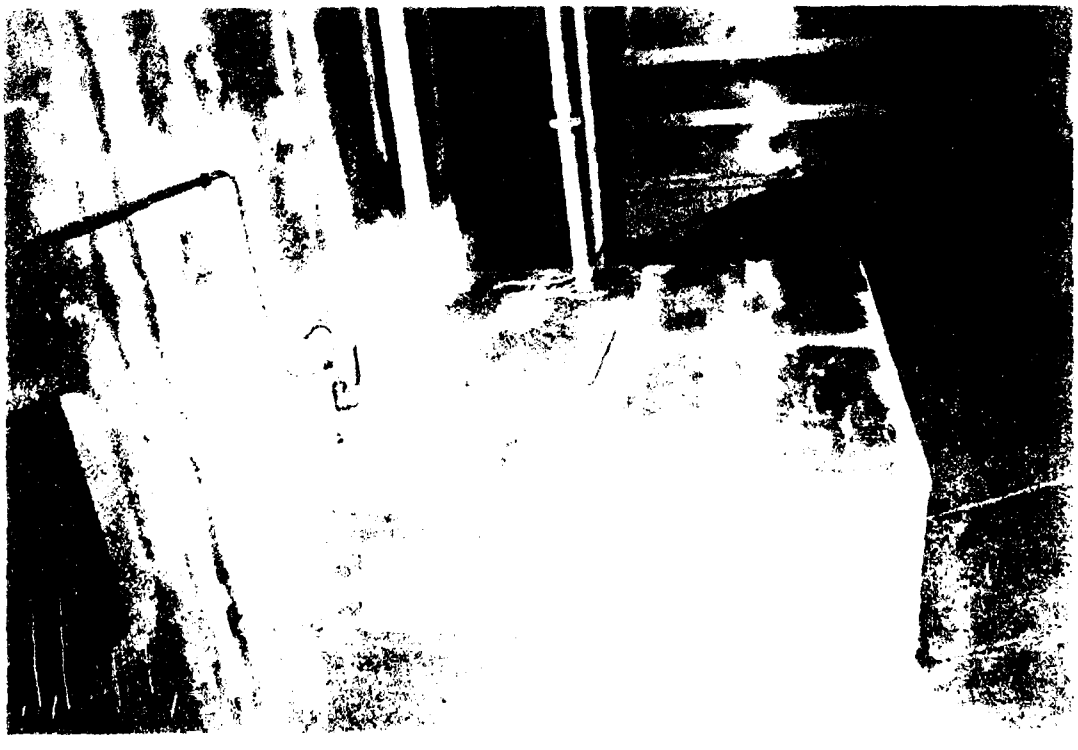

Figure 8-4(b) Basic Tank Style Proposed for Number 3 Non-Integral Fuel Tanks.

Reference 14 states, " For best performance and most comfortable ride the vessel should be loaded to place the longitudinal center of gravity approximately 1.5 ft aft of amidships and the lateral center of gravity on the centerline". This paragraph is referring to cushionborne operation and, in particular, to over hump operation, i.e., speeds in excess of 20 knots where proper LCG location is critical for optimum performance. This should be the optimum LCG position regardless of sea state or heading as long as the vessel is on-cushion. In order to ballast the present vessel to the optimum LCG at full load conditions, it is necessary to carry 1390 gallons of ballast water in the Number 3 Tanks which are located aft of Frame 14. This increases the FLD by 11,900 lb to a new total of 323,710 lb.

Values used to calculate this ballasted FLD condition are summarized in the following table. The ballast tank LCG is from the Tank Capacity Tables given in Appendix I of Reference 14. Midships is defined in Reference 14 as being 9/16 inch aft of Frame 9. LCG values are positive (+) if forward of amidships and negative (-) if aft of amidships.

Item	Weight(lb)	LCG (ft)	Moment (ft-lb)
Full Load Δ w/o Ballast	311,810	+ 0.07	21,827
Ballast in No. 3 Tanks	+11,900	-43.13	-513,247
Full Load Δ w/ Ballast:	323,710	- 1.52	-491,420

Carrying 1390 gallons of ballast on-board to maintain a 1.5 ft aft LCG for optimum performance at FLD is consistent with the Ballast Schedules in Appendix II of Reference 15. It is also consistent with rule-of-thumb operational reports of taking on ballast for 7 minutes per tank before leaving dockside at FLD. The ballast pump is rated at 75 GPM which puts 1050 gallons of sea water in the aft tanks.

The present necessity to carry this much ballast to maintain an optimum LCG is undesirable since it increases the vessel's displacement. This prompted investigating the proposed RCS installation in which the flow trunks are installed in the Number 2 Center Fuel Tank and the fuel displaced is installed in new non-integral tanks aft of Frame 13. FLD weight and moment estimates which follow show that this arrangement can be very advantageous because it will reduce the need to carry ballast.

FLD weight and moment estimates for all craft modifications associated with the RCS installation are tabulated below along with the new

FLD weight and LCG for the modified vessel.

Item	Weight (lb)	LCG (ft)	Moment (ft-lb)
Present Sea Bird @ FLD w/o Ballast	+311,810	+ 0.07	+ 21,827
1660 gal. Fuel Removed TK #2	- 11,730	-11.53	+135,247
Flow Trunk Struc.Mods. TK #2	+ 55	-11.53	- 634
Vent Valve Modules	+ 450	-11.53	- 5,189
Hydraulic System	+ 635	- 5.5	- 3,493
New #3 P/S Fuel Tanks	+ 1,700	-34.34	- 58,378
2385 gal. Fuel TK #3 P/S	+ 16,880	-34.50	-582,360
Modified Sea Bird @ FLD:	319,800	- 1.54	-492,980

As shown above, retrofit of the RCS reduces the nominal full load displacement at optimum LCG to 319,800 lb or 3,900 lb less than the present FLD (323,710). Additionally, the vessel's fuel capacity has been increased by 10% which will more than compensate for any speed loss or range penalty due to RCS operation. Therefore, we conclude that the RCS installation will have a favorable impact on weight and LCG. This could help other planned USCG retrofit projects such as vertical stacks, sound proofing and electronic gear installations, since these items will add weight forward of amidships. Without the RCS modifications, these installations will further aggravate the LCG problem and make it necessary to carry even more ballast in the aft tanks.

It will be necessary to check the modified craft's weight and LCG at 50% and 25% fuel load as part of a more detailed weight survey. Based on the ballast schedules in Appendix II of Reference 15, it is predicted that in all cases the modified craft will weigh less than the present vessel because the requirement to carry ballast in the aft tanks will be reduced.

It should be noted that the Key West SES Squadron reports that in a few extreme wind and sea conditions, performance may be best with the LCG positioned forward of Bell-Halter's published value (1.5 ft aft of amidships). Reports vary from carrying only a little ballast in the aft tanks to carrying small amounts of ballast in the forward tanks. This comment was surprising since model and full-scale SES experience would suggest a single optimum LCG for over hump operations, regardless of sea condition. Recent Navy experience with the SES-200 confirms this last statement. In fact, on the SES-200,LCGs forward of the published optimum are definitely undesirable from the standpoint of both performance and motions.

What may be happening is that very high head winds (>35 kts) acting on the sizeable frontal area are producing a significant bow-up moment. This effectively shifts the LCG aft and could explain why little or no ballast is required in the aft tanks at times. Regardless of the reason, it should be noted that the RCS installation has not hindered the operator's ability to ballast the craft to a forward LCG if desired. All three pairs of ballast

tanks (#1 Forward, #2 Forward and #3 Aft) will remain fully operational to fine-tune the longitudinal (LCG) and transverse (TCG) center of gravity positions. Additionally the RCS control unit (Section 8.2.3) can provide the SES operator with mean pitch and roll attitude displays. USCG SES operators at Key West indicated that these displays would be very helpful in assessing the vessel's trim and list for purposes of transferring fuel or ballast to optimize performance.

8.1.3 Impact on Stability

Analysis of the impact of the proposed modifications on intact and damage stability is outside the scope of this present effort. SES in general have excellent intact and damage stability characteristics due to the catamaran hull form and close spacing of full depth bulkheads. For the Sea Bird, a very preliminary stability investigation has been made which indicates there are no serious problems.

Installation of the vent valve stacks and modules on the weather deck may cause a slight rise in the vertical center of gravity ($\overline{KG}$). This change should be insignificant because the weight added above the weather deck (≈ 500 lb) is negligible compared to the 15.5 L.T. Coast Guard Certified load limit for deck cargo (Reference 15). On these preliminary grounds, no problems with intact stability are expected.

Watertight bulkhead spacing on the Sea Bird Class presently meets U. S. Navy two-compartment damage stability criteria (Reference 16). It will be necessary to perform floodable length calculations to ensure this standard still can be met after installation of the flow trunks and new fuel tanks. The flow trunk installation should not affect the two-compartment standard because the volume in question is treated as lost buoyancy regardless of whether it contains fuel oil or air ducting. In the stern, the new fuel tanks will cause some additional loss of reserve buoyancy and the impact will have to be checked. If the two-compartment standard cannot be met, it will be necessary to make the bulkhead at Frame 13 watertight. This would involve only straightforward structural details.

8.1.4 Impact on Machinery

Modifications required for installation of the RCS will not have a significant impact on the ship's machinery or its maintenance and operation. It will not be necessary to remove, relocate or extensively modify any of the ship's machinery in order to install the RCS. System operation will be easy because logic for performing self-checks, fault monitoring and shutdowns allows the RCS to be left unattended. Maintenance is relatively straightforward since it primarily involves lubricating the vent valves and inspecting the linkages.

The only machinery work that will be required is connecting the new fuel tanks into the fuel system and installing a belt drive and clutch mechanism to extract power from the starboard lift engine to drive the hydraulic pump. These are both straightforward tasks. Plumbing for the new fuel tanks will be identical to that used in the existing fuel system and should not present any problems. The lift engine has sufficient excess power to drive the hydraulic pump even at maximum fan rpm.

8.1.5 Impact on Ship Operation

Initially, MariDyne personnel were concerned that the proposed deck-mounted vent valve configuration might impact ship operations. There were two reasons for this concern:

1. The vent valve stacks would take up deck space which is presently used for cargo or other purposes.

2. Vent valve air flow would interfere with personnel movement on the deck during RCS operation.

The proposed vent valve configuration was discussed with the USCG SES Squadron at Key West on 8 April. The operators expressed the opinion that the deck-mounted vent valve configuration would not interfere with vessel operation. They did not feel that the deck area occupied by the vent valves was large enough to limit the vessel's cargo capacity. Also, they stated that during cushionborne operation in waves the deck is too wet for personnel to use. Cushion venting under the sidewalls and seals causes this wetness. Since no one normally will be on the weather deck, the vent valve air flow should not pose any problems.

8.2 CANDIDATE RIDE CONTROL SYSTEM DESCRIPTION

A general description of the proposed RCS installation and its impact on the Sea Bird Class SES was covered in the previous sections. In the sections which follow the various elements of the RCS, e.g., the vent valve modules, hydraulic system and electronics are described in more detail and some general hardware specifications are given. Additionally, system operation and maintenance are discussed.

8.2.1 Vent Valve Module Description

The vent valve installation proposed for the Sea Bird Class SES is similar to the installation on the SES-200 (see Figure 8-5) except there will be only two large vent valve modules instead of four smaller valves. Additionally, the Sea Bird vent valves will discharge the air flow aft instead of athwartships as is the case on the SES-200.

Each module will be 3 ft wide by 5 ft long and contain five louvers. General specifications for the module assembly are given in Table 8-1.

AD-A150 443 DESIGN DEVELOPMENT AND TESTING OF A PROTOTYPE DIGITAL RIDE CONTROL SYSTEM..(U) MARITIME DYNAMICS INC TACOMA WA J D ADAMS ET AL. JUN 83 MD-AR-1195-1 USCG-D-31-84 2/2

UNCLASSIFIED N00167-82-C-0079 F/G 13/10 NL

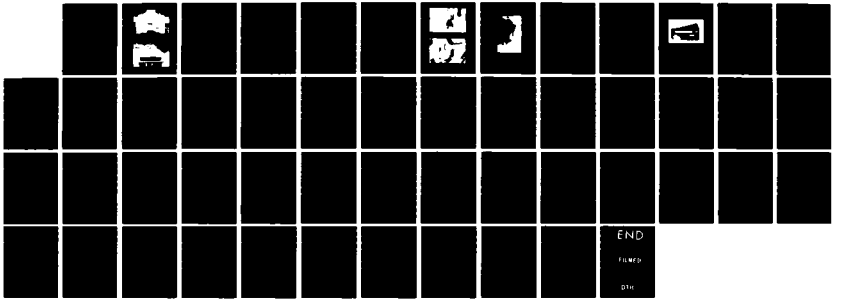

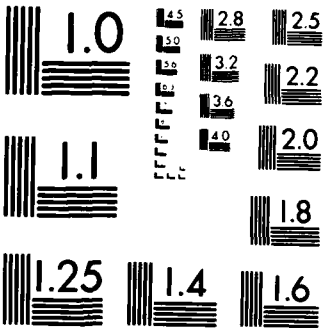

Figure 8-5(a) View Looking Forward at SES-200 Vent Valve Installation

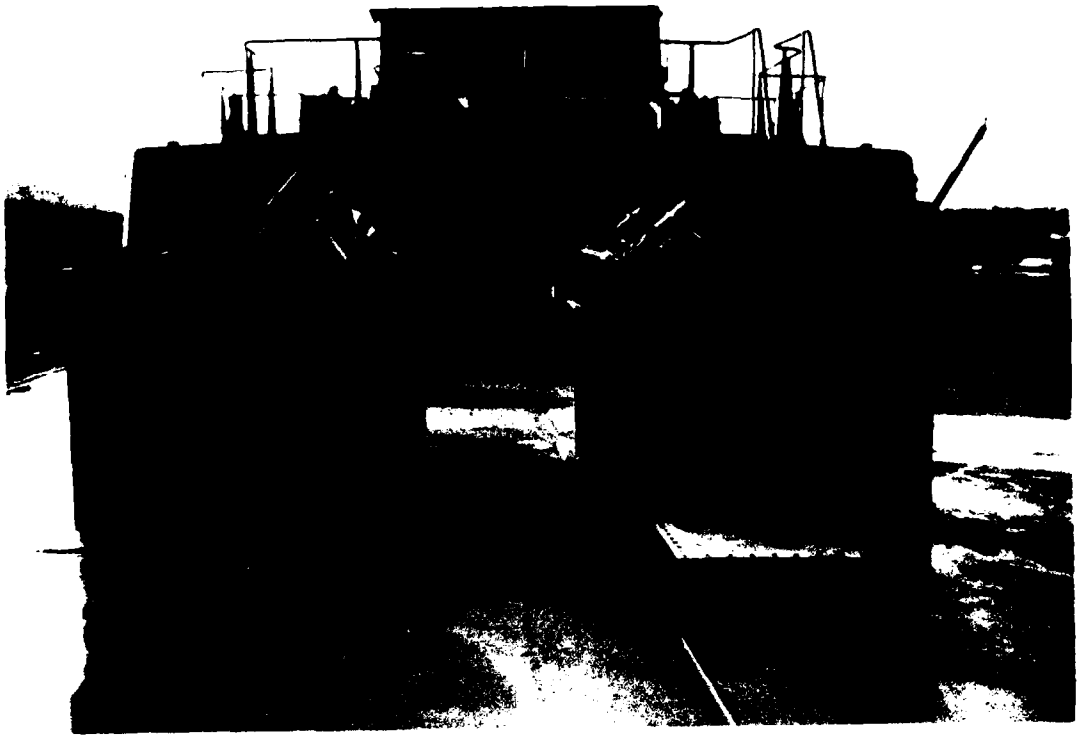

"Note" Sea Bird Class SES Vent Valve Modules will be similar except there will only be two modules not four and the vanes will discharge aft not athwartships. Sea Bird modules will be 3ft wide x 5ft long with 5 louvers per assembly.

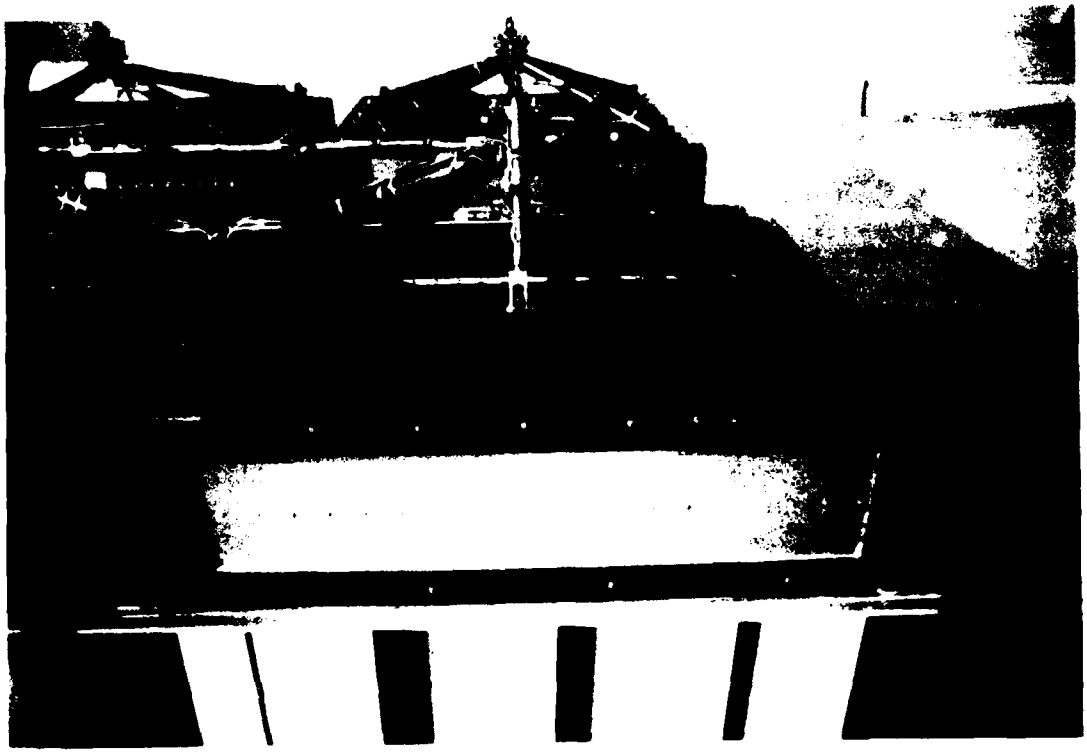

Figure 8-5(b) View Looking Down on SES-200 Vent Valve Module

TABLE 8-1

PRELIMINARY VENT VALVE MODULE SPECIFICATION
FOR
USCG SEA BIRD CLASS SURFACE EFFECT SHIP

ITEM	MANUFACTURER
Vent Valve Module Assembly Length: 5 ft Width: 3 ft Height: 24 in. Materials: 6xxx series Aluminum Extrusions Finish: Hard-Anodized Louvers: 5 Airfoil-type, 12 in. chord, 2 in. thickness Bearings: Commercial self-aligning Servovalve: Moog Series 34 Actuator: Sheffer HH Series LVDT: Schaevitz HPD Series	Maritime Dynamics, Inc. 1169 East Ash Avenue Fullerton, CA 92631

The louvers, channels, link bar and tubular frame are constructed from 6xxx series aluminum extrusions which have been hard-anodized to prevent corrosion. Self-aligning bearings are used throughout the mechanism to minimize radial internal clearances and avoid binding due to the combination of forces acting on the louvers. Bulb seals are fitted along the trailing edge of each louver and on the end frames to prevent air leakage when the system is not in use. Bulb seals also are installed at the ends of the louvers.

The mechanism is aerodynamically balanced such that cushion pressure will hold the louvers closed when hydraulic or electrical power has been secured. Aerodynamic closing torque in this condition is sufficient to prevent air from leaking between the seals. This is a fail safe feature.

Each module contains its own actuator, servovalve and linear variable differential transformer (LVDT) for actuator position feedback. All of these components are stock commercial items.

8.2.2 Hydraulic System Description

Figure 8-6 shows a simplified schematic of the Hydraulic System which will provide flow to the vent valve modules. It has approximately 50% fewer components than the system installed on the SES-200 because of the reduction in the number of vent valve modules. Table 8-2 lists general specifications for the system.

The hydraulic pump will be driven via a clutch assembly which engages a belt drive connected to the aft end of the starboard lift engine. Clutch engagement can be accomplished remotely from the bridge whenever the operator wishes to use the RCS. The pump selected would be a variable flow/constant pressure type rated at 3000 psig and 19 gpm at 1800 rpm.

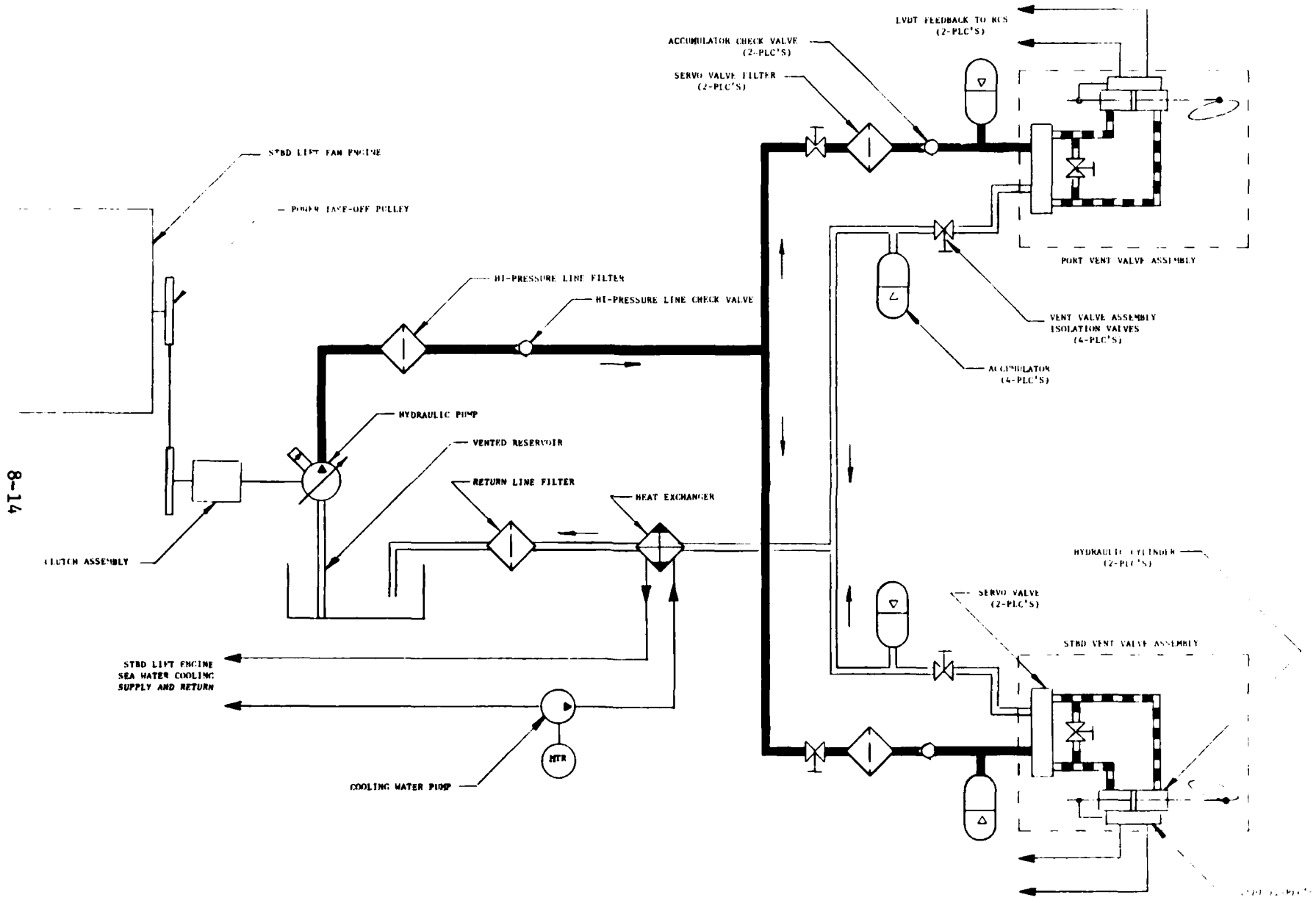

Figure 8-6 Sea Bird Class - RCS Hydraulic Schematic

TABLE 8-2
PRELIMINARY RCS HYDRAULIC SYSTEM SPECIFICATION
FOR
USCG SEA BIRD CLASS SURFACE EFFECT SHIP

Ratings/Requirements	Units
System Ratings:	
Nominal Pressure	3000 psig
Proof Pressure (for High Pressure Components)	4500 psig
Temperature Range	-40° F. to +250° F.
Fluid Type	Petroleum Based, MIL-H-5606, DTE*, etc.
Reservoir Volume	10 gal.
Pump Rating:	
Nominal Pressure	3000 psig
Flow @ Rated RPM	19 gpm @ 1800 rpm
Filtration Requirements:	
Main High Pressure	3 μm
VV High Pressure	10 μm
Main Low Pressure	10 μm

*Same as Sea Bird Hydraulic Steering System.

Hydraulic oil flows from the reservoir to the pump and then goes through the high pressure line filter and check valve. At this point, the flow splits and goes to the two vent valves. Each vent valve has its own shutoff valve, filter, check valve and accumulator on the high pressure side. On the return side, each system has an accumulator and shutoff valve. Oil returning from the vent valves passes through the heat exchanger and low pressure filter before dumping back into the reservoir. Either vent valve may be isolated using the supply and return line shutoff valves if it becomes necessary to secure one system.

All of the hydraulic system components except for those on the vent valve modules will be located in the lift engine compartment. Figure 8-7(a) shows the aft inboard side of the starboard lift engine with the engine foundation and related structure. A metal screen covers the vibration damper and the PTO pulley. The hydraulic pump and clutch mechanism will be installed on their own foundation close to the inboard rear corner of the starboard lift engine. They will be driven via a belt connected to the PTO pulley.

Figure 8-7(b) shows the forward inboard side of the starboard lift engine and a portion of Bulkhead #9. The area on the bulkhead between the lift engines is a suitable location for the hydraulic reservoir and return line filter. Beneath the reservoir there is enough room for the heat exchanger and cooling water pump. Cooling water can be tapped off the sea water intake located between the lift engines.

Figure 8-8 shows the center portion of the forward side of Bulkhead #10 which separates the lift engine compartment from the Number 2 Fuel Tank. The flow trunks will be located just aft of this bulkhead. Therefore, this makes an excellent mounting location for the accumulators, filters, check valves and shutoff valves for each vent valve system. This installation should not restrict the passageway between the lift engines.

8.2.3 Electronics Description

Figure 8-9 illustrates the major RCS electronic components and their interconnection. The control unit will be located on the bridge and interconnected with the vent valves and transducers via a junction box located at Bulkhead #10. Power for the system will be obtained from the ship's 115 v./60 Hz generator via a 5 amp circuit breaker. Interconnect cabling can be either waterblocked vinyl or armored, depending upon USCG requirements.

Preliminary specifications for the RCS electronics are listed in Table 8-3. A block diagram of the system developed for the SES-200 is illustrated in Figure 5-1, and Figure 8-10 shows a picture of the SES-200 control unit. A Sea Bird system block diagram and control unit would be similar with the exception that there would be hardware for two vent valves instead of four. Commercially rated components and power supply were used in the SES-200 system in order to save costs and avoid lead times which would impact the development. These commercial components were installed on modules which conform to MIL-STD-28787 (USN Standard Electronic Modules). The modules plug into a card cage and backplane which also conform to MIL-STD-28787. This arrangement permits the components which perform various functions (A/Ds, D/A, CPU, RAM, ROM) to be packaged as modules.

Figure 8-7(a) View Looking Outboard at Aft End of Starboard Lift Engine, Proposed Location for Installation of Power Take-Off and Hydraulic Pump.

Figure 8-7(b) View Looking Forward Between Lift Engines at Frame 9 Bhd., Proposed Location for Hydraulic Cooling Water Pump and Heat Exchanger.

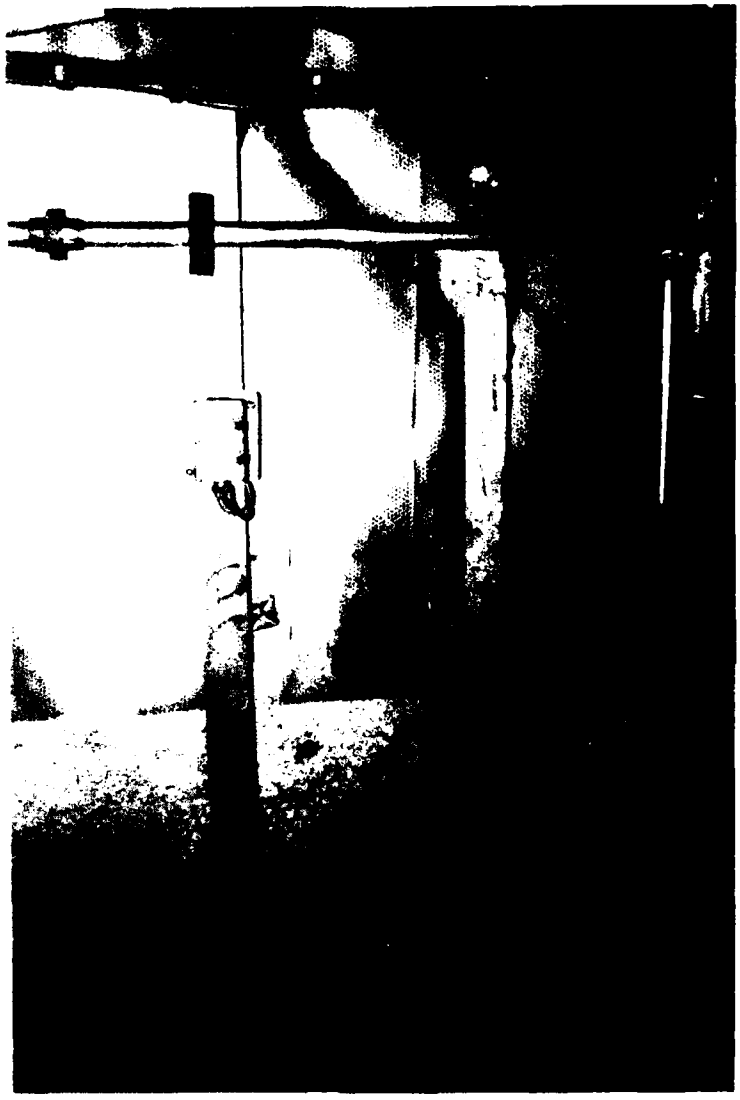

Figure 8-8 View Looking Aft at Frame 10 Bulkhead.
Proposed Location for Hydraulic Filters, Valves and Accumulators

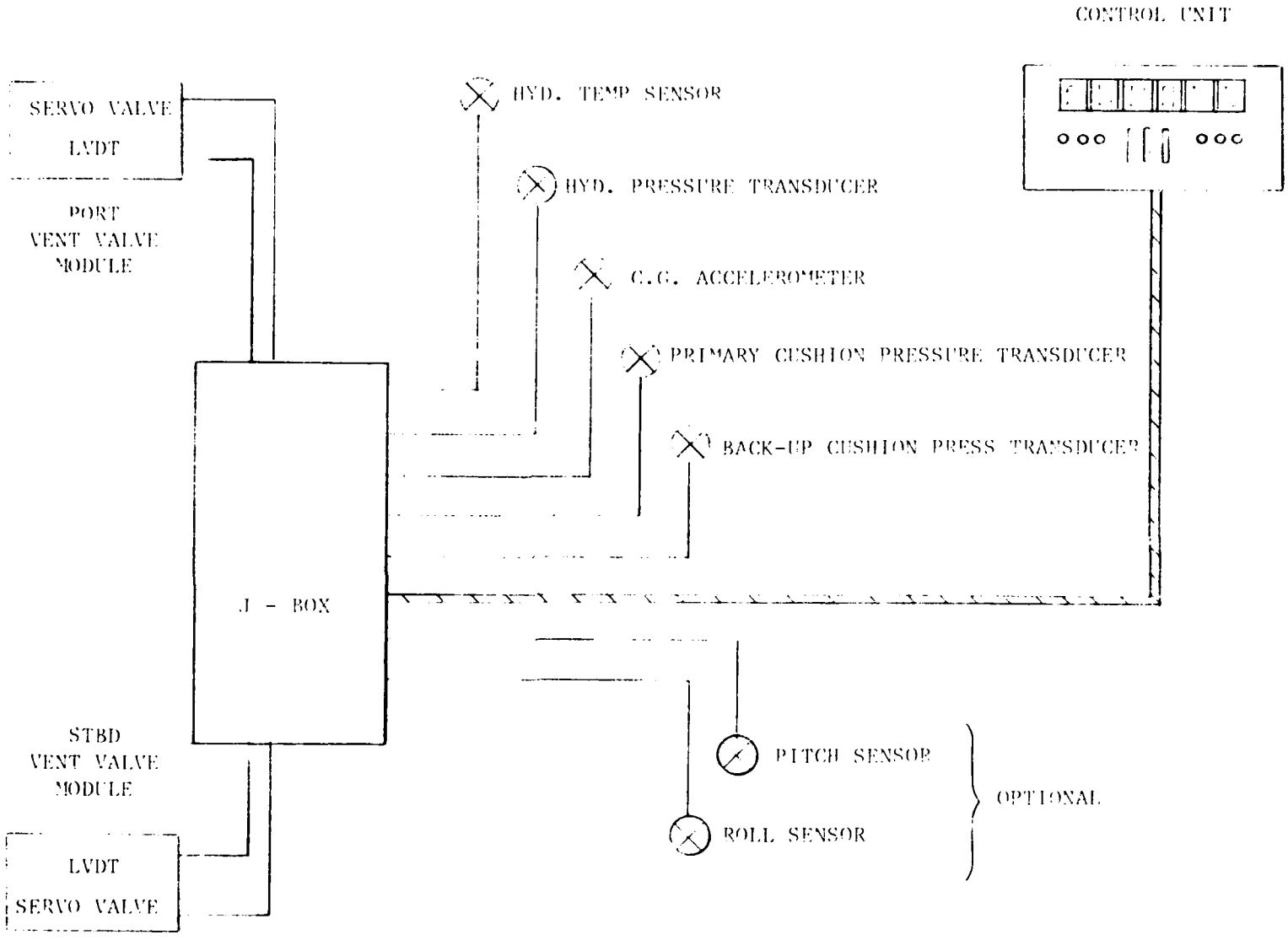

Figure 8-9 RCS Electronic Components and Interconnect Wiring

TABLE 8-3

PRELIMINARY RCS ELECTRONICS SPECIFICATION
FOR
USCG SEA BIRD CLASS SURFACE EFFECT SHIP

Item	Manufacturer
Digital Ride Control System: Card Cage: MIL-STD-28787 Component Modules: MIL-STD-28787 Digital/Analog Components: Temperature Range: - 55° C. to +125° C. Input Voltage Range: ±10% Power Supply: AC input: 95 - 135 VAC, 47 Hz - 500 Hz DC outputs: 5 VDC @ 6 amps ±15 VDC @ 1.5 amps +28 VDC @ 1.5 amps Line Regulation: 0.1% VDC_{out} + 10 mV (vor ±10% input change) Load Regulation: 0.1% VDC_{out} + 10 mV (for 1/2 to full load change) Temperature: -10° C. to +100° C. MIL-STD-810, MTD-502 Input Transient Protection: 1.2 kV spike 180 V Surge - 100 mSec. MIL-STD-704B & -C Humidity: MIL-STD-810,MTD-507 Acceleration: MIL-STD-810, MTD-513, 14 gs Vibration: MIL-STD-810, MTD-514, 15 gs Shock: MIL-STD-810, MTD-516, 40 gs Transducers: Cushion Pressure: Tavis, P-108S, 0-200 psfd Hydraulic Pressure: Genisco, 18A1035-43, 0-4000 psi Hydraulic Temperature: TBD Heave Acceleration: Kistler, 303 M1216, ±5 g Pitch and Roll: TBD	Maritime Dynamics, Inc. 8100 - 27th St. West Tacoma, WA 98466

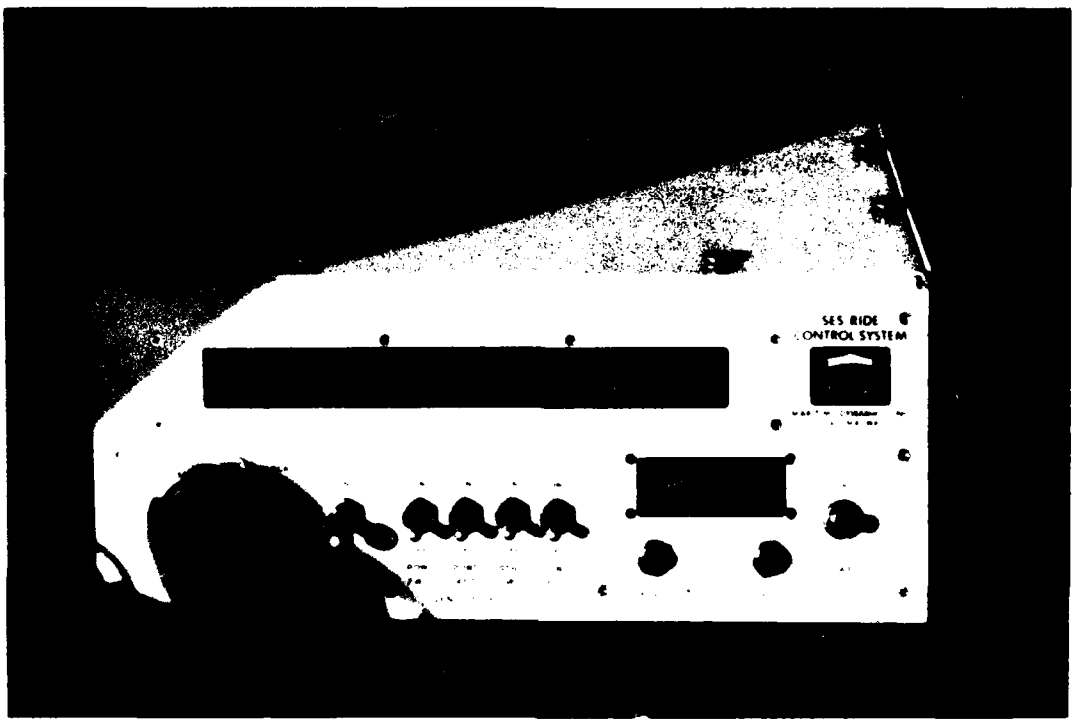

Figure 8-10 SES-200 Digital RCS Control Unit.

In a Sea Bird system, the components as a minimum will be upgraded [illegible] commercial specification on supply voltage and temperature (±5% [illegible] supply voltage, 0° to 75° C.) to the military specification [illegible], -55° to +125° C.). The power supply selected also will be [illegible] most military standards. The modules, card cage and backplane [illegible] same type as those used in the SES-200 system.

Ambient pressure transducers will be installed just above the [illegible] on the vertical stiffeners at Bulkhead 10. An 8 in. diameter [illegible] will be cut in the second deck just forward of Bulkhead 10 between the centerline and starboard buttock line 1 ft 6 in. in order to weld two [illegible] in. pressure taps to the wet deck. Aluminum 3/8 in. tube will connect the taps to the pressure transducers. Bulkhead fittings will be used for tube penetrations through the second deck. The access hole will be covered with a gasket and cover plate to maintain watertight integrity at the second deck level.

Pitch and roll angle transducers are shown as optional inputs to the RCS in Figure 8-9. These are not required for ride control law feedback. They are included because discussions with the USCG SES squadron indicated that mean pitch and roll attitude displays would be helpful in ballasting the craft for optimum performance. The digital RCS can perform the required calculations to make these displays without any significant increase in system complexity.

8.2.4 Operation

The theory of operation for the digital Ride Control System was covered in Section 5.1.2 and will not be repeated here. The SES-200 RCS was designed to have considerable flexibility for testing. This resulted in a configuration which requires more operator input than would be needed on a production unit. Therefore, for the Sea Bird Class, operation has been simplified to the following checklist:

Power-Up

1. Turn RCS "Power" switch on

Self-Check

1. Press "Self-Check" button - Verify Self-Check OK

Initialization

1. Enter Control Law Number 1, 2, 3, 4 for Sea States I-IV, respectively
2. Engage Hydraulic Clutch

Active Control

1. Turn "Active Control" switch on

Shutdown

1. Turn "Active Control" Off
2. Disengage Hydraulic Clutch

The RCS gain and bias will be automatically set at values which have been determined as optimum for the control law selected. If the operator desires, he may change the gain and bias to other values, but he cannot exceed limits which are stored in memory for each control law. The system can be left unattended once active control has been initiated. If a malfunction occurs, a warning message will be displayed and an audible alarm will sound. If the operator decides to reduce lift power for partial cushion or hullborne operations, the RCS will sense the reduction in mean cushion pressure. This will trigger a programmed shutdown which will slowly bring the gain down to zero and close the vent valves. Once full cushion operation has been re-established, the system automatically will restore active control.

Using thumbwheel switches on the front panel, the operator can display the mean values of hydraulic pressure, hydraulic temperature and cushion pressure. Also, he can display the standard deviation of heave acceleration and cushion pressure. If the optional pitch and roll inputs are installed, the RCC will display the mean values of these parameters. USCG SES operators at Key West indicated that this would be very helpful in assessing the vessel's trim and list for purposes of transferring fuel or ballast to optimize performance. The mean value displays will not vary due to pitch and roll oscillations because the dynamic part of the signal will be digitally filtered out. This should be a considerable improvement over the present method of using the bridge inclinometers which are unusable during operations in waves.

In addition to simplifying RCS operation for the USCG application, the self-check and fault monitoring routines will be improved. This should improve the maintainability and reliability of the system. Table 5-1 lists the self-check routines and Table 5-2 lists the fault monitoring routines presently incorporated in the software. It is expected that these lists will grow approximately 50% for the USCG application based on experience gained during digital RCS tests on the XR-1E and the SES-200.

8.2.5 Maintenance

Routine maintenance for the RCS will involve greasing the bearings in each vent valve module and inspecting the linkages for looseness. The hydraulic system fluid level will have to be checked and the system should be examined for evidence of leaks. Based on SES-200 experience, this entire exercise takes one person about 15 minutes and should be performed on a daily basis whenever routine engine checks are made.

Periodic maintenance that should be performed on 250 hour intervals involves sampling the hydraulic fluid for contamination. If contamination is found, all four (4) filter elements should be replaced. Air will have to be bled from the system anytime it is necessary to replace a component. This is accomplished by using the RCS to cycle the vent valves from 5% to 95% and back to 5%. Fluid circulation under these conditions will force the

air into the reservoir where it can escape. Yearly drydock periods are presently planned for the Sea Bird Class SES. During these periods, the bearings in each vent valve assembly should be removed, cleaned, repacked or replaced, and actuator piston and rod seals should be replaced.

No routine or periodic maintenance is required for the electronics. Self-check and fault monitoring routines should locate any failed components. The component modules are plug-in types which are thrown away upon failure, making replacement easy.

9. REFERENCES

1. Design, Development and Testing of a Ride Control System for the XR-1D Surface Effect Ship, Part I, Classical Control, Report No. MD-AR-1180-1, Maritime Dynamics, Inc., Tacoma, WA, September 1981.

2. Design, Development and Testing of a Ride Control System for the XR-1D Surface Effect Ship, Part II, Optimal Control, Report No. MD-AR-1180-2, Maritime Dynamics, Inc., Tacoma, WA, June 1981.

3. Design, Development and Testing of a Prototype Digital Ride Control System for Surface Effect Ships, Part I: SES-200 RCS Installation Plan, Report No. MD-R-1195-1, CDRL A001, Contract N00167-82-C-0079, Maritime Dynamics, Inc., Tacoma, WA, October 1982.

4. Design, Development and Testing of a Prototype Digital Ride Control System for Surface Effect Ships, Part VII: XR-1E Test Requirements, Report No. MD-R-1195-2, CDRL A007, Contract N00167-82-C-0079, Maritime Dynamics, Inc., Tacoma, WA, September 1982.

5. Test and Evaluation of the Bell-Halter 110-Foot Surface Effect Ship Demonstration Craft, P.K. Spangler, Report No. 6660-60, Naval Sea Systems Command Detachment, Norfolk, VA, February, 1981.

6. Technical and Operational Evaluation of the USCG Dorado (WSES-1), Report No. CG-D-44-82, USCG Research & Development Center, Avery Point, Groton, CT, August 1982.

7. SES-110 Acceptence and Evaluation Trials, May-June 1981, Surface Effect Ship Test Facility, Patuxent River, MD (PRELIMINARY).

8. SES-100A Ride Control System Test Requirements, Report No. MD-TN-1048-002, Maritime Dynamics, Inc., Tacoma, WA, October 1976.

9. A Review and Updating of Surface Effect Ships Seakeeping and Handling Qualities Specification HQ-1, Paragraph 3.6 - Habitability, TR-1031-1, Systems Technology, Inc., Hawthorne, CA, November 1974.

10. A Preliminary Investigation of Ride Control Feasibility for the Bell-Halter 110, Maritime Dynamics, Inc., Tacoma, WA, December 1982.

11. Bell-Halter Surface Effect Ship Development, AIAA Paper No. 81-2072, John Chaplin, Bell-Halter, Inc., New Orleans, LA

12. Program for Development of a Production SES Ride Control System, Maritime Dynamics, Inc., Presentation to U. S. Navy SES Office, May, 1981.

13. Ride Control for USCG Sea Hawk Class SES, Maritime Dynamics, Inc., Presentation to USCG, Office of Research and Development, March 1983.

14. USCG 110 SES Operations Manual, Contract DTCG23-82-C-30019, November 1982, Bell-Halter, Inc., New Orleans, LA.

15. Bell-Halter 110 SES, M.V. Speed Command, Operations Manual, Bell-Halter,Inc., New Orleans, LA.

16. The U. S. Coast Guard SES - Buying an Off-the-Shelf Vessel, D. G. Bagnell and S. A. Thomas, AIAA Paper AIAA-83-0620, U. S. Coast Guard Headquarters, Washington, D.C., February, 1983.

APPENDIX A

MEANS AND STANDARD DEVIATIONS

FOR

XR-1E MISSIONS 345, 346 and 348

TABLE A-1

XR-1E MISSION 345

TEST DATA

	TASK DESCRIPTION		ROLL (deg)	ROLLRATE (deg/sec)	PITCH (deg)	PITRATE (deg/sec)	YAWRATE (deg/sec)	CUSH3 (psf)	AZBOW (g)	AZCG (g)	SPEED P (kts)	WAVE HT (ft)	FVVPOSS (sq.ft)	AVVPOSS (sq.ft)	AVVPOSP (sq.ft)	TVVQ (cfs)	QTOT (cfs)	TRANSHP (shp)
#1	RCS OFF	AVG	-.20	.02	2.56	-.07	.00	64.7	1.00	.99	15.5	-	.01	.01	.01	7.9	385.2	72
		STD DEV	1.22	2.99	.61	1.74	.54	7.45	.165	.077	.63	.26	.00	.00	.00			
#2	RCS ON/1VV/5%	AVG	-.33	.07	2.49	-.11	.03	61.2	1.00	.99	14.7	-	.01	.38	.36	171.1	385.3	69
		STD DEV	.95	2.32	.82	2.29	.51	.57	.173	.065	.47	0.26	.00	.40	.40			
#3	RCS OFF	AVG	-.41	.04	2.73	-.12	-.02	66.4	1.00	.99	16.6	-	.01	.01	.01	7.8	372.9	70
		STD DEV	.78	1.52	.43	.48	.50	7.46	.132	.077	.73	0.24	.00	.00	.00			
#4	RCS ON/2VV/10%	AVG	-.47	.06	2.74	-.11	.04	65.0	1.00	.99	14.9	-	.01	.18	.16	83.1	376.4	70
		STD DEV	.86	.59	.66	.47	.75	3.13	.078	.033	.82	0.24	.00	.16	.16			
#5	RCS OFF	AVG	-.50	.01	2.98	-.11	-.04	66.2	1.00	.99	15.3	-	.01	.01	.01	7.7	385.0	72
		STD DEV	.70	1.67	.52	1.30	.25	5.44	.124	.060	.63	0.19	.00	.00	.00			
#6	RCS ON/2VV/15%	AVG	-.33	.08	3.08	-.12	.03	64.3	1.00	.99	14.2	-	.01	.29	.27	135.2	390.9	72
		STD DEV	.74	1.77	.33	.89	.35	3.90	.091	.034	.31	0.19	.00	.26	.26			
#7	RCS OFF	AVG	-.63	.06	3.00	-.12	.01	65.7	1.00	.99	14.6	-	.01	.01	.01	7.6	375.3	71
		STD DEV	.99	2.05	.41	.60	.55	5.61	.112	.064	1.03	0.20	.00	.00	.00			
#8	RCS ON/2VV/20%	AVG	.67	.07	2.72	-.12	.04	63.8	1.00	.99	14.9	-	.01	.23	.21	105.8	369.4	69
		STD DEV	.70	1.21	.51	.38	.54	2.43	.076	.025	1.15	0.20	.00	.15	.15			
#9	RCS OFF	AVG	-.49	.04	3.16	-.11		66.2	1.00	.99	14.7	-	.01	.01	.01	7.9	384.0	72
		STD DEV	.93	1.61	.32	.42		5.12	.100	.058	.54	0.25	.00	.00	.00			
#10	RCS ON/2VV/25%	AVG	-.71	.07	3.20	-.11	.03	64.4	1.00	.99	13.9	-	.01	.29	.26	131.3	389.1	71
		STD DEV	.80	1.56	.24	.39	.36	2.32	.072	.028	.40	0.25	.00	.19	.19			
#11	RCS OFF	AVG	-.83	.07	2.98	-.12	.02	65.3	1.00	.99	16.6	-	.01	.01	.01	7.9	370.8	69
		STD DEV	.96	1.93	.37	.60	.39	6.61	.123	.073	.69	0.19	.00	.00	.00			
#12	RCS ON/2VV/30%	AVG	-.92	.06	3.22	-.12	.09	63.1	1.00	.99	14.2	-	.01	.33	.30	150.0	378.7	68
		STD DEV	.94	1.98	.45	.37	.51	2.07	.066	.027	.64	0.19	.00	.19	.19			
#13	RCS OFF	AVG	-.55	.08	3.11	-.11	.02	65.5	1.00	.99	14.3	-	.01	.01	.01	8.0	381.4	70
		STD DEV	1.38	2.52	.30	.51	.74	5.57	.106	.065	.43	0.17	.00	.00	.00			
#14	RCS ON/2VV/35%	AVG	-.61	.06	2.92	-.12	.04	62.8	1.00	.99	13.6	-	.01	.39	.36	174.6	388.7	70
		STD DEV	1.05	1.90	.39	.43	.54	1.72	.063	.022	.52	0.17	.00	.18	.18			
#15	RCS OFF	AVG	-.70	.07	2.67	-.13	.01	65.7	1.00	.99	18.8	-	.01	.01	.01	8.0	376.6	70
		STD DEV	.99	1.82	.31	.46	.38	6.69	.125	.070	.76	0.19	.00	.00	.00			
#16	RCS ON/2VV/40%	AVG	-.61	.06	2.59	-.12	.04	60.8	1.00	.99	14.8	-	.01	.45	.42	200.8	389.6	63
		STD DEV	1.01	1.83	.35	.45	.38	1.97	.072	.022	.68	0.19	.00	.22	.22			

TABLE A-2

XR IE MISSION 346

TEST DATA

	TASK DESCRIPTION		ROLL (deg)	ROLL RATE (deg/sec)	PITCH (deg)	PITRATE (deg/sec)	YAWRATE (deg/sec)	QDSHB (psf)	AZBOW (g)	AZ C (g)	SPEED P (kts)	WAVE HT (ft)	FVVPOSS (sq.ft)	AVVPOSS (sq.ft)	AVVPOSP (sq.ft)	TVVQ (cfs)	QTDT (cfs)	TFAIRSHP (shp)
#1	RCS OFF	AVG	-.55	.04	2.74	-.11	25	66.9	1.00	.99	17.1	-	.01	.01	.01	7.5	380	72
		STD DEV	1.31	2.71	.33	.71	.53	9.15	.162	.097	1.86	0.21	.00	.00				
#2	RCS ON/2VV/5%	AVG	-.28	.04	.08	-.09	.03	64.0	1.00	.99	17.7	-	.01	.35	.33	160.5	386	70
		STD DEV	1.14	2.67	.44	.74	.32	6.21	.136	.065	1.11	0.21	.00	.37	.37			
#3	RCS OFF	AVG	-.17	.02	2.60	-.10	.03	67.8	1.00	.99	19.4	-	.01	.02	.02	11.7	375	72
		STD DEV	0.65	1.52	.32	.74	.32	11.16	.193	.113	1.28	0.21	.00	.09	.08			
#4	RCS ON/2VV/10%	AVG	-.29	.03	2.39	-.09	.00	64.5	1.00	.99	17.4	-	.01	.36	.33	165.1	385	71
		STD DEV	0.49	1.02	.30	.65	.28	5.54	.122	.058	.79	0.21	.00	.36	.36			
#5	RCS OFF	AVG	-.57	.03	3.05	-.11	-.06	66.2	1.00	.99	14.3	-	.01	.01	.01	7.3	387	72
		STD DEV	1.10	2.53	.29	.74	.46	7.27	.137	.083	.45	0.21	.00	.00	.00			
#6	RCS ON/2VV/15%	AVG	-.55	.06	3.04	-.10	-.23	64.9	1.00	.99	13.9	-	.01	.34	.31	154.5	391	72
		STD DEV	1.15	2.58	.30	.69	.35	3.76	.095	.045	.52	0.20	.00	.32	.31			
#7	RCS OFF	AVG	-.60	.05	3.32	0.10	-.02	67.0	1.00	.99	14.1	-	.01	.01	.01	7.4	385	73
		STD DEV	.97	2.12	.29	.72	.49	7.05	.123	.080	.44	0.20	.00	.00	.00			
#8	RCS ON/2VV/20%	AVG	-.61	.04	2.92	.11	.10	63.9	1.00	.99	14.1	-	.01	.39	.36	178.4	389	71
		STD DEV	.79	1.67	.30	.70	.42	4.19	.103	.045	.49	0.20	.00	.36	.36			
#9	RCS OFF	AVG	-.63	.05	3.22	-.10	.13	66.2	1.00	.99	14.5	-	.01	.01	.01	7.5	382	72
		STD DEV	.88	1.99	.34	.86	.36	8.47	.155	.098	.37	0.22	.00	.00	.00			
#10	RCS ON/2VV/25%	AVG	-.62	.04	2.97	-.11	-.11	63.5	1.00	.99	13.8	-	.01	.46	.43	209.7	387	70
		STD DEV	.60	1.38	.32	.82	.43	4.10	.107	.047	.44	0.22	.00	.39	.39			
#11	RCS OFF	AVG	-.48	.04	2.62	-.10	.05	64.1	1.00	.99	16.8	-	.01	.01	.01	7.5	379	71
		STD DEV	1.32	2.95	.38	.94	.42	10.9	.196	.121	.46	0.24	.00	.00	.00			
#12	RCS ON/2VV/30%	AVG	-.54	.05	2.44	-.10	.04	60.7	1.00	.99	14.8	-	.01	.54	.51	242.9	386	69
		STD DEV	1.27	2.92	.36	1.01	.38	5.24	.137	.057	.43	0.24	.00	.47	.47			
#13	RCS OFF	AVG	-.53	.05	2.89	-.12	.06	65.4	1.00	.99	16.2	-	.01	.01	.01	7.5	377	71
		STD DEV	1.24	2.04	.43	.88	.38	10.96	.194	.123	.68	0.24	.00	.00	.00			
#14	RCS ON/2VV/35%	AVG	-.66	.05	2.48	-.12	.05	61.2	1.00	.99	15.1	-	.01	.53	.51	240.2	384	68
		STD DEV	.93	1.91	.38	.84	.44	4.4	.116	.048	.59	0.22	.00	.43	.43			
#15	RCS OFF	AVG	-.53	.05	2.75	-.11	.07	65.9	1.00	.99	17.8	-	.01	.01	.01	7.5	374	71
		STD DEV	.55	1.23	.33	.90	.32	11.39	.202	.123	.64	0.22	.00	.00	.00			

TABLE A-2

XR-1E MISSION 34o

TEST DATA

	TASK DESCRIPTION		ROLL (deg)	ROLLRATE (deg/sec)	PITCH (deg)	PITRATE (deg/sec)	YAWRATE (deg/sec)	CUSH3 (psf)	AZBOW (g)	AZCG (g)	SPEED P (kts)	WAVE HT (ft)	FVVPOSS (sq.ft)	AVVPOSS (sq.ft)	AVVPOSP (sq.ft)	TVVQ (cfs)	QTOT (cfs)	TFANSHP (shp)
#16	RCS ON/2VV/40%	AVG	-.53	.03	2.34	-.11	.13	60.2	1.00	.99	15.4	-	.01	.61	.58	274.0	383	67
		STD DEV	.55	1.42	.37	1.03	.37	5.16	.137	.059	.51	0.22	.00	.47	.47			
#17	RCS OFF	AVG	-.28	.0.	.12	-.13	-.06	64.2	1.00	.99	15.8	-	.01	.01	.01	7.6	366	70
		STD DEV	1.21	2.42	.53	1.37	.47	1.89	.227	.131	.88	0.28	.00	.00	.00			
#18	RCS ON/2VV/45%	AVG	-.42	.04	2.70	-.12	.07	58.5	1.00	.99	14.8	-	.01	.69	.66	305.2	379	65
		STD DEV	1.26	2.72	.58	1.36	.57	5.92	.155	.059	.66	0.28	.00	.51	.51			
#19	RCS OFF	AVG	-.48	.06	3.38	-.12	.23	64.3	1.00	.99	15.3	-	.01	.01	.01	7.7	384	71
		STD DEV	1.23	2.51	.57	1.26	.62	11.11	.211	.125	1.57	0.28	.00	.00	.00			
#20	RCS ON/2VV/50	AVG	-.42	.04	2.52	-.11	-.09	58.2	1.00	.99	15.2	-	.01	.72	.69	317.0	387	67
		STD DEV	.79	1.53	.53	1.41	.40	6.24	.163	.061	.66	0.32	.01	.54	.54			
#21	RCS OFF	AVG	-.51	.03	2.94	-.12	.05	64.2	1.00	.99	17.1	-	.01	.01	.01	7.5	384	71
		STD DEV	1.15	1.75	.60	1.30	.48	14.24	.261	.157	1.65	0.32	.00	.00	.00			

TABLE A-3

XR-1E MISSION 366

TEST DATA

TEST CONDITION		ROLL (deg)	P RATE (deg/sec)	PITCH (deg)	Q RATE (deg/sec)	YAW RATE (deg/sec)	QSHS psf	AZCON g	AZCG g	SPEED KTS	WAVE HT (ft)	FVVPOSS (sq.ft)	AVVPOSS (sq.ft)	AVVPOSP (sq.ft)	TVVQ (cfs)	QTOT (cfs)	TRANSHP (shp)
#1 RCS OFF	AVG	-.77	65	-.28	.1	.06	66.3	1.00	.99	20.7	-	.01	.01	.01	7.3	358	72
	STD DEV	.40	53	.27	51	31	7.76	.145	.080	.79	0.14	.00	.00	.00			
#2 RCS ON/2VV/5%	AVG	-.74	.06	2.31	.11	-0-	65.5	1.00	.99	16.9	-	.01	.20	.18	93.5	370	69
	STD DEV	.41	.53	.51	.49	.44	4.36	.105	.041	1.26	0.14	.00	.20	.19			
#4 RCS OFF	AVG	.43	.06	2.49	-.11	.20	68.9	1.00	.99	21.0	-	.01	.01	.01	7.3	364	73
	STD DEV	.90	1.87	.26	26	.33	8.59	.156	.091	.47	0.14	.00	.00	.00			
#3 RCS ON/2VV/3%	AVG	-.33	.07	2.33	-.13	.11	64.6	1.00	.99	14.6	-	.01	.37	.34	170.6	366	68
	STD DEV	.29	.47	.27	.45	.41	3.32	.09	.029	.61	0.14	.00	.25	.25			
#5 RCS OFF	AVG	-.52	.06	2.35	-.11	.08	68.7	1.00	.99	21.9	-	.01	.01	.01	7.5	361	73
	STD DEV	.31	.50	.38	.61	.29	10.99	.188	.114	.36	0.16	.00	.00	.00			
#6 RCS ON/3VV/5	AVG	-.73	.07	2.41	-.11	.17	67.2	1.00	.99	21.3	-	.16	.18	.15	120.1	365	70
	STD DEV	.24	.48	.31	.54	.27	5.23	.116	.050	.70	0.16	.17	.16	.16			
#7 RCS OFF	AVG	-.38	.08	2.50	-.13	.03	67.2	1.00	.99	18.6	-	.01	.01	.01	7.4	366	69
	STD DEV	.31	.69	.21	.48	.24	8.0	.144	.085	1.013	0.16	.00	.00	.00			
#8 RCS ON/2VV/35	AVG	-.26	.06	2.56	-.10	.05	67.9	1.00	.99	20.1	-	.01	.42	.39	202.2	429	78
	STD DEV	.297	.65	.20	.59	.32	5.73	.131	.053	.42	0.16	.00	.34	.34			
#9 RCS OFF	AVG	-.59	.07	2.25	-.11	.10	67.5	1.00	.99	20.7	-	.01	.01	.01	7.6	351	36
	STD DEV	.27	.55	.21	.53	.27	10.63	.185	.108	.42	0.18	.00	.00	.00			
#10 RCS ON/3VV/25%	AVG	-.65	.07	2.46	-.11	.08	67.2	1.00	.99	20.7	-	.29	.30	.28	211.2	434	111
	STD DEV	.21	.48	.20	.55	.23	5.63	.131	.054	.49	0.18	.24	.23	.23			
#11 RCS OFF	AVG	-.58	.08	2.48	-.12	-.05	66.7	99	.99	20.7	-	.01	.01	.01	7.6	371	70
	STD DEV	.28	.70	.21	.60	.26	12.7	.208	.130	.33	0.17	.00	.00	.00			
#12 RCS ON/3VV/40%	AVG	-.24	.07	2.83	-.11	.07	67.2	.99	.99	18.3	-	.44	.45	.42	319.5	569	137
	STD DEV	.29	.60	.18	.62	.30	5.03	.123	.049	.46	0.17	.29	.28	.28			
#13 RCS OFF	AVG	-.14	.07	2.57	-.10	.04	66.7	.99	.99	20.0	-	.01	.01	.01	7.5	374	71
	STD DEV	.37	.68	.23	.60	.36	11.73	.204	.124	.70	0.17	.00	.00	.00			
#14 RCS ON/2VV/5%	AVG	-.22	.06	2.55	-.10	.04	64.6	.99	.99	18.5	-	.01	.30	.27	136.0	380	69
	STD DEV	.28	.69	.29	.59	.32	6.03	.132	.063	.48	0.18	.00	.32	.32			
#15 RCS OFF	AVG	-.23	.06	2.26	-.12	.01	66.6	.99	.99	22.5	-	.01	.01	.01	7.4	372	70
	STD DEV	.26	.57	.22	.65	.34	14.07	.241	.157	.57	0.18	.00	.00	.00			

TABLE A-3

A6-1E MISSION 34G

TEST DATA

	TASK DESCRIPTION		ROLL (deg)	ROLLRATE (deg/sec)	PITCH (deg)	PITRATE (deg/sec)	YAWRATE (deg/sec)	CUSH3 (psf)	AZBOW (g)	AZCG (g)	SPEED P (kts)	WAVE HT (ft)	FVVPOSS (sq.ft)	AVVPOSS (sq.ft)	AVVPOSP (sq.ft)	TVVQ (cfs)	QTOT (cfs)	TFANSHP (shp)
#16	RCS OFF	AVG	-.83	.07	2.56	-.14	.05	67.8	.99	.99	21.3	-	.01	.01	.01	7.5	447	116
		STD DEV	.37	.66	.25	.60	.27	14.25	.242	.155	.98	0.18	.00	.00	.00			
#17	RCS ON/2VV/5	AVG	-.66	.07	2.29	-.11	-.03	67.3	.99	.99	22.2	-	.01	.30	.27	139.3	435	114
		STD DEV	.17	.46	.19	.57	.25	9.23	.18	.097	.30	0.18	.00	.32	.32			
#18	RCS ON/3VV/5	AVG	-.69	.08	2.35	-.12	.08	67.5	.99	.99	22.2	-	.19	.21	.18	140.3	431	113
		STD DEV	.24	.59	.17	.54	.24	8.36	.165	.083	.39	0.18	.21	.21	.20			

APPENDIX B

WAVE HEIGHT POWER SPECTRA

FOR

XR-1E MISSIONS 345, 346, 347

PSD

XBIE M-305 = WAVE HEIGHT 11:02:00-11:10:20

MAX % ERROR = 22.3607 MEAN = .0026

BANDWIDTH = .04 ST. DEV = .258

DELTA TIME = .100 AVERAGE HIGHEST 1/3RD

NYQUIST FREQ = 5.00 1.002

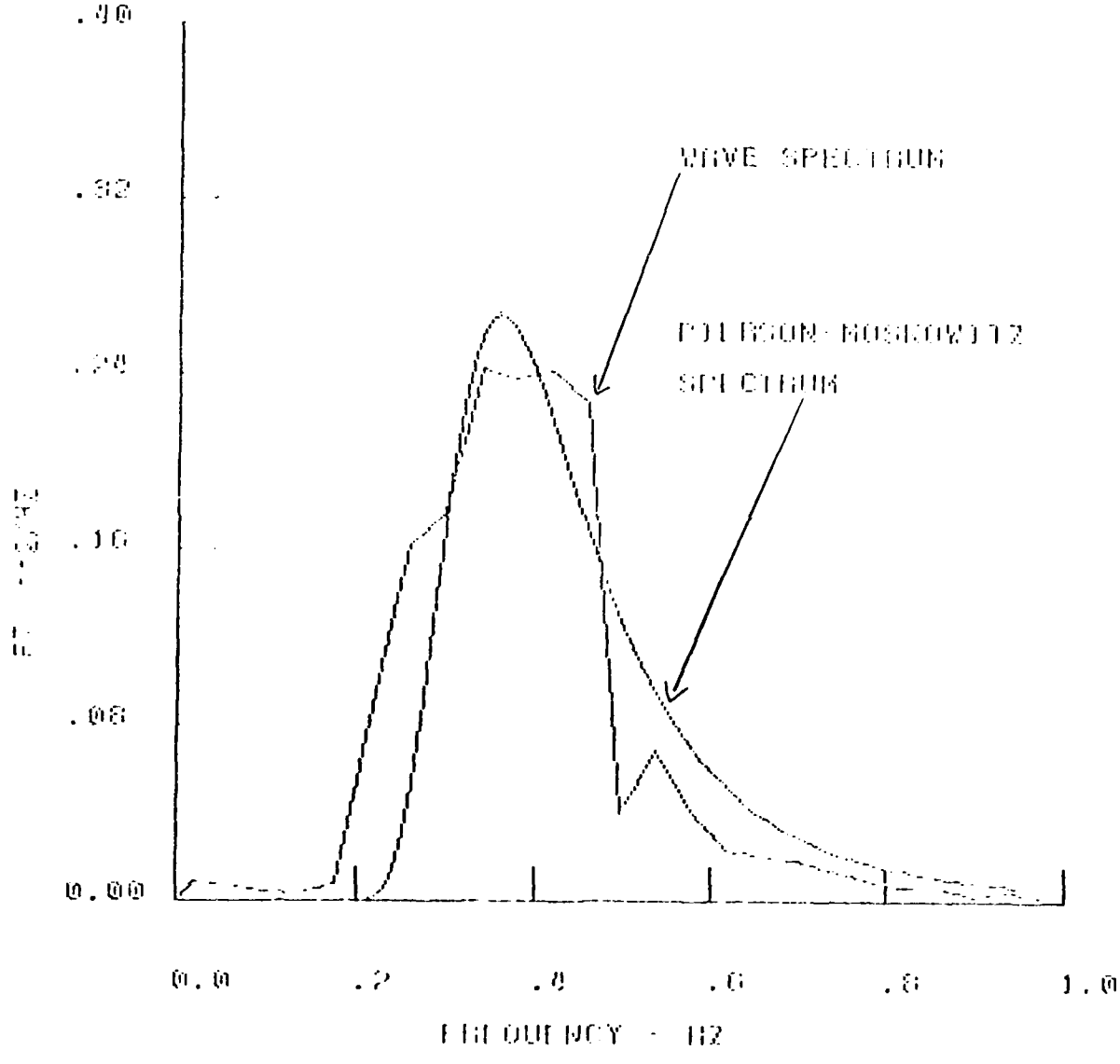

PSD

XMIC M-345	WAVE HEIGHT	11:22:55-11:31:15	
MAX % ERROR	22.3607	MEAN =	.3891
BANDWIDTH	.04	ST. DEV =	.240
DELTA TIME	.100	AVERAGE HIGHEST 1/3RD =	.917
NYQUIST FREQ	5.00		

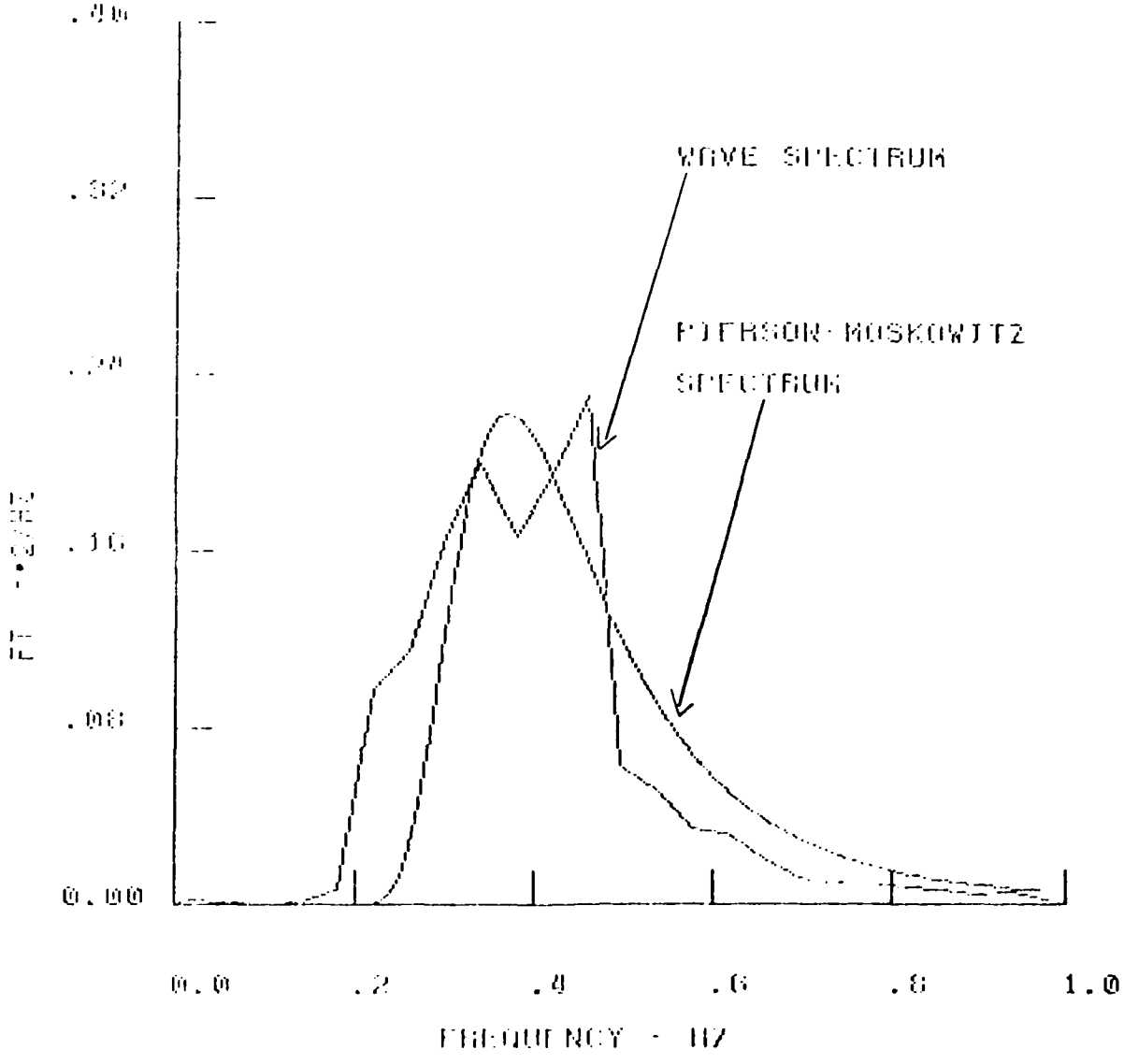

PSD

XFILE M-345	= WAVEHEIGHT	11:42:50-11:51:15	
MAX % ERROR	22.3607	MEAN =	.3760
BANDWIDTH	= .04	ST. DEV =	.194
DELTA TIME	.100	AVERAGE HIGHEST 1/3RD =	
NYQUIST FREQ =	5.000		

758

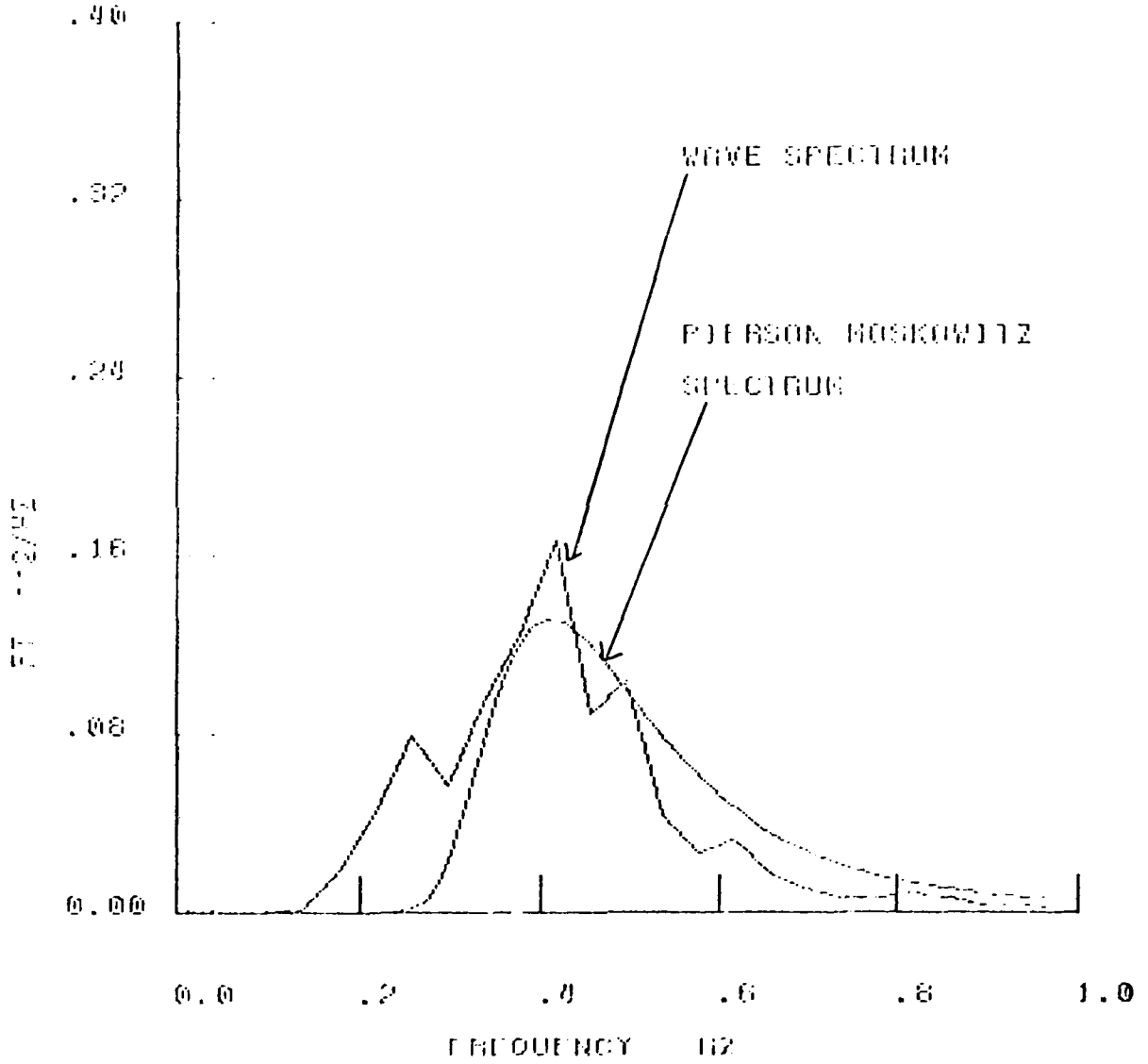

PSD

XFILE M-345	WAVEHEIGHT	11:58:55-12:07:15	
MAX % ERROR	22.3607	MEAN =	.3599
BANDWIDTH =	.04	ST. DEV =	.196
DELTA TIME	.100	AVERAGE HIGHEST 1/3RD =	
NYQUIST FREQ	5.00		

.784

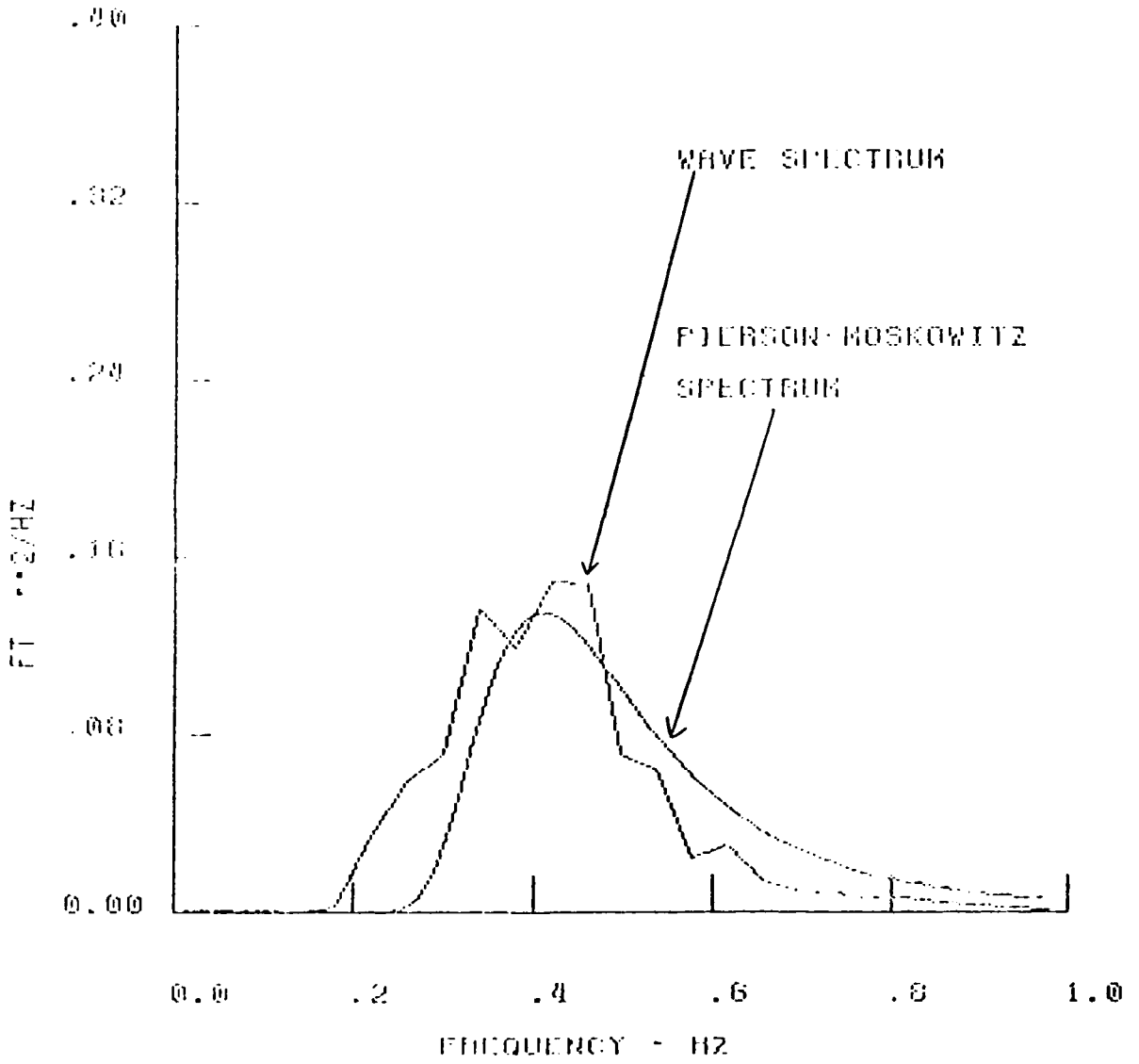

PSD

XRIE M-345	WAVEHEIGHT	12:17:00-12:25:20	
MAX % ERROR =	22.3607	MEAN =	.2898
BANDWIDTH =	.04	ST. DEV =	.251
DELTA TIME	.100	AVERAGE HIGHEST 1/3RD =	
NYQUIST FREQ =	5.00		

.761

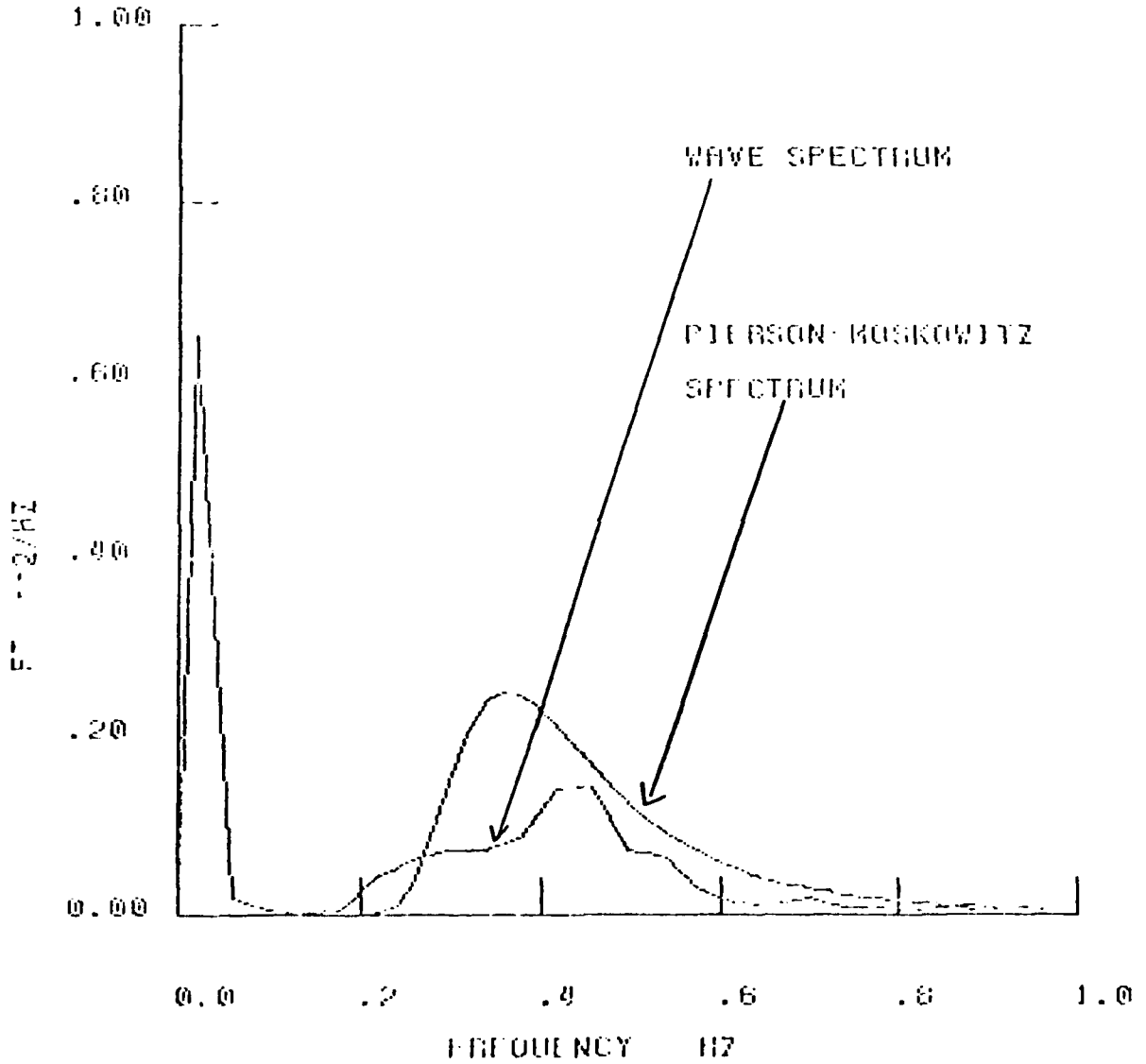

PSD
XHIE M-345 = WAVEHEIGHT 12:38:00-12:41:20
MAX % ERROR = 22.3607 MEAN = .3222
BANDWIDTH = .04 ST. DEV = .191
DELTA TIME = .100 AVERAGE HIGHEST 1/3RD =
NYQUIST FREQ = 5.00 .750

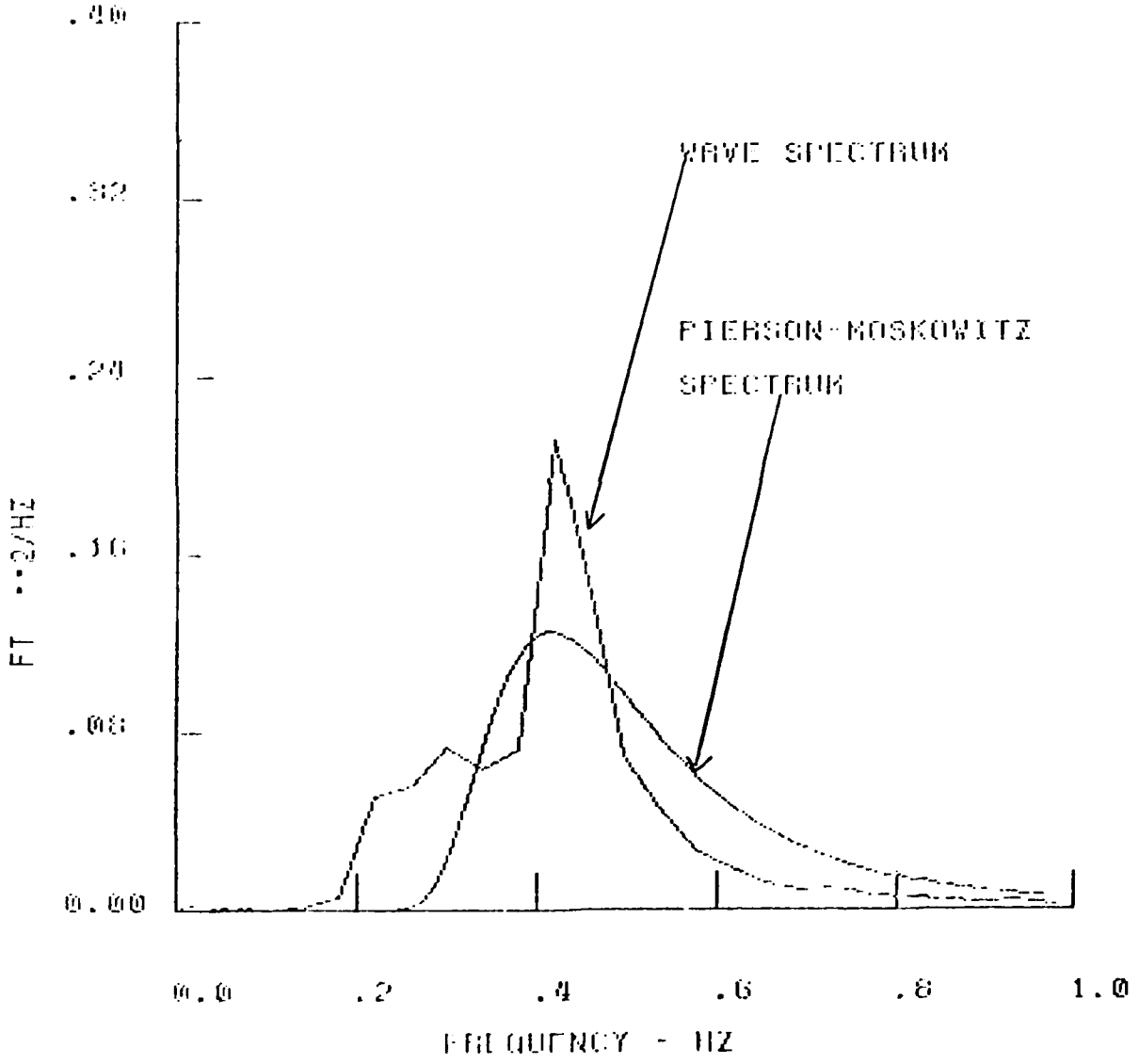

PSD
XBIE M-345 = WAVEHEIGHT 12:46:00-12:54:20
MAX % ERROR = 22.3607 MEAN = .3148
BANDWIDTH = .04 ST. DEV = .171
DELTA TIME = .100 AVERAGE HIGHEST 1/3RD =
NYQUIST FREQ = 5.00

.664

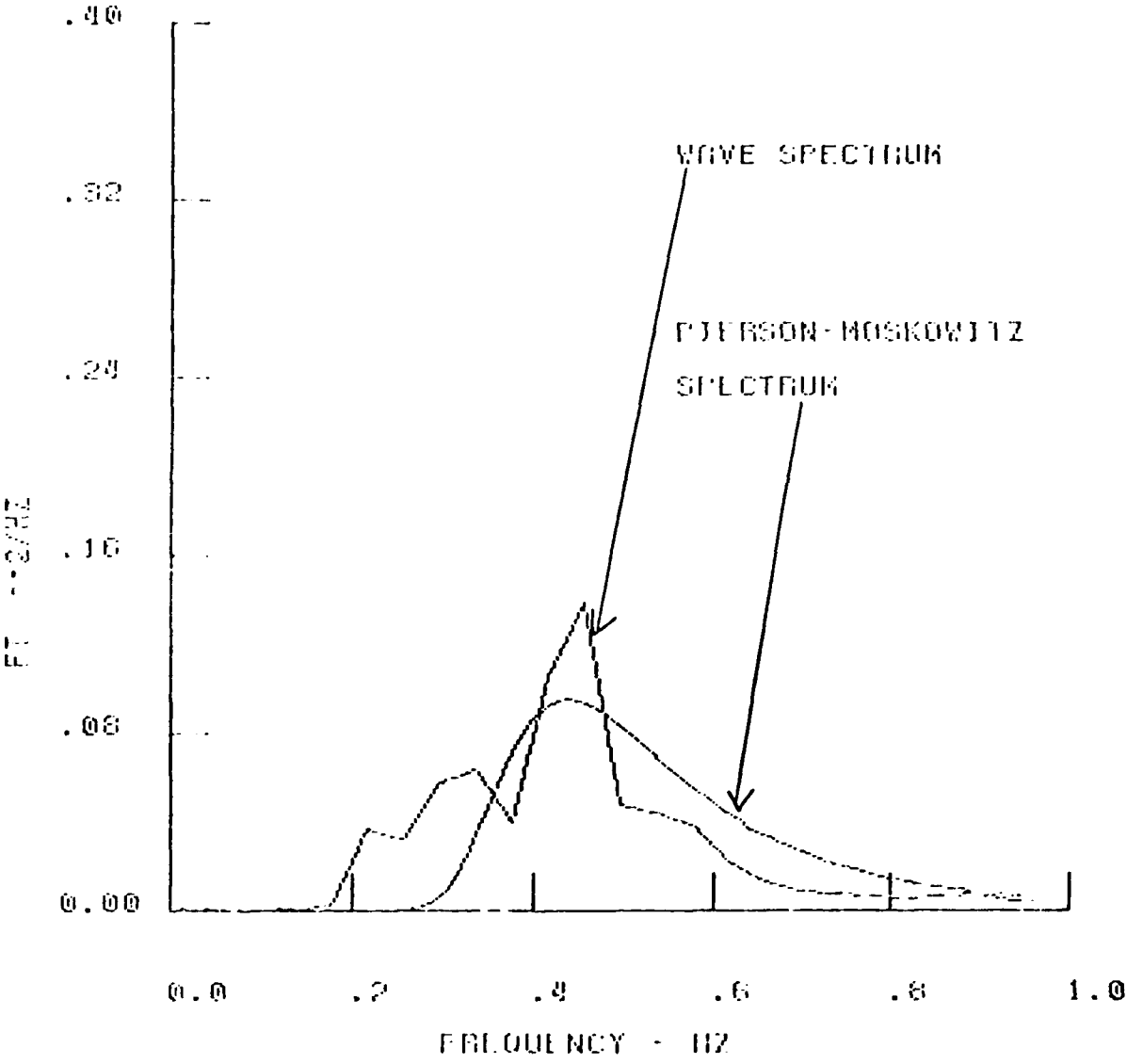

PSD

XBIE M-345	WAVEHEIGHT	13:02:00-13:10:20	
MAX % ERROR	22.3607	MEAN =	.2881
BANDWIDTH =	.04	ST. DEV	.185
DELTA TIME	.100	AVERAGE HIGHEST 1/3RD =	
NYQUIST FREQ =	5.00		

724

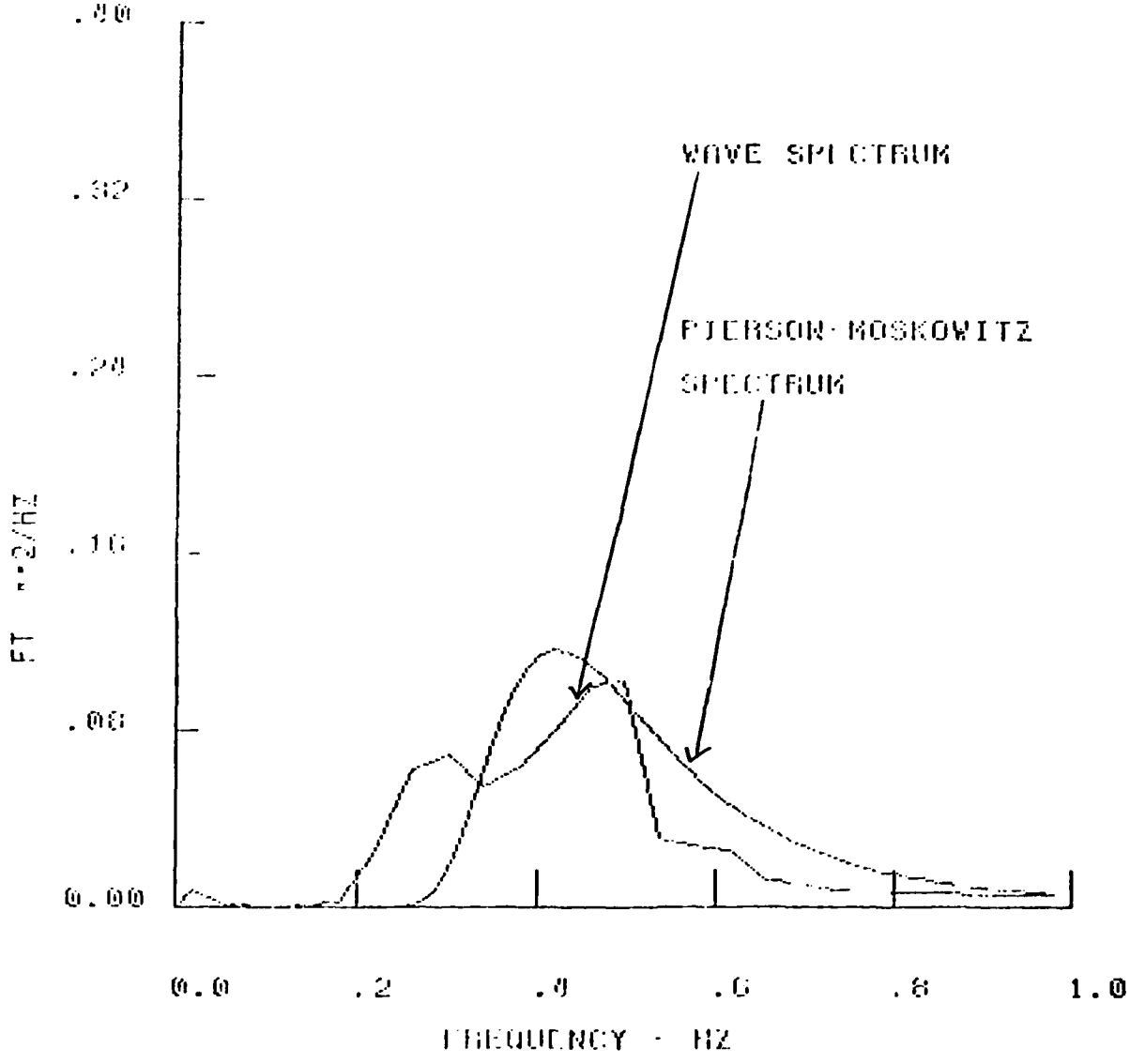

PSD

M346-1 WAVEHEIGHT 11:28:00-11:36:20

MAX % ERROR = 22.3607 MEAN = .1530

BANDWIDTH = .04 ST. DEV = .210

DELTA TIME .100 AVERAGE HIGHEST 1/3RD =.85

NYQUIST FREQ = 5.00

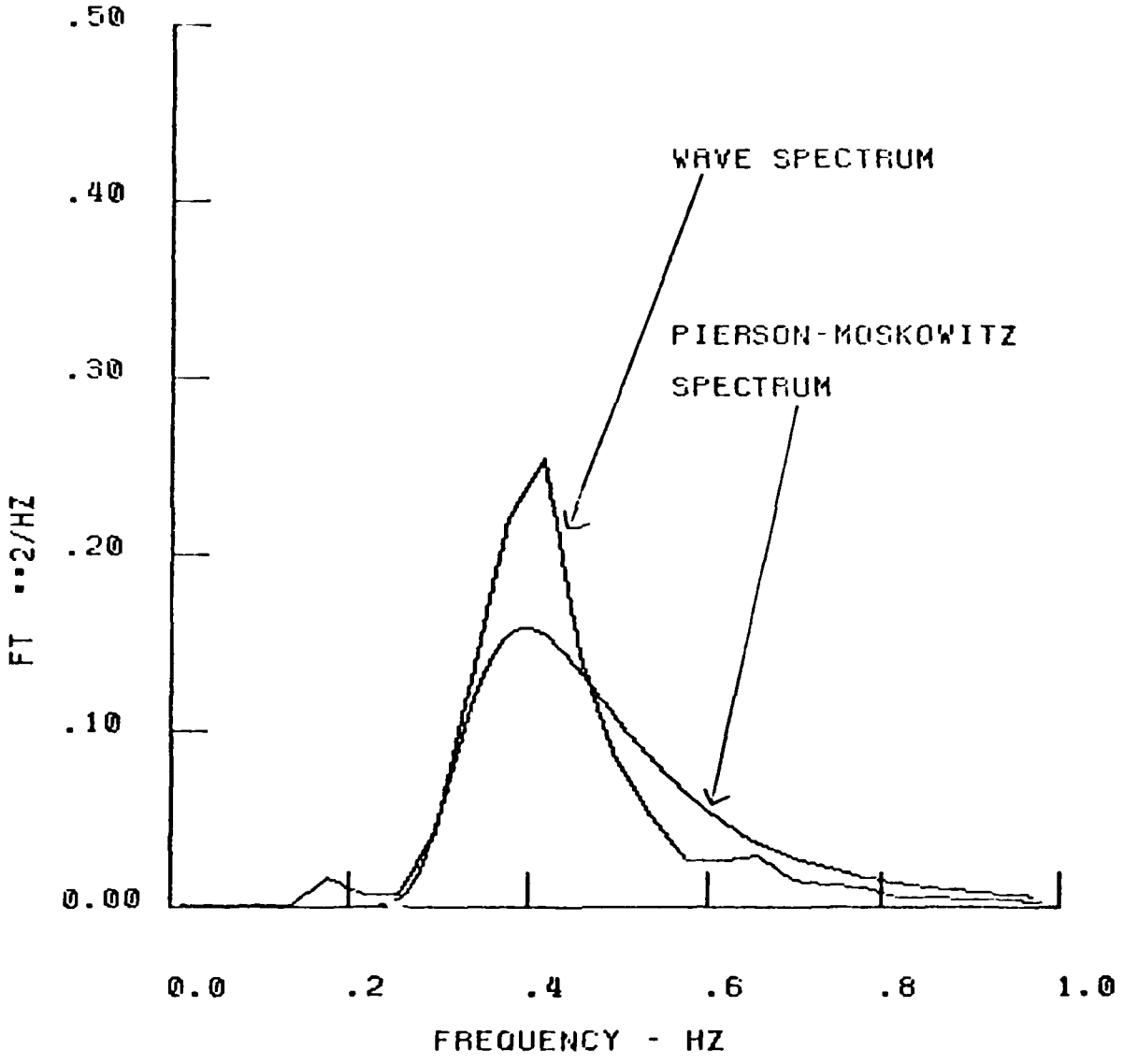

PSD

M346-2 WAVEHEIGHT	11:37:00-11:45:20
MAX % ERROR = 22.3607	MEAN = .1463
BANDWIDTH = .04	ST. DEV = .198
DELTA TIME .100	AVERAGE HIGHEST 1/3RD = .82
NYQUIST FREQ = 5.00	

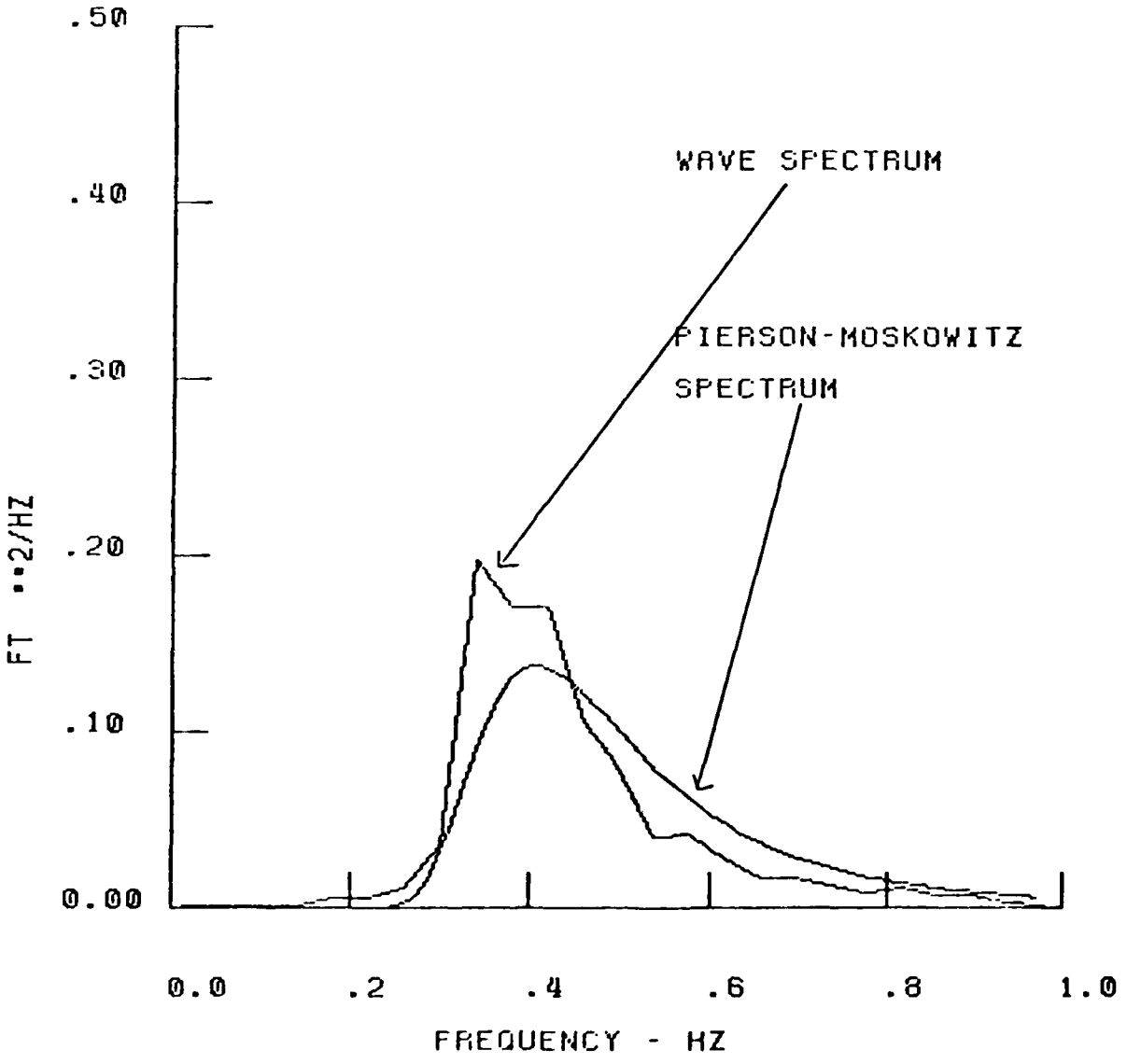

PSD

M346-3	WAVEHEIGHT	11:54:40-12:03:00	
MAX % ERROR =	22.3607	MEAN =	.1372
BANDWIDTH =	.04	ST. DEV =	.202
DELTA TIME	.100	AVERAGE HIGHEST 1/3RD =	.81
NYQUIST FREQ =	5.00		

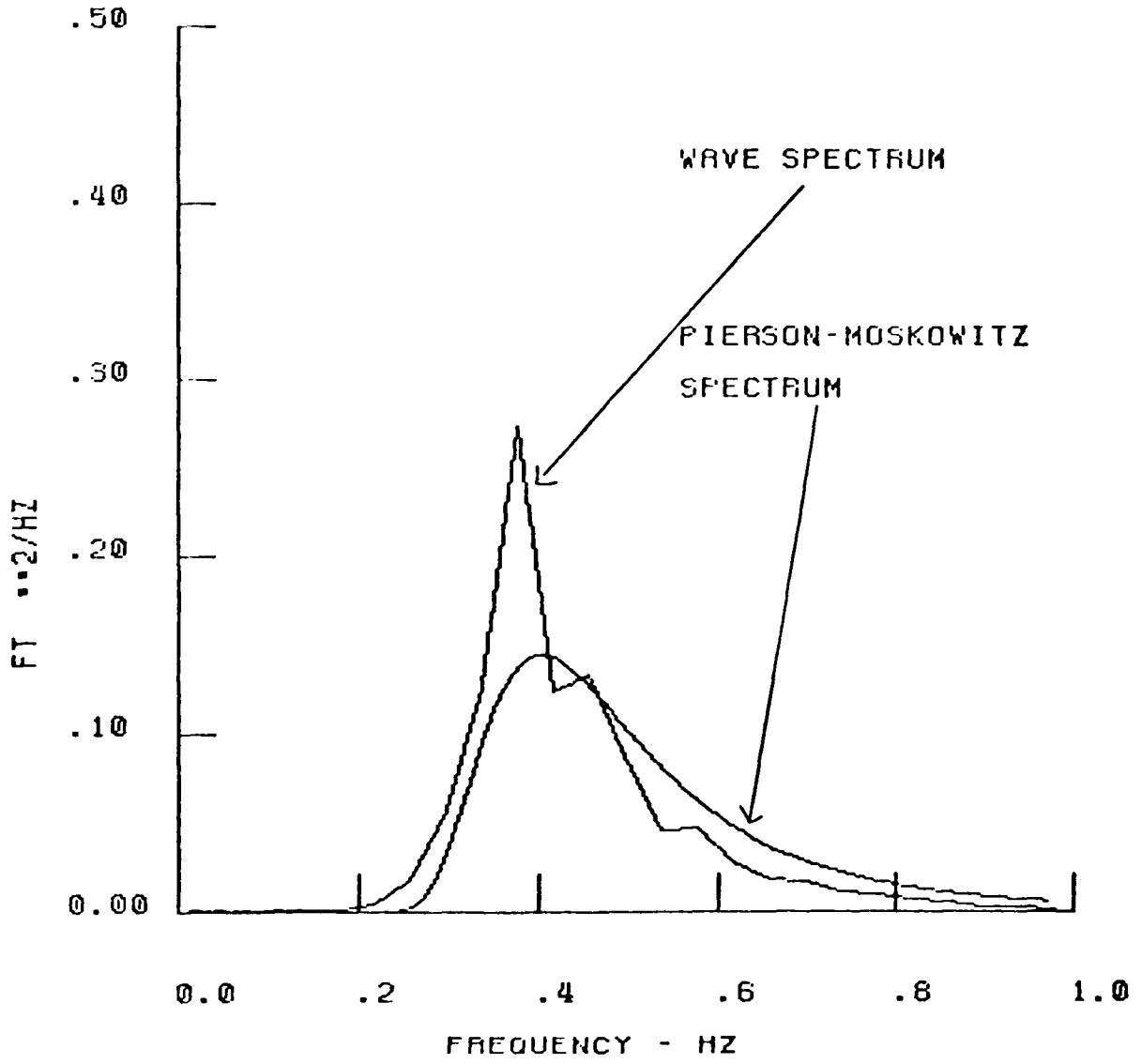

PSD

M346-4	WAVEHEIGHT	12:03:10-12:11:30	
MAX % ERROR =	-22.3607	MEAN =	.1338
BANDWIDTH =	.04	ST. DEV =	.214
DELTA TIME	.100	AVERAGE HIGHEST 1/3RD =	.86
NYQUIST FREQ =	5.00		

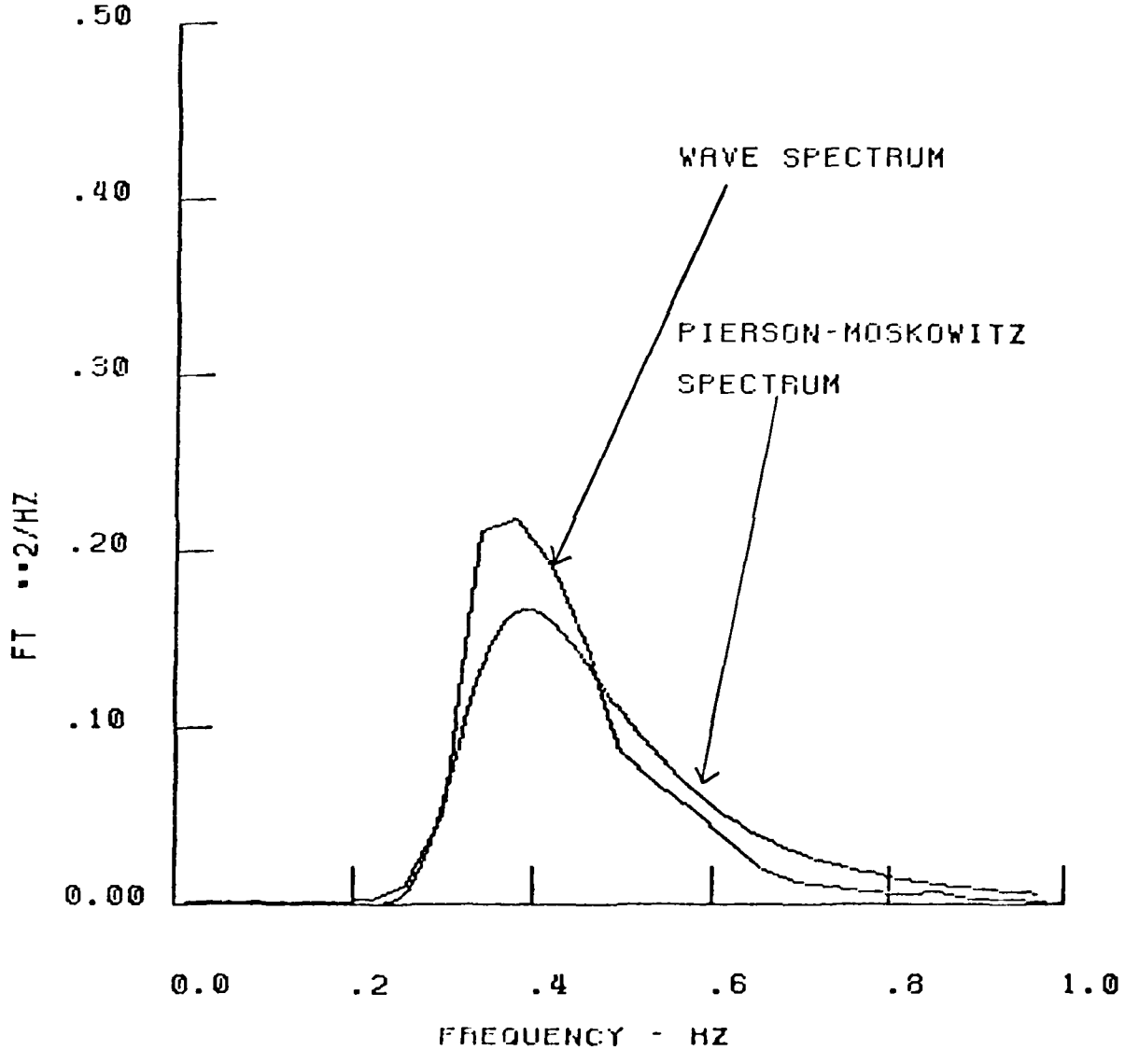

PSD

M346-5 WAVEHEIGHT 12:27:30-12:35:50

MAX % ERROR = 22.3607 MEAN = .1262

BANDWIDTH = .04 ST. DEV = .236

DELTA TIME .100 AVERAGE HIGHEST 1/3RD = .94

NYQUIST FREQ = 5.00

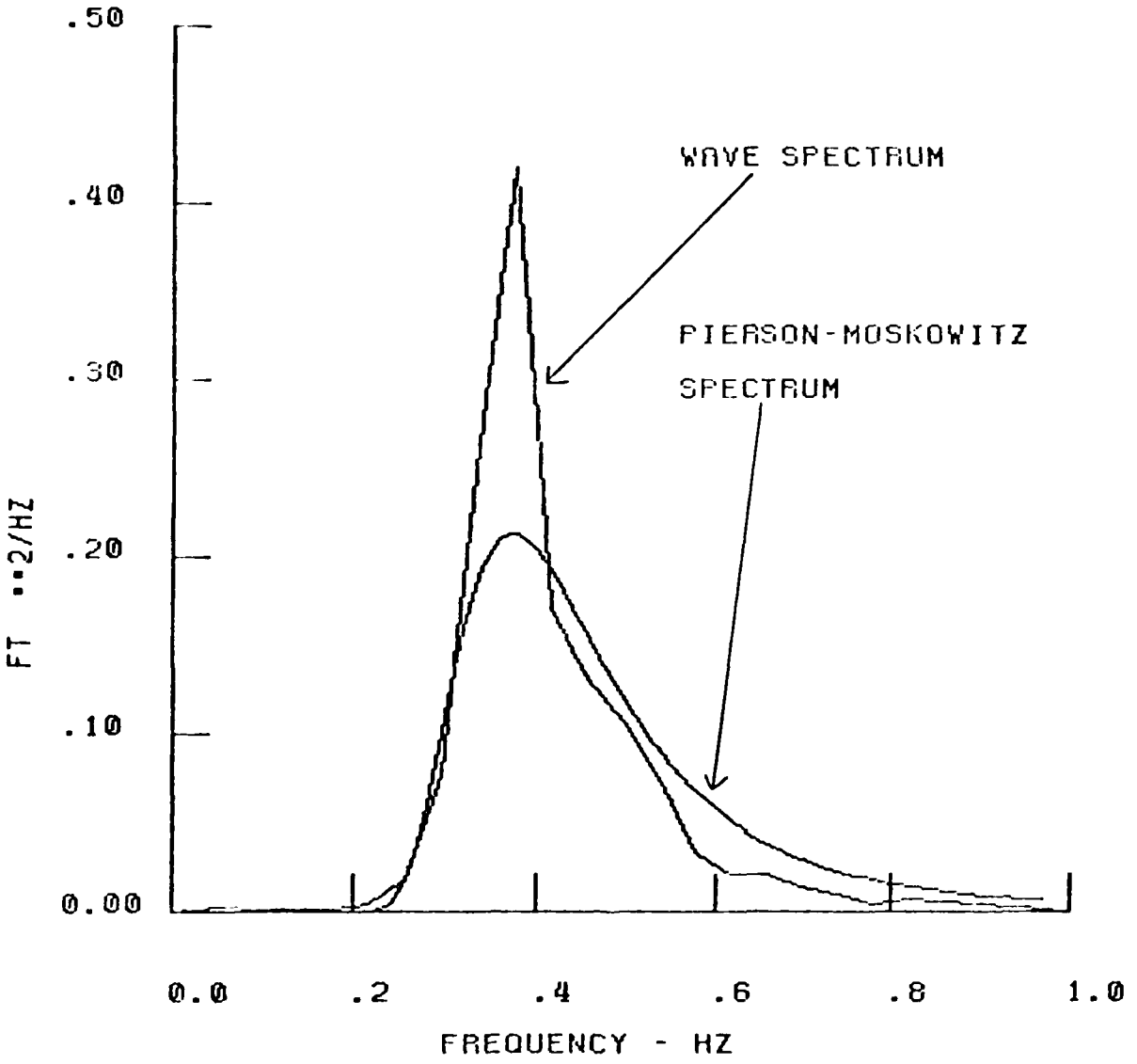

PSD
M346-6 WAVEHEIGHT
MAX % ERROR = 22.3607
BANDWIDTH = .04
DELTA TIME .100
NYQUIST FREQ = 5.00

12:36:00-12:44:20
MEAN = .1230
ST. DEV = .216
AVERAGE HIGHEST 1/3RD = .87

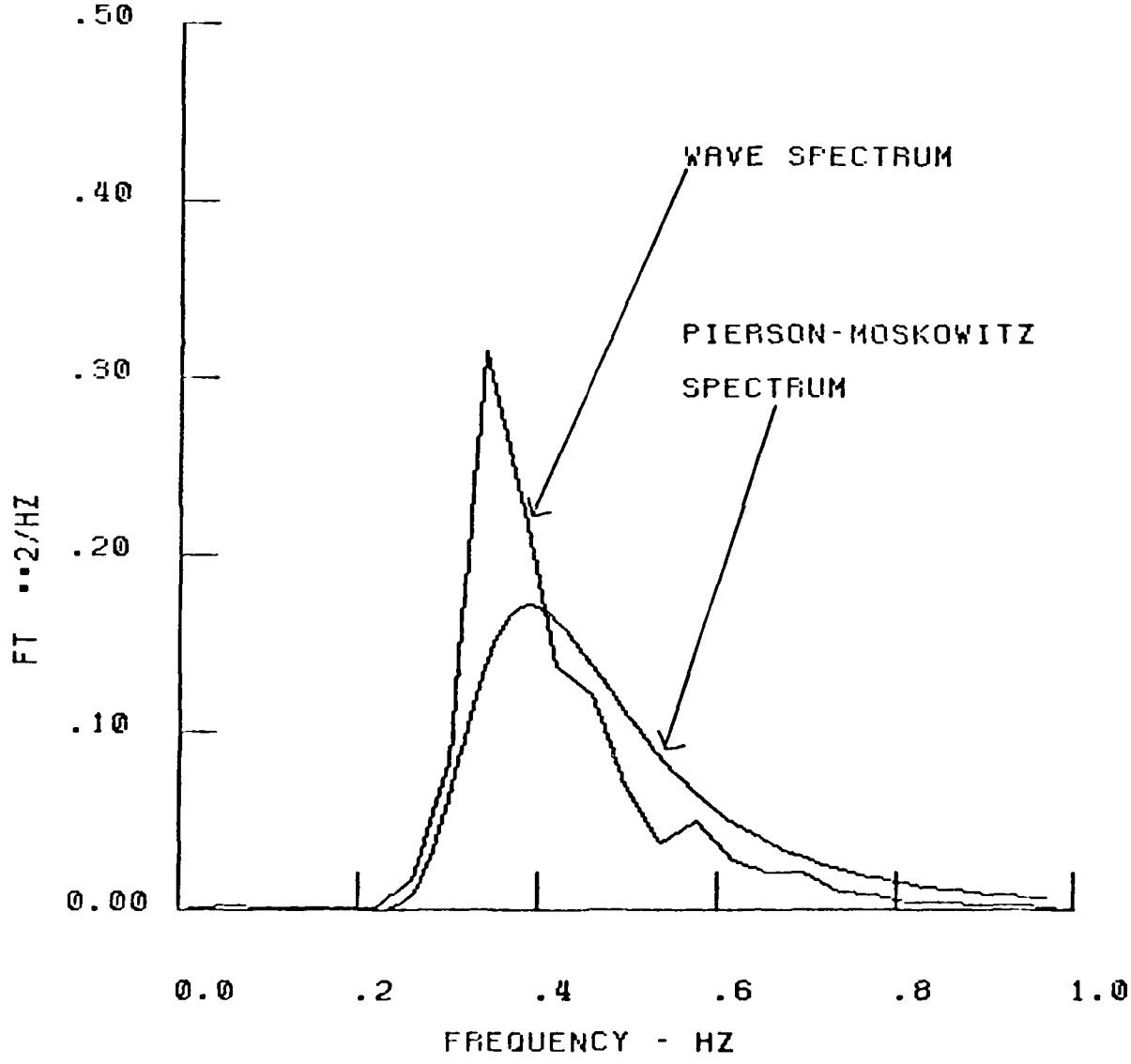

PSD
M346-7 WAVEHEIGHT
MAX % ERROR = 22.3607
BANDWIDTH = .04
DELTA TIME .100
NYQUIST FREQ = 5.00

13:01:00-13:09:20
MEAN = .1173
ST. DEV = .283
AVERAGE HIGHEST 1/3RD =
1.12

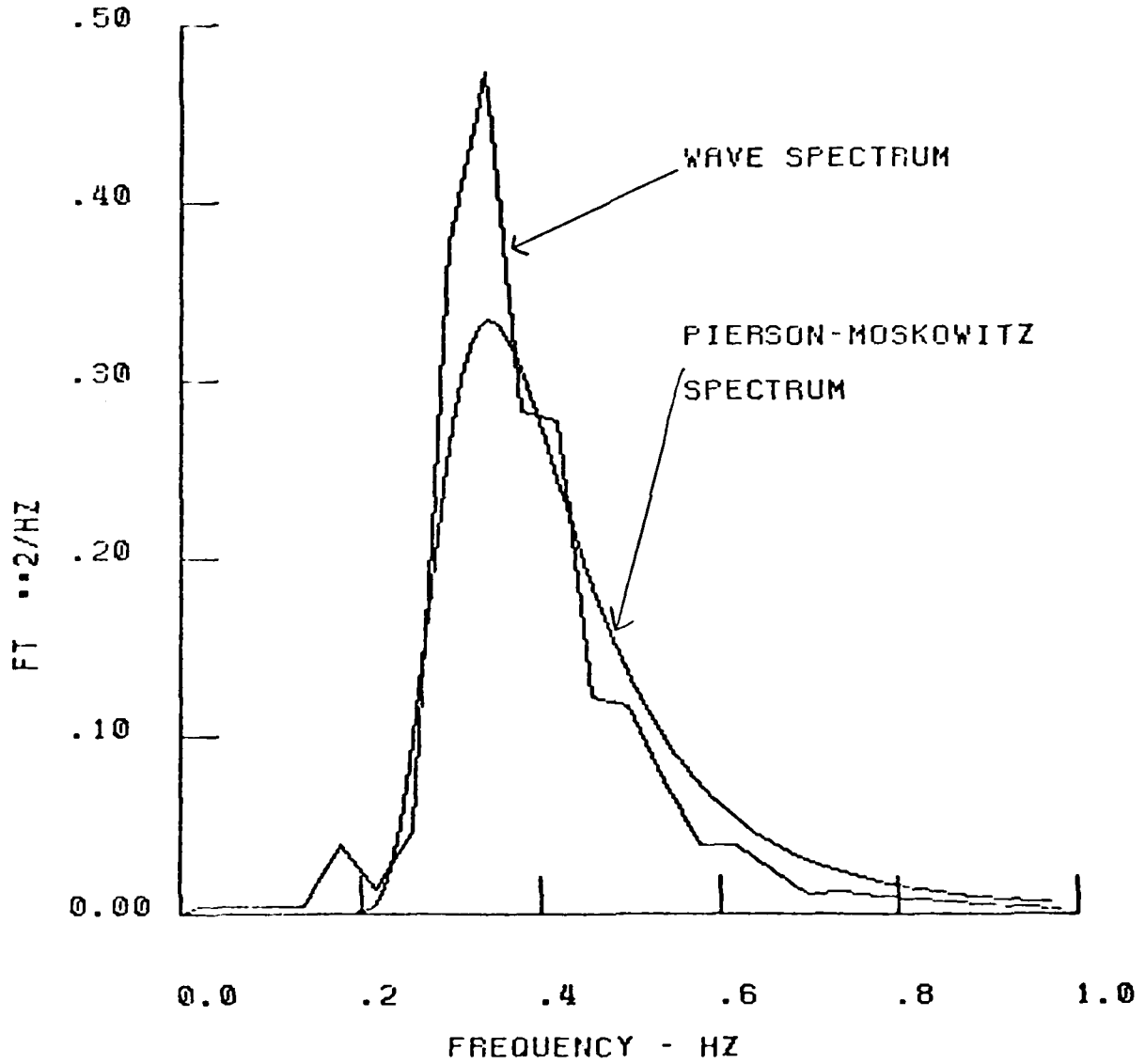

PSD
M346-8 WAVEHEIGHT
MAX % ERROR = 22.3607
BANDWIDTH = .04
DELTA TIME .100
NYQUIST FREQ = 5.00

13:06:10-13:14:30
MEAN = .1195
ST. DEV = .322
AVERAGE HIGHEST 1/3RD =
1.27

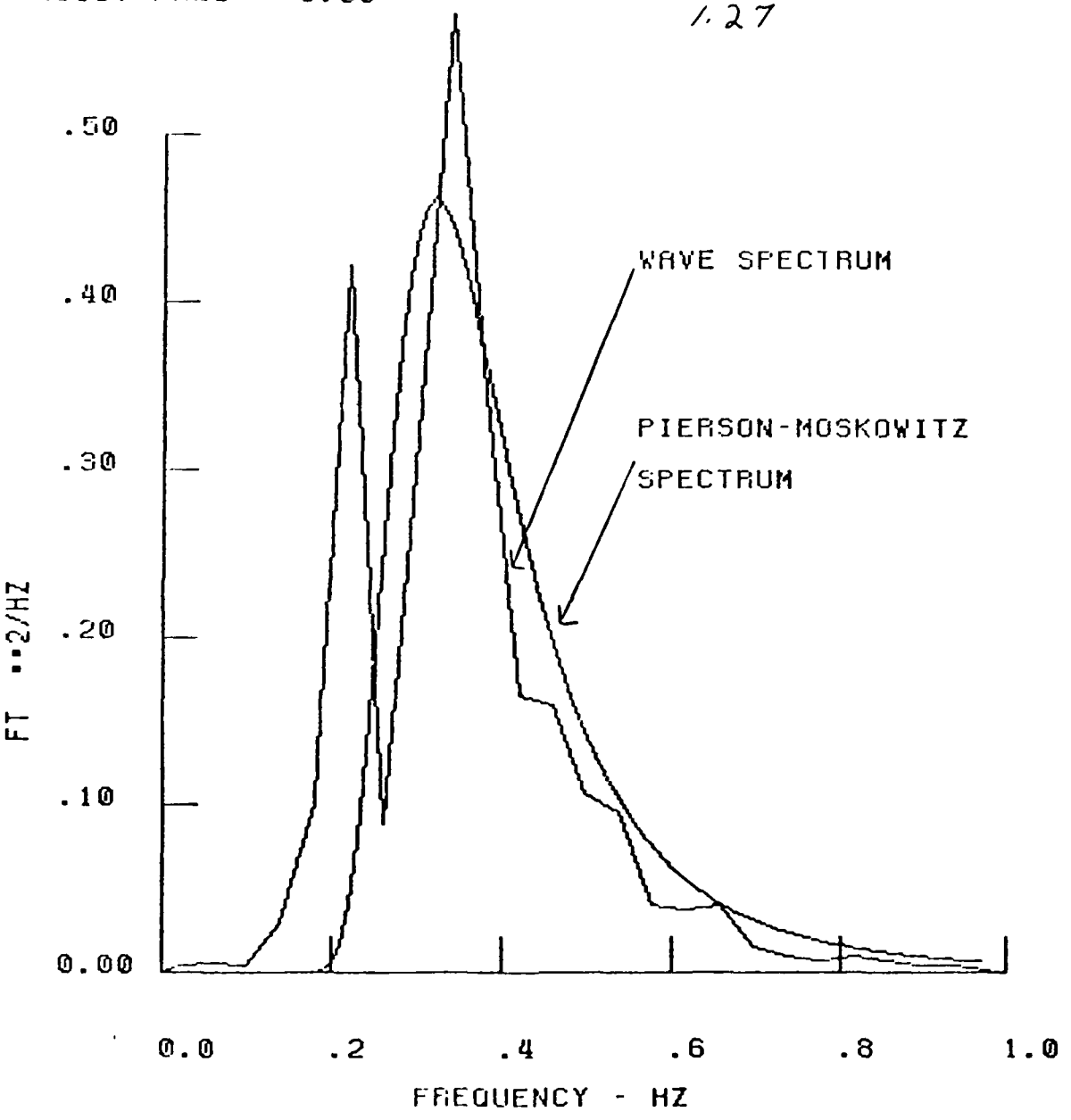

PSD
M348-1 WAVEHEIGHT
MAX % ERROR = 22.3607
BANDWIDTH = .04
DELTA TIME .100
NYQUIST FREQ = 5.00

11:03:00-11:11:20
MEAN = .1842
ST. DEV = .144
AVERAGE HIGHEST 1/3RD = .57

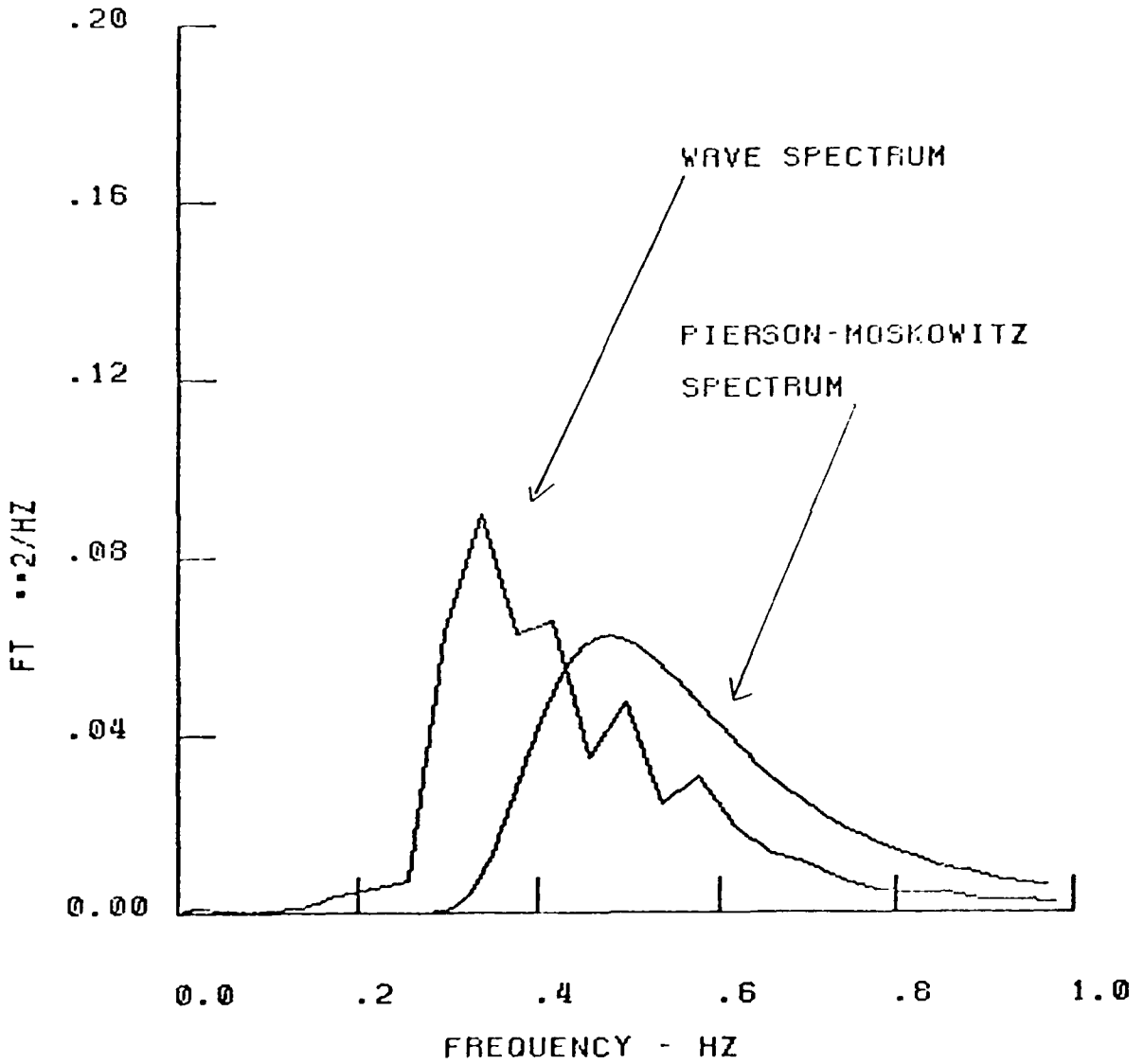

PSD

M348-2 WAVEHEIGHT 11:11:30-11:19:50

MAX % ERROR = 22.3607 MEAN = .1689

BANDWIDTH = .04 ST. DEV = .145

DELTA TIME .100 AVERAGE HIGHEST 1/3RD = .57

NYQUIST FREQ = 5.00

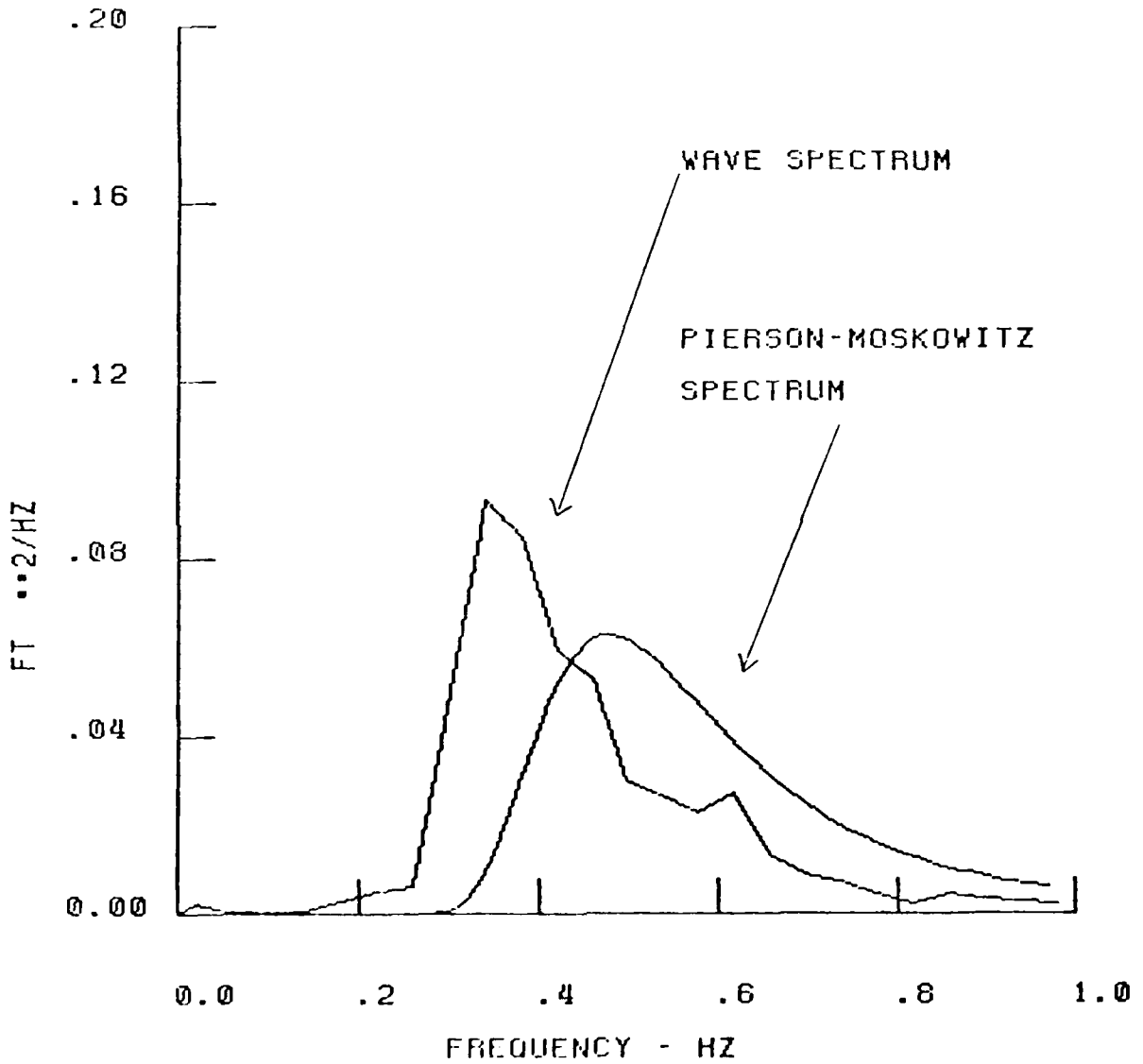

PSD

M348-3	WAVEHEIGHT	11:20:00-11:28:20	
MAX % ERROR =	22.3607	MEAN =	.1579
BANDWIDTH =	.04	ST. DEV =	.156
DELTA TIME	.100	AVERAGE HIGHEST 1/3RD =	62
NYQUIST FREQ =	5.00		

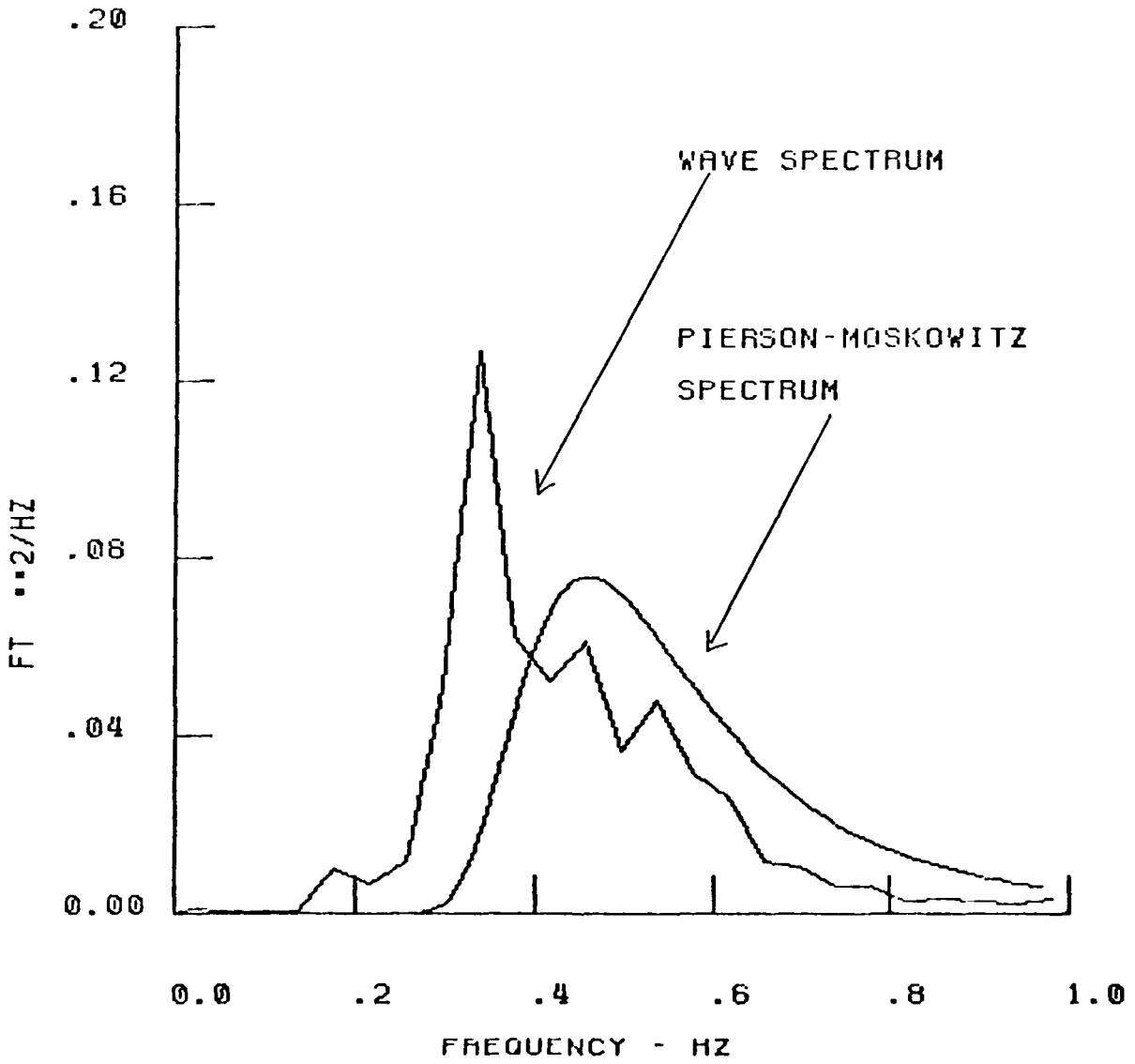

PSD

M348-4 WAVEHEIGHT	11:47:00-11:55:20
MAX % ERROR = 22.3607	MEAN = .1200
BANDWIDTH = .04	ST. DEV = .156
DELTA TIME .100	AVERAGE HIGHEST 1/3RD = .63
NYQUIST FREQ = 5.00	

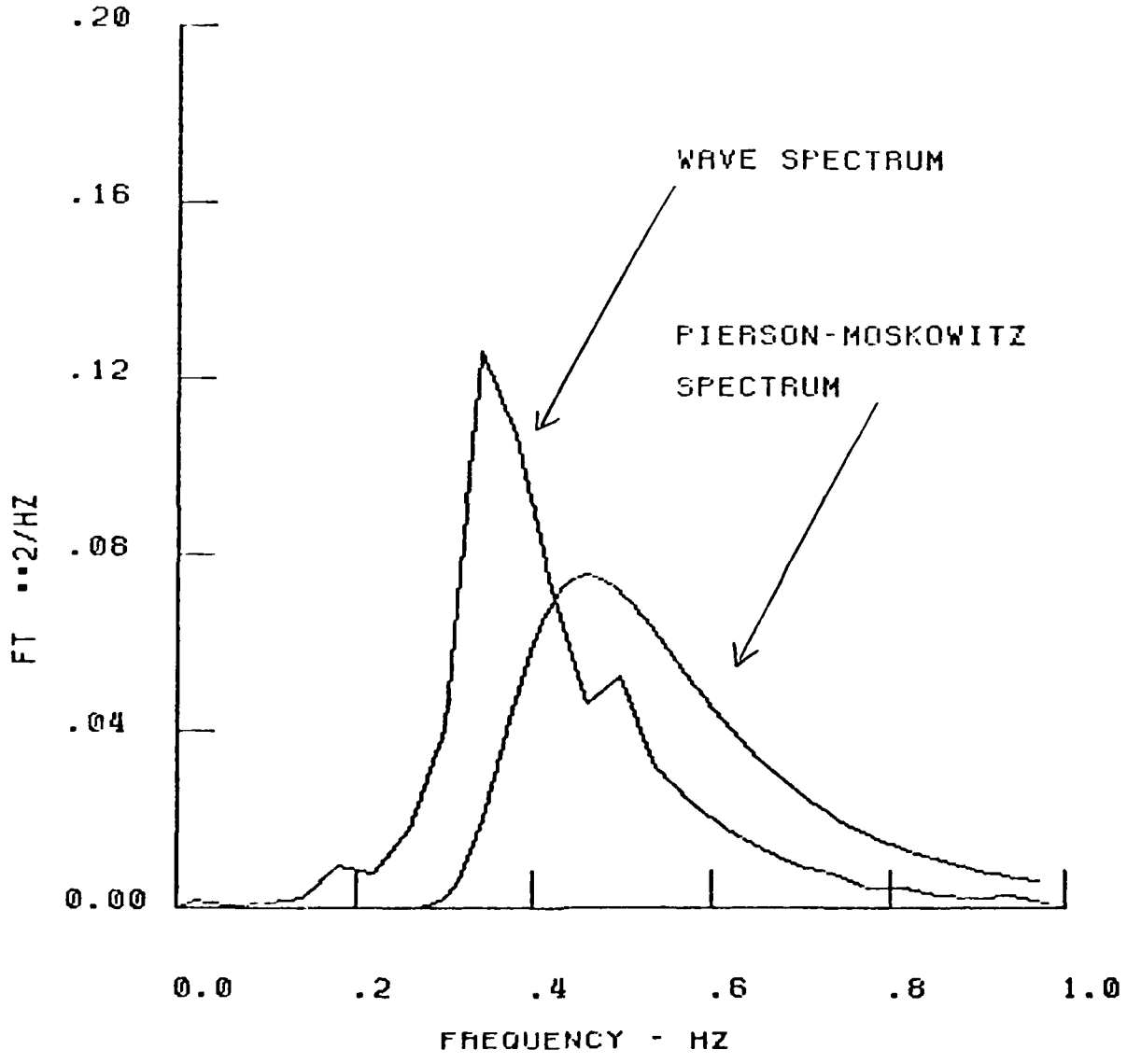

PSD

M348-5 WAVEHEIGHT

MAX % ERROR = 22.3607

BANDWIDTH = .04

DELTA TIME .100

NYQUIST FREQ = 5.00

11:56:40-12:05:00

MEAN = .1059

ST. DEV = .176

AVERAGE HIGHEST 1/3RD = .71

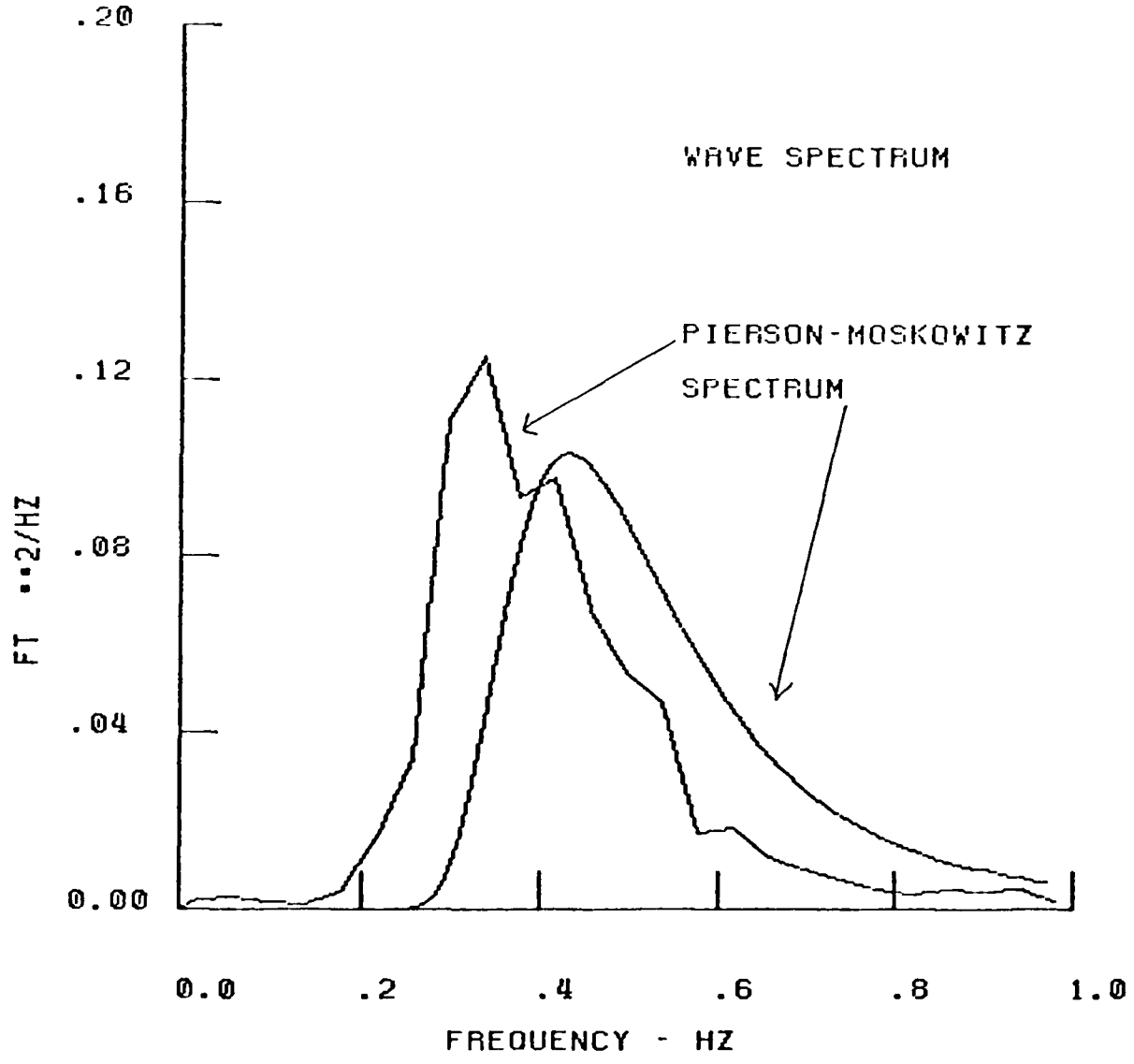

PSD

M348-7	WAVEHEIGHT	12:30:40-12:39:00	
MAX % ERROR =	22.3807	MEAN =	.0789
BANDWIDTH =	.04	ST. DEV =	.170
DELTA TIME	.100	AVERAGE HIGHEST 1/3RD =	70
NYQUIST FREQ =	5.00		

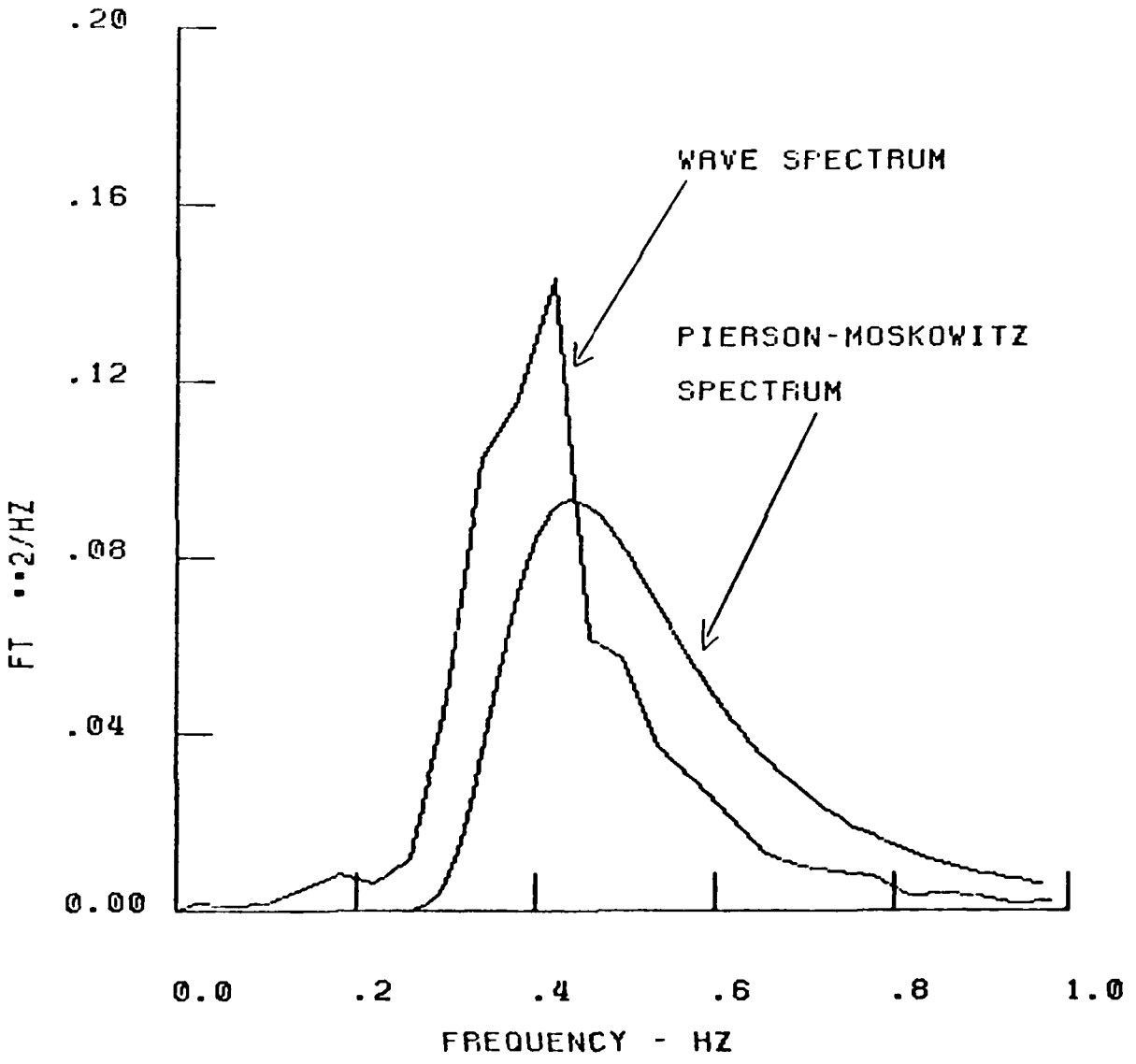

PSD

M348-8 WAVEHEIGHT		12:39:10-12:47:30	
MAX % ERROR =	22.3607	MEAN =	.0700
BANDWIDTH =	.04	ST. DEV =	.175
DELTA TIME	.100	AVERAGE HIGHEST 1/3RD =	.73
NYQUIST FREQ =	5.00		

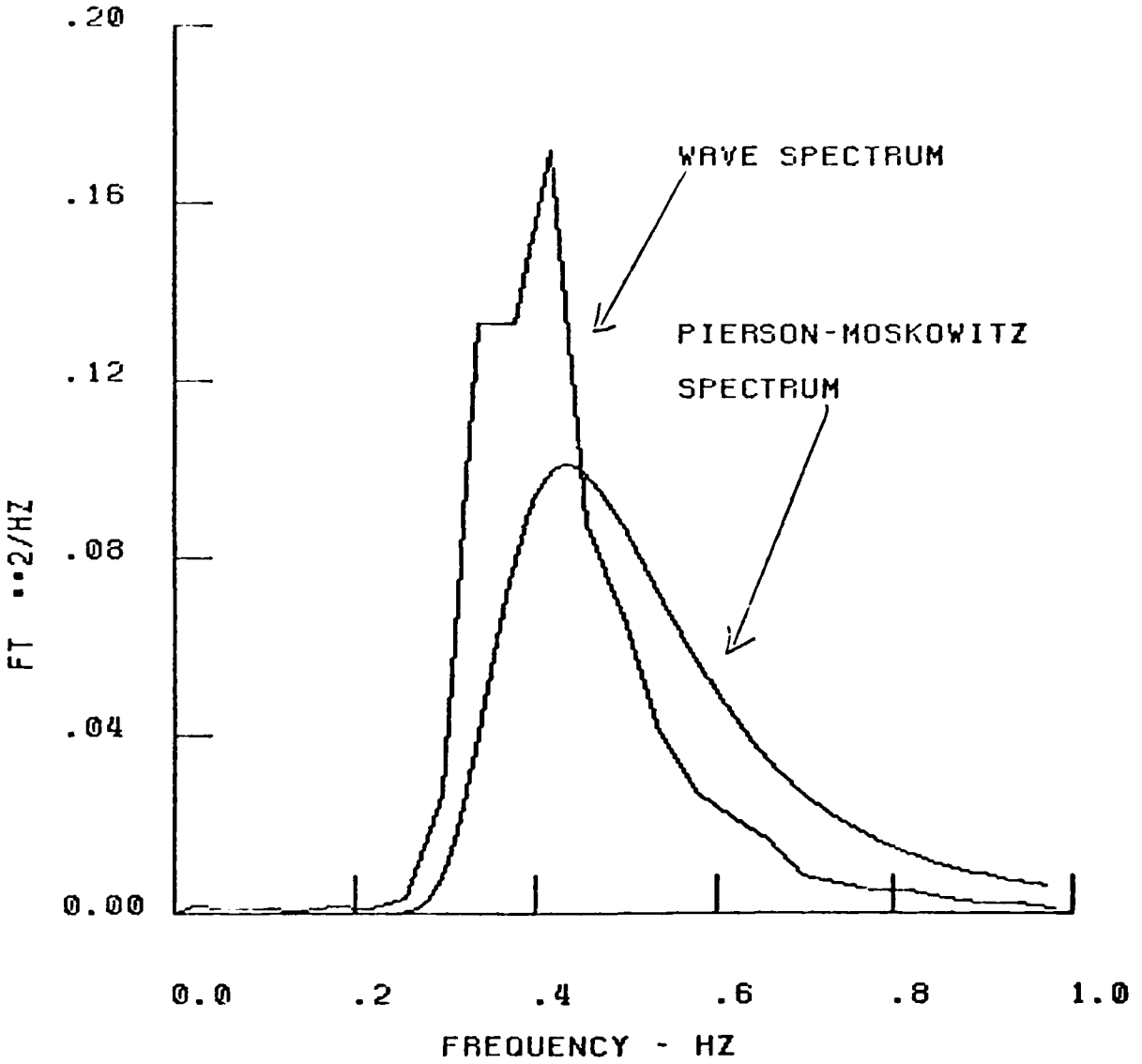

PSD

M348-9 WAVEHEIGHT 12:43:40-12:52:00

MAX % ERROR = 22.3607 MEAN = .0650

BANDWIDTH = .04 ST. DEV = .176

DELTA TIME .100 AVERAGE HIGHEST 1/3RD = .73

NYQUIST FREQ = 5.00

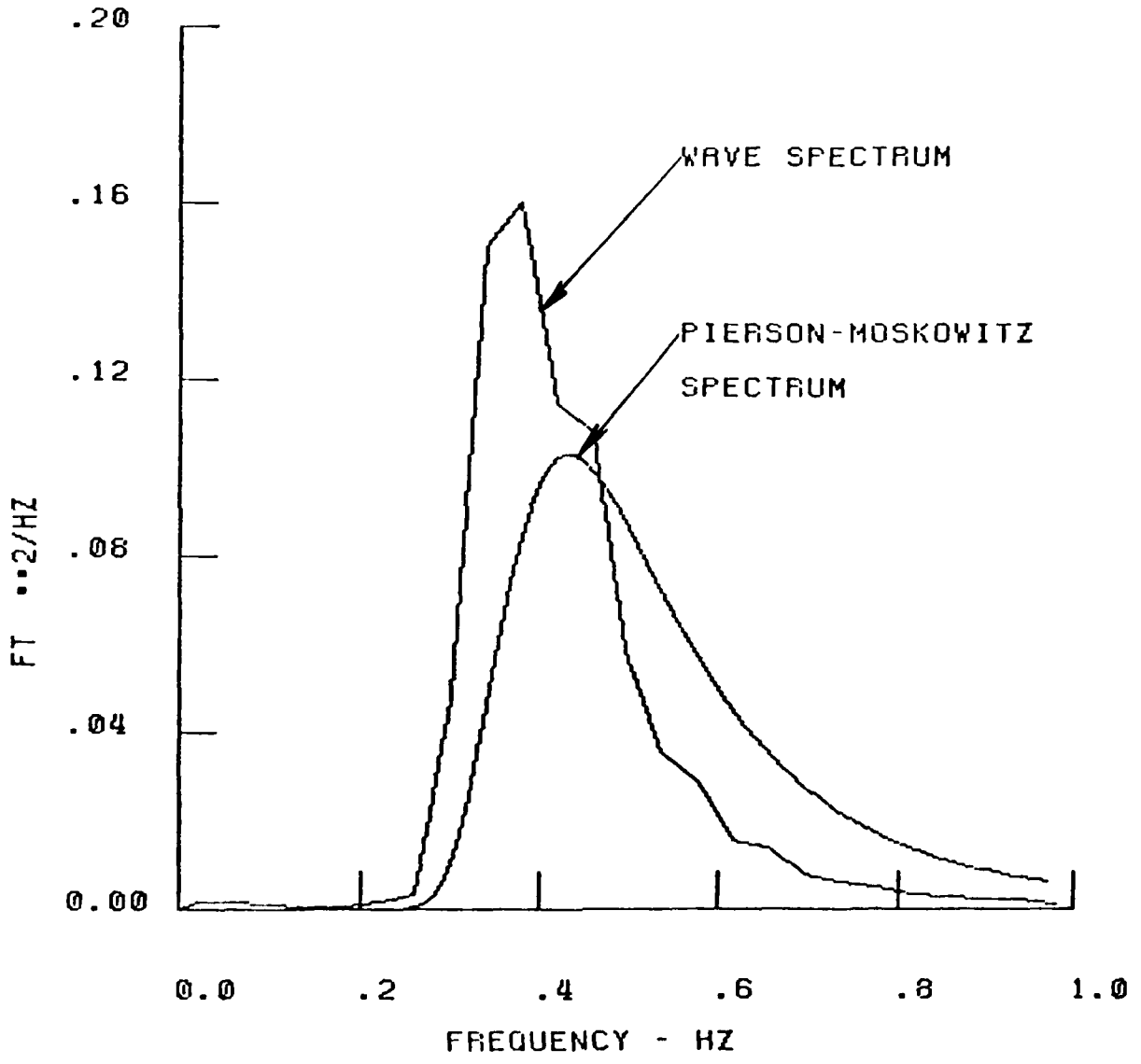

APPENDIX C

VENT VALVE CONFIGURATION TRADEOFF STUDY

C. VENT VALVE CONFIGURATION TRADEOFF STUDY

Retrofitting the Sea Bird Class SES with ride control will affect both the hull structure and arrangements in order to install the flow trunks and vent valve modules. Three candidate locations were selected for the vent valve installation based on examination of the Sea Bird general arrangement drawings. These locations are illustrated in Figure C-1. USCG and MariDyne representatives performed a shipboard inspection of these locations on 7 and 8 April to determine which was most suitable. During this inspection, it was discovered that none of the candidate locations were acceptable and that the vent valves could be easily retrofitted at a new location not previously considered. This new proposed location is discussed in Section 8.

The original candidate locations and the factors which led to their elimination from further consideration are described below.

1. Sidehull Exhaust Between Frames 2 and 3

This configuration would utilize space between Frames 3 and 4 which is presently part of the A/C Machinery Room for the flow trunk connection to the cushion. Vent valve modules would also be located in this space. From the A/C Machinery Room, the trunks would penetrate Frame 3 then turn 90° and discharge through the sidehulls between Frames 2 and 3. Forward of Frame 3, the trunks would occupy space which is presently part of the rope lockers.

This configuration was eliminated from further consideration for the following reasons:

a. The air inlets from the cushion into the trunks would be between the bow seal finger attachment tracks which extend aft from Frame 1 to Frame 4. Flow oscillations in the trunks might cause the finger material to flap during RCS operation and this could reduce the life of the fingers.

b. The additional weight due to the RCS installation would be added forward of amidships. This is unfavorable from the standpoint of optimum performance because it is already necessary to carry ballast in the aft tanks to maintain proper LCG and trim. If additional weight is added forward of amidships, it will be necessary to carry additional ballast in the aft tanks and this will cause a further increase in weight.

2. Vertical Exhaust Between Frames 11 and 12

This configuration is similar to the SES-200 vent valve installation, i.e., vertical ducts with the modules located on short stacks above the weather deck. The entrances from the cushion into the trunks are made between buttock lines not occupied by the seal air ducts or plenums. The trunks would be located between the centerline and Buttock Line 3 ft 0 in. on the starboard side and between Buttock Lines 4 ft 6 in. and 7 ft 6 in. on the port side.

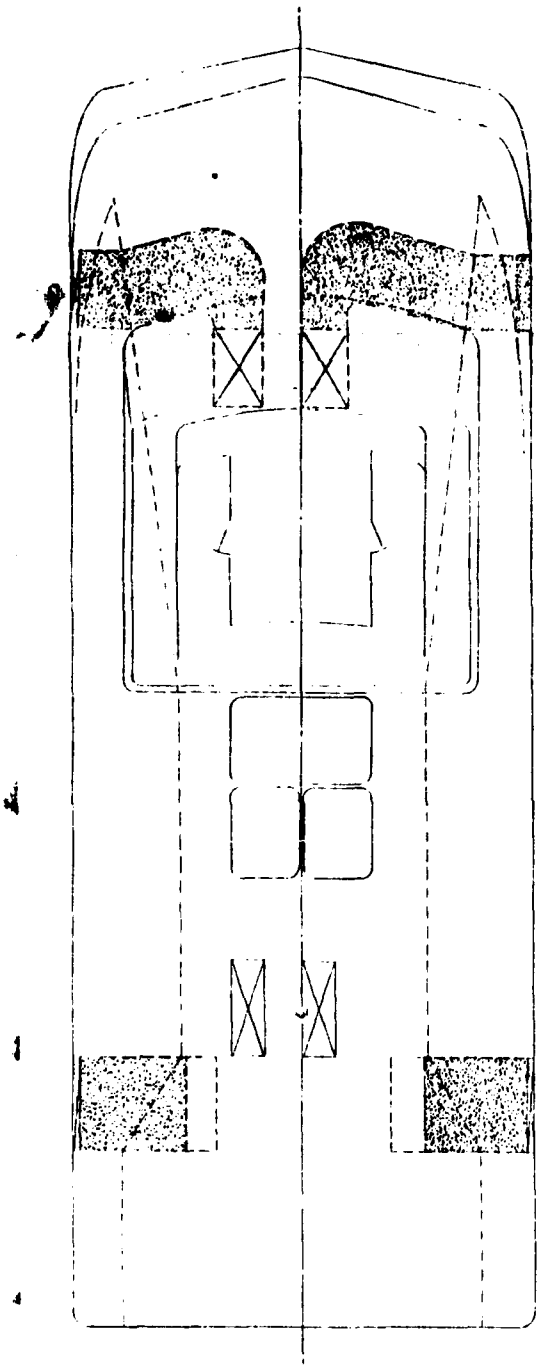

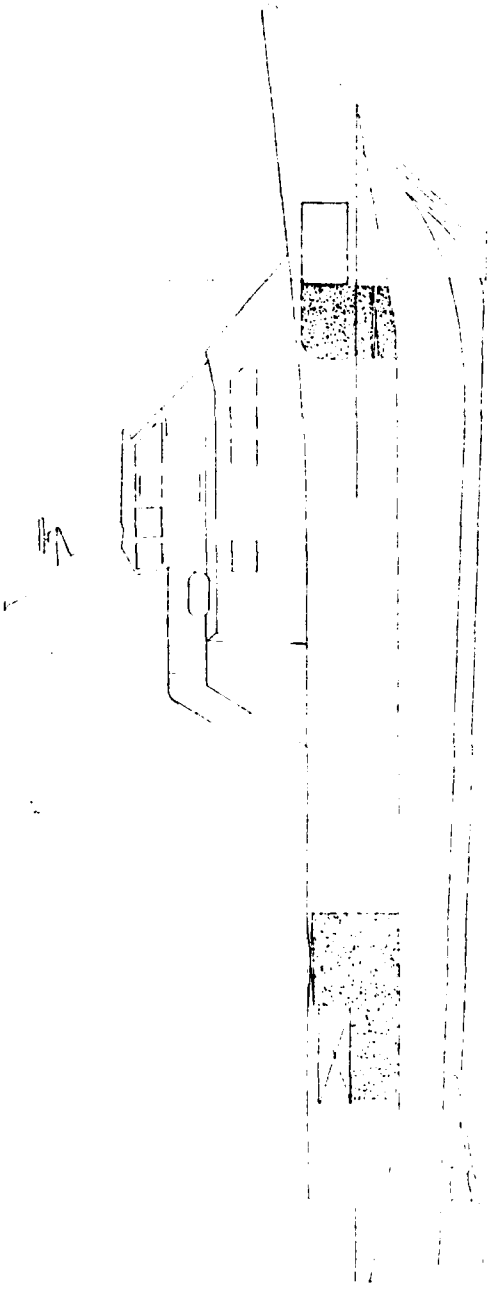

Reasons for eliminating this configuration are as follows:

a. It would require relocating some of the main electrical panels, controls and junction boxes located on the aft side of Frame 11. This would be expensive and time consuming since it would undoubtedly lead to complete rewiring of some systems.

b. It would take up part of the main deck space presently occupied by the soft patch which is used to remove the main and auxiliary generators. This would necessitate installing two new soft patches over the sidehulls to remove the generators. This would not be good structural design practice because it creates two new cutouts in the weather deck skin/stringer assembly.

3. Sidehull Exhaust Between Frames 12 and 13

In this configuration, the flow trunk connection to the cushion would be between Buttock Lines 7 ft 6 in. and 10 ft 6 in. on both the port and starboard sides. The trunks would rise vertically from these openings, turn outboard 90° and discharge through the sidehulls. Vent valve modules would be mounted where the flow trunks attach to the sidehull skin/stringer assembly.

This configuration was always considered less than optimum because of the considerable distance between the vent valves and the craft's center of gravity. Experience has shown that it is desirable to locate vent valves close to the LCG. Additionally, it has been found that the lowest frequency lift system acoustic modes are typically associated with the stern seal and the pressure in the aft cushion. Location of the vent valves in the stern could aggravate any coupling between the RCS and these modes and thereby reduce RCS effectiveness.

Other reasons for eliminating this configuration are as follows:

a. It would be necessary to relocate the Envirovac Sewage Treatment Plant, plus all associated plumbing.

b. It would be necessary to relocate the refrigerator and freezers on the port side and the toolbox/spare parts bins on the starboard side.

END

FILMED

3-85

DTIC